

Lorenz Steiner, BSc

**Pd-catalyzed cross-coupling and oxidative homo-coupling
of aryllithium reagents generated
in-situ via ortho-directed lithiation**

MASTERARBEIT

zur Erlangung des akademischen Grades

Master of Science

Masterstudium Chemie

eingereicht an der

Technischen Universität Graz

Betreuer

Univ.-Prof. Dipl.-Ing. Dr. techn., Wolfgang Kroutil

Institut für Chemie
Karl-Franzens Universität Graz

MSc, Hugo Helbert
Faculty of Science and Engineering, University of Groningen (NL)

EIDESSTATTLICHE ERKLÄRUNG

Ich erkläre an Eides statt, dass ich die vorliegende Arbeit selbstständig verfasst, andere als die angegebenen Quellen/Hilfsmittel nicht benutzt, und die den benutzten Quellen wörtlich und inhaltlich entnommenen Stellen als solche kenntlich gemacht habe. Das in TUGRAZonline hochgeladene Textdokument ist mit der vorliegenden Masterarbeit identisch.

Datum

Unterschrift

Contents

Zusammenfassung	1
Abstract.....	1
Introduction.....	1
Cross-coupling reactions	1
Development of cross-coupling reactions.....	2
Palladium catalysts.....	4
Palladium complexes as catalysts	4
Palladium metal as catalyst.....	6
Organometals for Coupling-Reactions.....	8
Organolithium compounds by directed metalation.....	9
Oxidative coupling.....	10
Oxidants.....	11
Aim of the project.....	12
Results.....	14
Arnottin.....	14
Retrosynthesis.....	14
Forward synthesis.....	15
Regioselective Lithiation of 4	15
Forward synthesis.....	16
Alternative route development.....	18
Oxidative homo-coupling of aryllithium compounds.....	20
Method development.....	20
Temperature Studies.....	22
Sterically hindered substrates	24
Preliminary Results.....	26
Conclusions and Prospect.....	27
Experimental.....	28
References.....	33
Appendix.....	36
NMR-Spectra.....	37
GC-MS Chromatograms.....	58

- This page is intentionally left blank -

Zusammenfassung

Palladium-katalysierte Kupplungsreaktionen von Aryllithiumverbindungen wurden untersucht. Für eine neuartige Syntheseroute für die Herstellung von Arnottin I, einem Naturstoff aus der Substanzklasse der Coumarine, wurden Palladium-Nanopartikel erfolgreich als Katalysator für die Kreuzkupplung von Aryllithiumreagenzien mit Arylbromiden eingesetzt. Darüber hinaus wurde eine von Pd-PEPPSI IPent und Pd-PEPPSI SIPr katalysierte, neuartige Methode für die oxidative Homokupplung von Aryllithium- und Heteroaryllithiumreagenzien mit 1,2-dichlorethan als Oxidans entwickelt. Dabei wurde bei sterisch ungehinderten Systemen voller Umsatz innerhalb von Sekunden bis Minuten bei einer Katalysatorladung von 1 mol % beobachtet. Alle Aryllithiumreagenzien wurden *in-situ* durch Lithiierung über *ortho*-dirigierende Gruppen hergestellt.

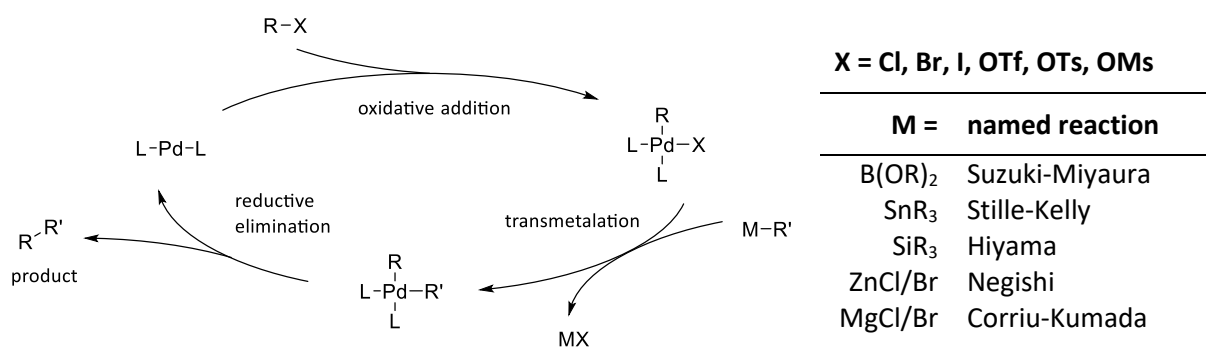
Abstract

Palladium-catalyzed coupling reactions of aryllithium compounds were studied. Palladium nanoparticles were employed as catalyst in the successful cross-coupling of an aryllithium with an aryl bromide in an attempt to synthesize Arnottin I, a natural product of the coumarin family. Workaround strategies further proved the applicability of this method. Additionally, a method for catalytic oxidative homo-coupling of aryllithium and heteroaryllithium compounds was successfully developed with Pd-PEPPSI IPent and Pd-PEPPSI SIPr catalyst. This reaction is fast for sterically unhindered systems, reaching full conversion within seconds to minutes at room temperature with catalyst loadings of 1 mol %. All aryllithium compounds were generated *in-situ* by directed lithiation strategies.

Introduction

Cross-coupling reactions

Chemistry revolves around the formation and cleavage of bonds, and organic chemistry even more so around the formation of C-C bonds. An organic chemist must be equipped with a toolbox of reactions that will allow them to design a synthetic route towards any desired product. One very powerful reaction class for the formation of sp^2 - sp^2 bonds, which are otherwise hard to access, is palladium-catalyzed cross-coupling. Indeed, the godfathers of this reaction, Richard Heck, Ei-Ichi Negishi and Akira Suzuki, were awarded the chemistry Nobel prize in 2010 “for palladium-catalyzed cross-couplings in organic synthesis”.^[1]



Scheme 1 Generally accepted mechanism of Pd-catalyzed cross coupling and the respective named cross-coupling reactions.

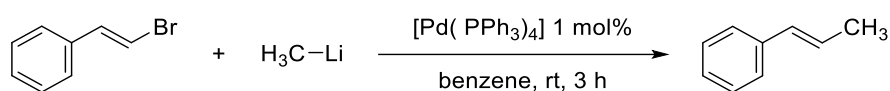
The generally accepted mechanism of this class of reactions starts by the palladium catalyst undergoing oxidative addition with an organic halide, followed by a transmetalation step from an organometallic compound. Subsequently, the C-C bond forms upon reductive elimination, which regenerates the Pd-catalyst into the catalytic cycle (Scheme 2). The choice of the catalyst is not limited to Pd, and Au,^[2,3] Ru^[4,5] and Rh^[6-8] are among the most widely used alternatives. Due to economic reasons and growing environmental awareness the development of catalysts based upon more abundant metals such as Cu,^[9] Fe^[10,11] and Ni^[12,13] is ongoing. Despite these efforts Pd catalysts will probably continue to be the first choice, as their development builds on decades worth of research.

Development of cross-coupling reactions

The history of C-C bond formation from carbon-transition metal bonds dates back to at least 1869, when Glaser reported the successful homocoupling of phenyl acetylene cuprate to the corresponding dialkyne.^[14] His method involved stoichiometric use or excess of copper for the completion of the reaction, and a catalytic method was out of reach for quite some time. It was not until the late 1930's to early 1940's that the transition metal catalysis slowly became a reality.^[15] The next two decades saw the establishment of standard reactions for the following three elements: copper for acetylene chemistry, nickel for coupling reactions and palladium for olefin chemistry. However, nowadays we strongly associate coupling-reactions with palladium, a trend that was arguably kickstarted in 1968 by Richard Heck. His work on palladium at Wacker and Höchst lead to the discovery that organomercury compounds would react with alkenes in the presence of a palladium catalyst. In seven back-to-back publications in 1968 he described his findings on the catalytic activity of $\text{Li}_2[\text{PdCl}_4]$, and thus started an era of investigation to come.^[16-23]

Alternatives to mercury were highly anticipated, as these compounds are extremely toxic. The effort of Kumada and Corriu generated a method for the coupling of Grignard reagents, however they still relied on nickel catalysts, as existing palladium catalysts were still too low in activity.^[24] The use of phosphine ligands by Kumada for the nickel catalyst in these reactions finally paved the way for the development of more active palladium catalysts to come.^[25,26]

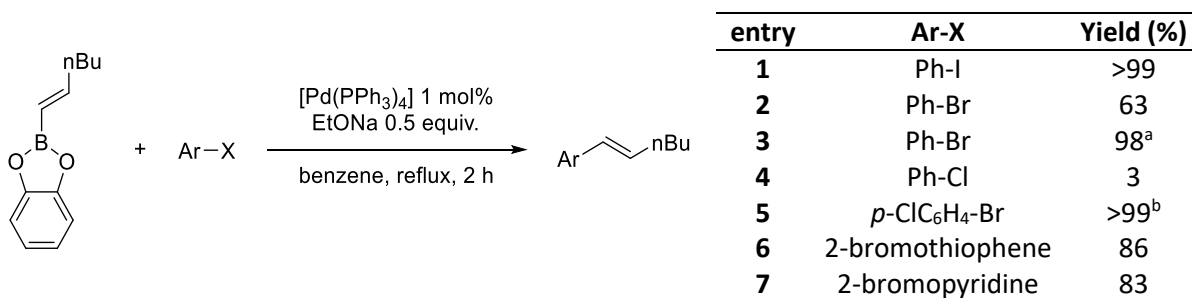
And indeed, in 1975 Murahashi employed $[\text{Pd}(\text{PPh}_3)_4]$ in the coupling reaction of styrene with methyl lithium (and methyl magnesium bromide, respectively),^{[27] [28]} and found palladium to be the superior catalysts over nickel in this case (Scheme 2).



Scheme 2 Murahashi's findings in 1975.

Organolithium and Grignard reagents are highly reactive nucleophiles and will readily react with a broad spectrum of electrophiles, including carbonyls of any sort, and many positively polarized carbon atoms. Therefore, the desire for a method using a less reactive organometallic reaction partner was present. It would not be long before Negishi looked into the possibility of using organo-zinc, -aluminum, and -boron compounds for cross-coupling. He found success and reported the coupling of arylzinc chlorides in 1977.^[29,30] Building on earlier reports, John Stille also looked for an alternative to Li and Mg, and focused on the use of organotin in the late 1970's, and found Sn and Zn reagents as an attractive replacement.^[31,32] Though performable under milder conditions organozinc reagents are not air stable, and organotin reagents are highly toxic.

A real solution to all these problems came in 1979. Akira Suzuki together with Norio Miyaura focused on organoboron compounds, which had previously thought to be inert in cross-coupling by Negishi,^[33] and which Heck was only able to couple by the use of stoichiometric amounts of palladium.^[34] The two published the now infamous two-page paper in 1979,^[35] which would soon be one of the most influential publications in the field of cross-coupling chemistry.



Scheme 3 Examples from Suzuki's and Miyaura's 1979 publication.^[35] ^a reaction time is 4 h. ^b reaction time is 3 h.

This was a significant breakthrough in the applicability of cross-coupling reactions! Organoboron compounds are usually not air- and moisture sensitive, and the by-products of the reaction are easily removable inorganic salts of little toxicity. These properties would make the Suzuki-Miyaura reaction the most well-known of all the cross-coupling reactions up to this point. It is the posterchild of coupling reactions taught throughout organic chemistry courses in universities, and it truly kickstarted the development of more active catalysts in the years following its discovery.

Palladium catalysts

The right choice of a palladium catalyst for a coupling reaction is not trivial. Indeed, most chemical suppliers offer a vast selection of catalysts ready for use, as well as palladium precatalysts and salts. From the latter a powerful catalyst can be generated *in-situ* when combined with the right ligands.

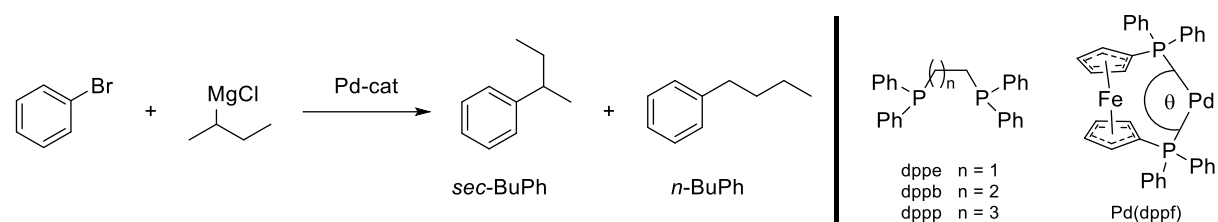
From this assortment the resourceful chemist is tasked to make the most sensible choice for any given catalytic problem, as the much sought-after all-purpose catalyst is yet to be found, if it exists at all. The insights and efforts of chemists working in the development of highly active catalysts will be discussed in the following paragraph.

Palladium complexes as catalysts

The most commonly employed palladium complex for catalysis in the early days of coupling reactions was [Pd(PPh₃)₄], a rather poor catalyst viewed from today's perspective. With it, chemists were able to couple aryl- and alkenyl iodides as well as highly activated bromides, but the corresponding chlorides proved to be too inactive. This is commonly explained by the high dissociation energy of C-Cl bonds, compared to C-Br and C-I bonds.

Already in 1979, Kumada could show the correlation between bite angle of bidentate phosphine ligands and reaction rate.^[36] By accelerating the rate of reductive elimination, the time for isomerization of the *s*-butyl-group to the thermodynamically more stable *n*-butyl isomer is impeded, leading to a more defined product isomer mixture.

Table 1 Cross-coupling of *sec*-BuMgCl with bromobenzene using Pd-catalysts with different bite angles.



entry	catalyst	time (h)	bite angle θ (°)	<i>sec</i> -BuPh (%)	<i>n</i> -BuPh (%)
1	PdCl ₂ (dppf)	1	99.1	95	0
2	PdCl ₂ (dppb)	8	94.5	51	25
3	PdCl ₂ (dppp)	24	90.6	43	19
4	PdCl ₂ (dppe)	48	85.8	0	0
5	Pd(PPh ₃) ₄	24	-	4	6

Another major breakthrough in catalyst design was in 1999, when Fu first reported the coupling of unactivated aryl chlorides with [Pd₂(dba)₃] in the presence of bulky alkyl phosphine ligands in Heck and Suzuki-Miyaura reactions.^[37,38] Within a year, he could expand the substrate scope in the Suzuki-Miyaura to aryl and vinyl triflates as well.^[39] From these findings many were inspired, and a number of sterically demanding, electron rich phosphine ligands were developed over the next years, notable examples of which are highlighted in Figure 1.

A major downside to the use of free phosphine ligands in combination with a suitable palladium salt is the commonly air-sensitive nature of bulky alkyl phosphine ligands. In extreme cases, these are even known to be pyrophoric (e.g. P(*t*-Bu)₃), and thus it is highly desirable having those Pd-P bonds already in place in what is known as a preformed catalyst. The years around 2000 saw the rise of Pd(0) preformed catalysts, mainly [Pd(*Pt*-Bu₃)₂] and [Pd(*PO*-tol₃)₄].^[40,41] However, these catalysts would still deteriorate over time unless stored under inert conditions or at low temperatures. A better alternative poses the use of Pd(II) preformed catalysts, as they are generally bench-stable. One noteworthy example from this class are the so-called PEPPSI catalysts (Pyridine Enhanced Precatalyst Preparation and Stabilization and Initiation).^[42,43] The *N*-heterocyclic carbene (NHC) ligand is known to strongly bind to palladium, thus making dissociation unlikely, and in turn Pd(NHC)L_n catalysts highly active. Catalysts of the type Pd(NHC)₂L_n on the other hand are rather inactive, due to the slow dissociation of the NHC-ligand, making the formation of the active catalyst in solution unlikely.^[44,45]

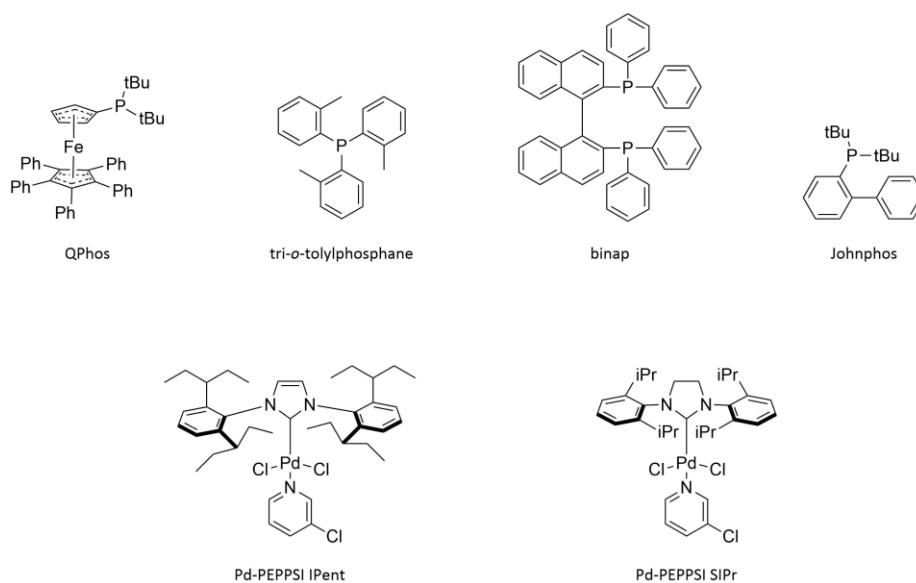
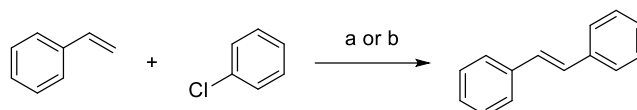


Figure 1 commonly employed ligands for Pd-catalysts used in cross-coupling and *N*-heterocyclic precatalysts Pd-PEPPSI IPent and Pd-PEPPSI SIPr

Palladium metal as catalyst

Metallic palladium as a catalyst in coupling reactions was already used in the early 1970's by Heck in the form of Pd-black,^[46] and Julia as Pd supported on carbon.^[47] The mechanism of catalysis is still debated, as the true nature of the catalyst is hard to study. The two schools of thought are that the catalytic steps either take place in solution from leached palladium, or at defect sites directly on the palladium surface. The advent of palladium nanoparticles in catalysis did not settle this argument and extensive research will be needed for a definite answer to the mechanism. The field of palladium metal catalysis is, to make an understatement, vast and complicated. Highly active systems are commonly described in the literature, and indeed the subject alone would demand for a whole thesis. Biffis *et al* wrote an excellent review on the matter, that the interested reader is referred to.^[47] In the following paragraph some reaction schemes will be given in order to exhibit the possible outstanding activity of palladium metal as catalyst.

In 1990 Kaneda *et al* could present the successful coupling of styrene with chlorobenzene catalyzed by Pd supported on MgO to obtain stilbene.^[48] By reducing Pd(acac)₂ they were able to obtain a catalyst with a surface area of 268 m² g⁻¹ Pd that would yield a turnover number of 1620 (mol stilbene / g Pd). Mukhopadhyay *et al* obtained stilbene and similar products in a reaction catalyzed by Pd supported on charcoal in water in the presence of PEG-400 and sodium formate.^[49] They found that hydrogenation of stilbene could be suppressed by the choice of the employed base.



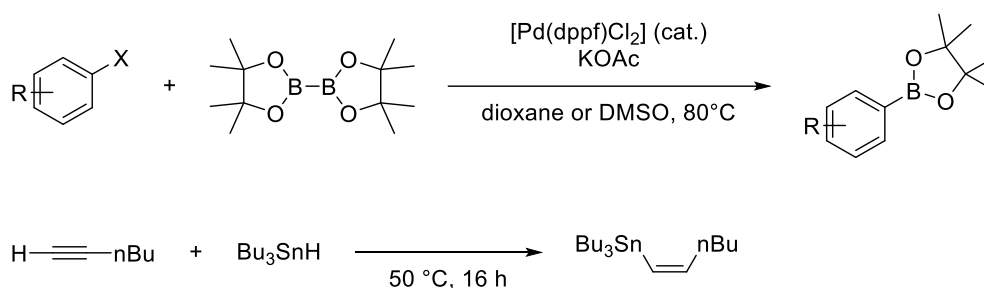
Scheme 4 a) styrene (44.0 mmol), chlorobenzene (44.0 mmol), sodium formate (70 mmol), Pd/C (0.7 mol %), PEG-400 (8.5 mol %), Na₂CO₃ (125 mmol), H₂O (50 mL), 100 °C, 5.5 h; conversion 80 % (60 % stilbene, <5 % hydrogenated stilbene, 25 % biphenyl); b) styrene (10 mmol), chlorobenzene (7.5 mL, 74 mmol), Pd/MgO (0.002 mg Pd), Na₂CO₃ (3.3 mmol), 150 °C, 5 h; TON 1620.

Yamada *et al* developed a highly active metalloenzyme-inspired polymeric imidazole Pd catalyst (MEPI-Pd) capable of quantitatively coupling *p*-iodotoluene with benzyl boronic acid with an astounding catalyst loading of only 2.8 * 10⁻⁵ mol %.^[50] Other derivatives were obtained in yields of >95 % with a catalyst loading of 6.6 * 10⁻³ mol %.

Feringa *et al* developed a method for the ultrafast cross-coupling of aryl bromides with organolithium bases employing Pd-nanoparticles. These highly active nanoparticles are generated by treating [Pd(*t*-Bu)₂] in toluene with molecular oxygen and subsequent reduction with the lithium base.^[51] They were able to couple 2-bromo-naphthalene quantitatively with *n*-BuLi within 5 seconds with a catalyst loading of 5 mol %.

Organometals for Coupling-Reactions

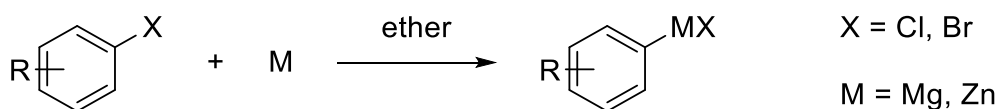
In its most basic form a cross-coupling reaction involves a more nucleophilic, negatively polarized (commonly C-BR₂, C-SnR, C-SiR₃, ...), and an electron deficient, positively polarized reaction partner (commonly C-Br, C-I, C-OTf, ...). These organometallic reactants have different advantages (i.e. functional group tolerance, methods of preparation, ...) and disadvantages. Organoboron compounds are expensive to make and organotin compounds are highly toxic. Organometallic reagents for cross-coupling are commonly synthesized by transmetalation from more electropositive organometals, such as organolithiums or Grignard reagents.^[52-54] Arylboronic acids may be prepared by the Miyaura borylation reaction,^[55] and organotins^[56-58] and alkenylboronic acids^[59] are also commonly synthesized by hydrometallation.



Scheme 5 Top: Miyaura reaction for the synthesis of arylboronic acids from aryl bromides and iodides. Bottom: hydrosilylation of a terminal alkyne with Bu₃SnH.^[60]

All these methods will add another step to any synthetic route involving these compounds. In addition to that, another disadvantage shared by all the organometals mentioned above is the low atom efficiency. The use of a large molecule that will only transfer a relatively small side chain is something that is frowned upon more and more as the green chemistry aspect is gaining importance in modern days.

Kumada- (C-MgX, X=Br, I) and Negishi-coupling (C-ZnX, X=Br, I) are variations that tackle these problems by generating the reactive organometal *in-situ* from the corresponding organohalide and elemental Mg or Zn. Furthermore, as the reaction proceeds the only byproducts are Mg- or Zn-salts, which are low in toxicity, and are easily removed by an aqueous workup. These organohalides themselves are prepared from suitable precursors, which adds another synthetic step.



Scheme 6 General approach for the *in-situ* preparation of aryl magnesium and zinc halides.

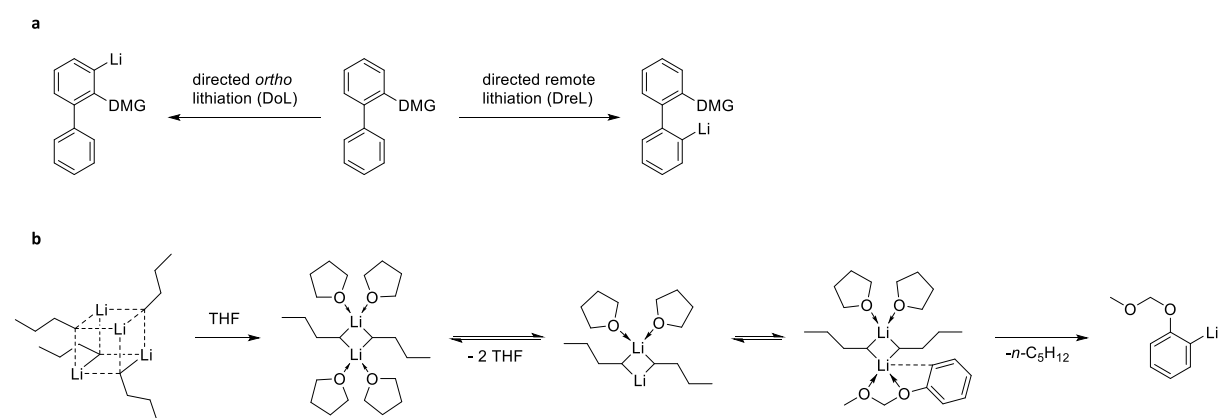
Organolithium compounds by directed metalation

One way of avoiding the use of organohalides as precursors to organometals is metalation through *directed ortho lithiation* (DoL) and *directed remote lithiation* (DreL). This now well established method for the lithiation of a variety of aromatic compounds with a strong lithium base was discovered by Gilman and Wittig as early as 1939.^[61,62]

Commercially available organolithium bases are often present as polyhedral aggregates in solution.^[63] The degree of aggregation depends on the solvent and the bulkiness of the lithium base. *n*-BuLi is present as a hexamer in hydrocarbons,^[64] tetrameric in diethyl ether^[64] and a mixture of tetramer and dimer in THF.^[65] The sterically more demanding *s*-BuLi is a mixture of hexamer and tetramer in hydrocarbons,^[66,67] and breaks down to a mixture of dimer and monomer in THF.^[68] *t*-BuLi is present as a tetramer in hydrocarbons.^[69,70] In diethyl ether is present as dimer, and in THF as monomer.^[71]

A lower degree of aggregation is associated with higher reactivity. Organolithium bases are thus either activated by the choice of a coordinating solvent (e.g. THF, diethyl ether, dioxane), or by the use of additives [e.g. tetramethylethylenediamine (TMEDA), hexamethylphosphoric triamide (HMPT)].

Once activated, a butyl lithium base can take part in directed metalation. A *directing metalation group* (DMG) will allow for selective deprotonation by spatially guiding the alkyllithium base into proximity of a proton. Directing groups are Lewis basic residues which lower the activation energy of the deprotonation by coordination of the lithium ion.^[72]



Scheme 7 ^a DoL vs. DreL in a schematic diaryl system. ^b Mechanism of *ortho* lithiation of methoxy methoxy benzene with *n*-BuLi in tetrahydrofuran.

DMG's can be ranked by their ability to promote DoL, often allowing the prediction of the lithiation site if two or more directing groups are present in the same molecule.^[73-75] A strong directing group is not only determined by its electronic properties, but also steric influences play a role. This can be demonstrated by the fact, that the methoxy-methyl (MOM) ether moiety is classified as a strong directing group, whereas the methoxy-ethyl ether is already significantly weaker. To summarize, the site

of lithiation may also be influenced by choice of solvent, lithium base, reaction temperature and time, or the use of additives, such as TMEDA. The chemistry of directed metalation and lithiation has been studied extensively, and reviews published on this field are far from scarce. With these resources at aid the talented resourceful chemist will may always find a way to lithiate any given aromatic system where desired.

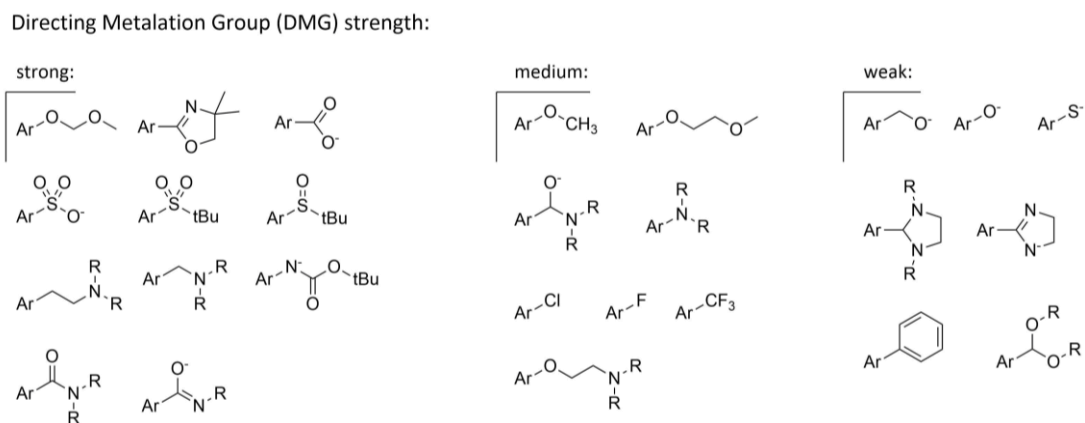


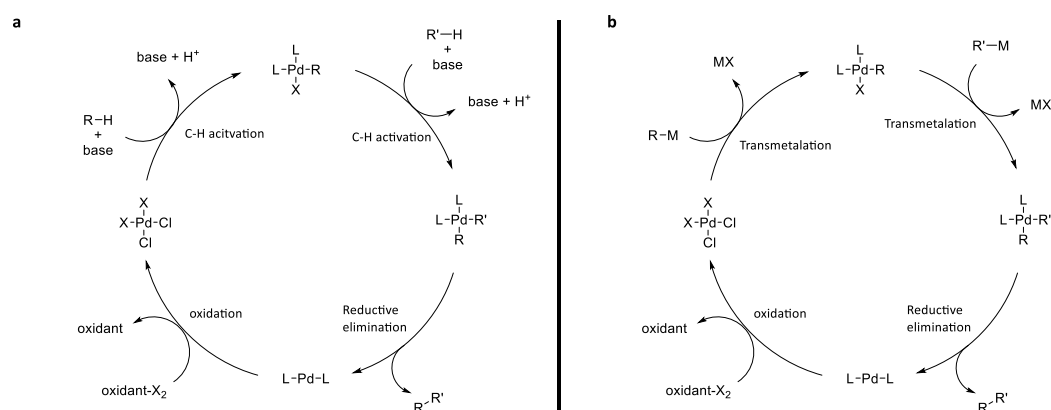
Figure 2 Common directing metalation groups adapted from Paul Krawczuk's "Directed Metalation: A Survival Guide".^[76]

Oxidative coupling

So far, we established the most important factors for successful cross-coupling reactions between a positively polarized reagent (organohalide) and a negatively polarized reagent (organometal). The overall reaction is electroneutral, allowing for the Pd catalyst to switch between the oxidized and reduced form throughout the reaction via the well-established *oxidative addition-transmetalation-reductive elimination* mechanism. However, it is also possible to couple a pair of negatively polarized reactants in a reaction that will formally oxidize one reaction partner and transfer two electrons to the Pd(II) catalyst yielding catalytically inactive Pd(0), hence the name of the reaction: oxidative coupling. The reoxidation of the inactive catalyst to Pd(II) is necessary to keep the reaction electroneutral, yet the exact nature of the oxidation step is not fully understood. The choice of oxidant is not trivial, as will be explained further down, and can alter the reaction pathway and selectivity. Substrates for oxidative couplings are often not prefunctionalized and rely on C-H activation, usually either through oxidative addition, sigma bond metathesis or concerted metalation-deprotonation. In any case a base is necessary to facilitate the deprotonation and increase the rate of reaction.^[77]

Commonly employed organometal reagents include organozinc- and Grignard reagents, but also organotin, -silicon, -indium, and -boranes have been reported in synthesis.^[78] The coupling of mixed systems, that is an organometal and a hydrocarbon, have also been reported in the literature. A mechanism for the coupling of two nucleophiles can be derived from the well-established catalytic cycle

for cross-coupling reactions (Scheme 8). In both cases the catalytic cycle initiated by the coordination of the reagent to Pd(II), either through C-H activation or transmetalation. Another subsequent C-H activation or transmetalation step is followed by reductive elimination of the product. The catalytically inactive Pd(0) species is then reoxidized to start the cycle anew. Oxidative heterocoupling, i.e. the coupling of two different nucleophiles to yield an unsymmetrical product, is one of the major challenges of this methodology to overcome. Selective hetero-double-transmetalation could be achieved when using desyl chloride as an oxidant.^[78–80]



Scheme 8 catalytic cycle for catalytic oxidative coupling ^a through C-H activation and ^b use of organometallic reagents.

Oxidants

The classification of oxidative coupling reactions by the oxidant seems to be the most meaningful, as they have more influence in the reaction mechanism than the metal center itself. The differentiation in metal based and metal free oxidants is a good starting point for further classification. Metal based oxidants are well established, having the advantage of suitable reduction potential and a basic anion that will aid in C-H activation. $[\text{Cu}(\text{OAc})_2]_2$ is the most widely used oxidant,^[77] as Cu(II) has a reduction potential well suited for Ru, Rh and Pd, and the acetate counterions will act as a base in order to activate the reagent. Ag(OAc), as a standalone oxidant or in combination with $[\text{Cu}(\text{OAc})_2]_2$, facilitates the activation of catalyst chloride salts by the formation of insoluble AgCl.^[81] However, the use of stoichiometric amounts of transition metal salts is undesirable both in cost and regarding their environmental impact.

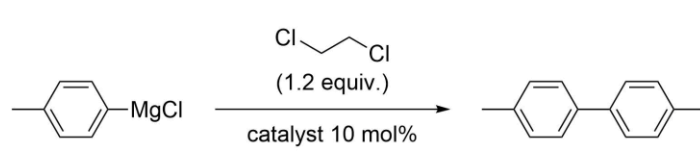
Table 2 Commonly employed oxidants for oxidative coupling reactions.

Metal based oxidants	Metal free oxidants
[Cu(OAc) ₂] ₂	Radical precursor ^[82]
Ag(OAc)	Benzoquinone / O ₂ ^[83]
Cu/Ag mixture	Molecular oxygen (O ₂) ^[82,84]
Cs(OAc) + internal oxidant	(N ₂ O) Laughing gas ^[85]
	Desyl chloride
	Dibromo ethane
	<i>This work:</i> dichloro-ethane

Metal free oxidants are an attractive alternative, producing side products more easily to deal with while on the other hand also having a lower price tag on them. Benzoquinone in combination with an oxidant (e.g. molecular oxygen or electric current) is an attractive system for substrates that are not nucleophilic enough for the attack at the electrophilic C=O bond. Some examples allow for the use of molecular oxygen or air alone, however these examples are scarce. Kiefer *et al* reported the successful oxidative homocoupling of some aryl Grignard reagents mediated by N₂O as an oxidant.^[86] Of the used catalysts they found [Fe(acac)₂] to give the best results of this kind of coupling.

An unwanted reaction in the polymerization of vinyl chlorides is β-Cl elimination.^[77,87-89] Figueroa *et al* showed that hexachloro ethane would undergo oxidative addition followed by β-Cl elimination on a Ni(0) complex.^[90] 1,2-Dichloro-ethane has been used for the catalytic oxidative coupling of aryl Grignard reagents at room temperature, yielding homo-coupled diaryl system (Table 3).^[91,92]

Table 3 Coupling of *p*-tol-MgCl with dichloro-ethane at room temperature.

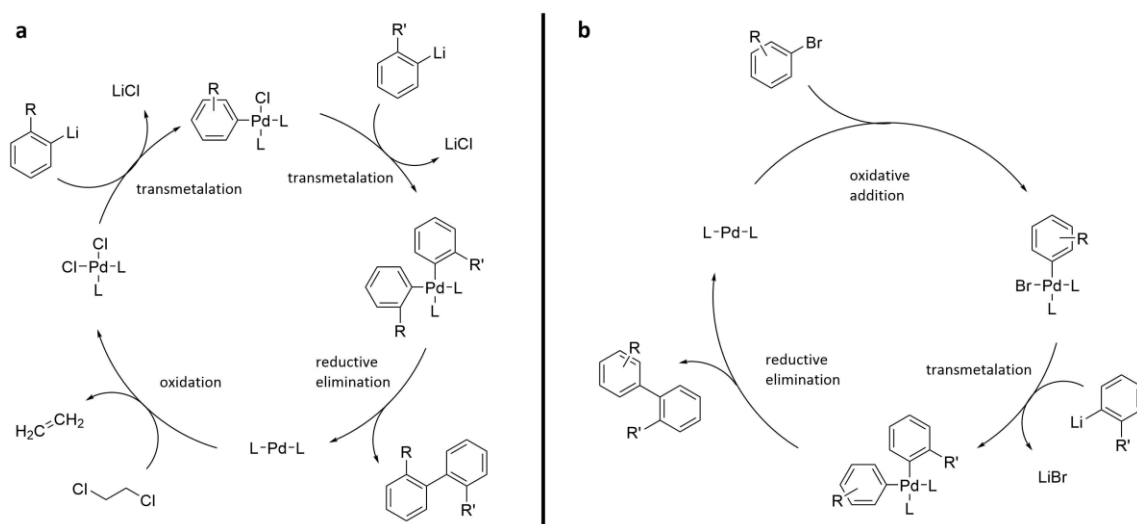
	Entry	Catalyst	Yield (%)
	1	MnCl ₂	96
	2	NiCl ₂	85
	3	CuCl ₂	60
	4	MgCl ₂	30
	5	FeCl ₃	95

Aim of the project

Organometals for cross-coupling are commonly prepared by transmetalation from organolithium or Grignard reagents. This adds at least one more step to any procedure relying on a cross-coupling step. On the bases of the information above we set out to develop a fast and convenient method for the cross-coupling and oxidative coupling of aryllithium compounds (Scheme 9). These would be generated *in-situ* by directed lithiation strategies. In 1975, Murahashi reported the successful coupling of a variety of

alkyllithium reagents with vinyl halides.^[93] However, they had to use stoichiometric amounts of $\text{Pd}(\text{PPh}_3)_4$. We now know well, that $\text{Pd}(\text{PPh}_3)_4$ is ill-suited for more challenging substrates, and rarely gives decent turnovers unless when used in combination with highly reactive organometals. Revisiting these organolithium compounds with today's catalysts might revile new interesting reaction pathways prior thought impossible with these highly reactive reagents.

Feringa *et al* reported the successful and efficient coupling of aryl and alkenyl bromides with aryllithium compounds,^[94–96] however only ever one natural product was prepared by them.^[94] We set out to further proof the applicability of this methodology by synthesizing Arnottin I, employing organolithium cross-coupling chemistry where possible. In addition to that, we worked towards developing a reliable and fast procedure for the catalytic, oxidative coupling of aryllithium compounds. Developing this method would pose a challenge, since publications on this topic are scarce. Our literature research could only bring up one publication from 1998, where stoichiometric amounts of oxovanadium species are used.^[97] Whilst at the end of our optimization process, Liu *et al* published on a method for catalytic oxidative coupling of aryllithium compounds.^[98] Their method uses MnCl_2 as a catalyst and molecular oxygen as an oxidant, however they rely on very low temperatures, and their method is less straight forward and also slower than the method developed by us. Therefore, we believe to still add a valuable contribution to this field.



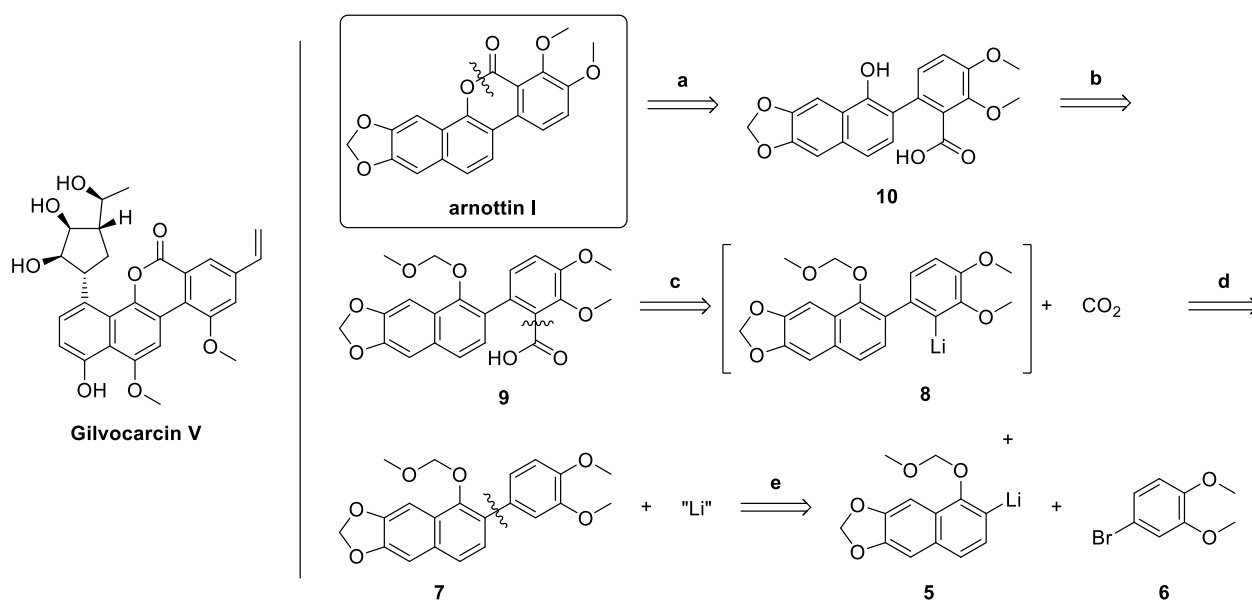
Scheme 9 ^a Catalytic cycle for the oxidative homocoupling of an aryllithium where R and R' are directing groups and 1,2-dichloro-ethane acts as oxidant for the regeneration of catalytically active Pd(II). ^b Catalytic cycle for cross-coupling reactions of *in-situ* generated aryllithium where R' is a directing group with an aryl bromide.

Results

Arnottin

Retrosynthesis

Arnottin I is a natural product found, and isolated from the bark of *Zanthoxylum*^a *arnottianum*,^[99] and shares a key structural feature with the antibiotic drug Gilvocarcin V.^[100] Its structure was determined in 1993,^[99] and since then, several successful strategies for the synthesis of Arnottin I have been published,^[101,102] the latest of which is reported in 2015 by Chad Lewis *et al.*^[103] Scheme 10 details our retrosynthetic analysis for a novel synthesis of Arnottin I. The first disconnection (a) is made at the lactone, arriving at a free carboxylic acid and a naphthol motif (**10**). A protection step (b) to convert alcohol **10** into a methoxy methyl ether (MOM) **9** is then needed, as the next disconnection (c) at the carboxylic acid arrives at the aryllithium species **8**. A retro-directed remote lithiation (d) arrives at a biaryl synthon **7**, that is disconnected at the aryl-aryl bond (e) to arrive at aryllithium **5** and 4-bromoveratrole (**6**).

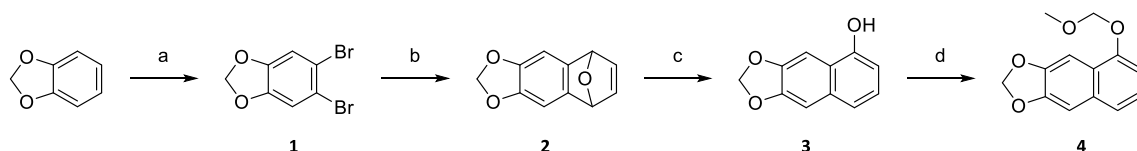


Scheme 10 Retrosynthetic analysis of Arnottin I and structure of Gilvocarcin V.

^a In chemical literature often incorrectly named *Xanthoxylum arnottianum*.

Forward synthesis

The starting material for the synthesis of Arnottin I was prepared according to literature procedures (Scheme 11). A double bromination of benzo dioxole^[104] gave **1**, from which the aryne species was generated and reacted with furan in an Diels-Alder reaction.^[105] Catalytic ring opening of **2** yielded **3**,^[106] which was reacted with chloro methoxy methyl ether (MOMCl) to yield **4**.^[107]

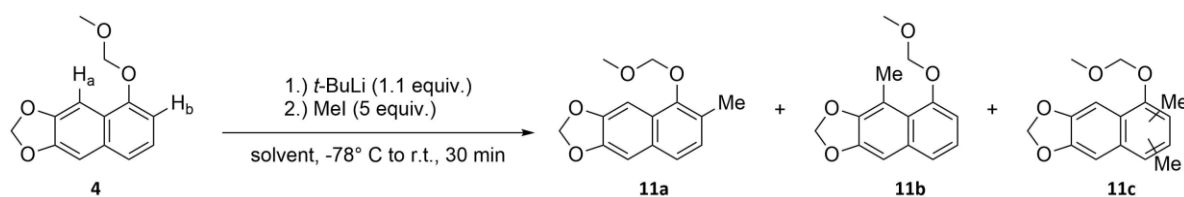


Scheme 11 Synthesis of starting material **4**. a) NBS (2.1 equiv.), TMSCl (0.1 equiv.), MeCN, rt, 16 h, 99 %; b) *n*-BuLi (1.1 equiv.), furan (8 equiv.), toluene/THF (1:7), -78 °C, 30 min then r.t. 2 h, 70 %; c) TsOH (0.2 equiv.), methylene chloride, r.t., 2 h, 66 %; d) NaH (2.2 equiv.), MOMCl (1.8 equiv.), THF, rt, 16 h, 68 %.

Regioselective Lithiation of **4**

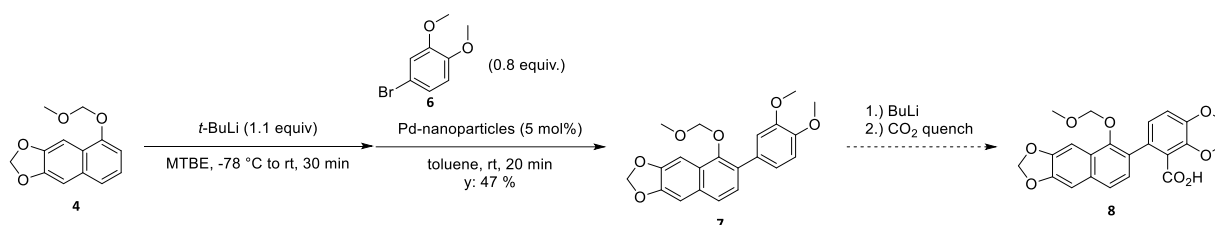
Conditions for the regioselective deprotonation of **4** were investigated. A solution of **4** in dry ethereal solvent was treated with *t*-BuLi, quenched with methyl iodide, and the resulting reaction mixture was analyzed by GC-MS (Table 4). Although *n*-BuLi is preferably used over *t*-BuLi, due to the noticeably higher reactivity of the latter, preliminary experiments with *n*-BuLi as lithium base were unsuccessful. We expect the protons closest to the MOM-ether (H_a and H_b) to be most acidic. Furthermore, we hypothesize that an increasingly bulky solvent would favor the deprotonation of H_b over H_a . When THF was used as (co-)solvent, many unassignable peaks were found in the GC-MS, which are likely associated with the degradation of the solvent. Deprotonation in methyl tertiary butyl ether (MTBE) and diethyl ether are comparable in regioselectivity, though marginally less conversion was detected in the latter. We hypothesize that increasingly bulky solvent would favor the deprotonation of H_b over H_a . In dibutyl ether however, conversion drops significantly, as the steric effect might hinder deprotonation too much.

Table 4 Distribution of the product mixture (given in [%]) found upon quenching lithiated **4** in ethereal solvents (mixtures) with methyl iodide. The structure of **11a** is assumed, as coupling of **4** with **6** gave the desired product **7** as determined by NMR studies. The exact structure of **11b** was not determined by NMR. Values are taken directly from the area under the corresponding peak in the GC-MS chromatogram. No correction factor was taken into account.



entry	Solvent	starting material	(1a)	(11b)	(11c)	non-identified by-product
A	THF	64	15	5	4	12
B	toluene/THF (95:5)	47	21	9	7	16
C	toluene/THF (90:10)	67	4	1	4	24
D	toluene/THF (75:25)	34	4	1	6	55
E	MTBE	9	76	2	12	<1
F	Et ₂ O	15	78	3	12	<1
G	<i>n</i> -Bu ₂ O	36	47	4	13	<1

Forward synthesis



Scheme 12 Cross-coupling of *in-situ* lithiated **4** with **6** to arrive at **7**, and proposed subsequent lithiation and carboxylation to arrive at **8**.

4 was successfully coupled with bromo veratrole (**6**) in a two-step reaction (Scheme 12) to give **7**, employing Pd-nanoparticles as a catalyst.^[51] Lithiation of the cross coupled product in one pot could not be achieved, however. **7** was isolated, and its structure was determined by a 1D-NOESY NMR (Nuclear Overhauser Effect Spectroscopy) experiment (Figure 3). The number, position, multiplicity, and coupling constants of the peaks detected strongly support the successful synthesis of compound **7**.

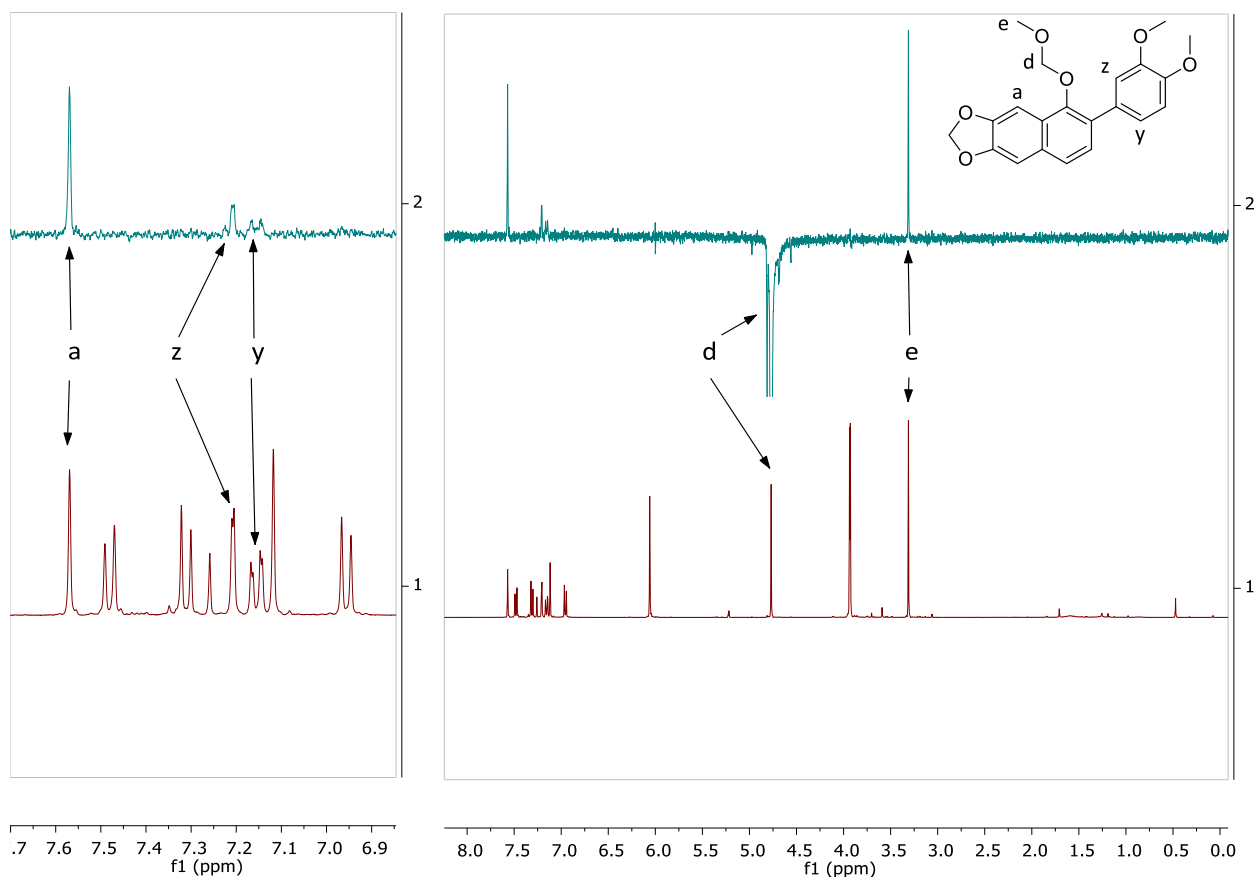
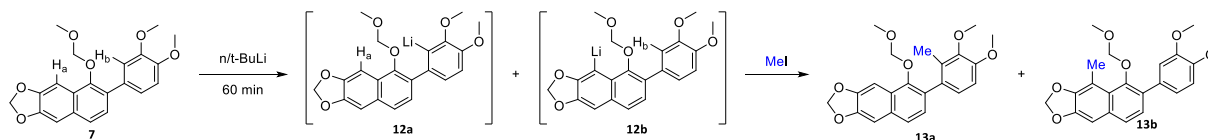


Figure 3 1D-NOESY spectrum stacked on top of a ^1H -NMR spectrum of **7** with a zoomed view of the between 7.7 – 6.9 ppm. Upon irradiation of proton d (s, 4.77 ppm), protons a (s, 7.57 ppm), z (d, 7.21 ppm, $J=2.0$ Hz), y (dd, 7.15 ppm, $J=8.2$ Hz, 2.0 Hz), and e (s, 3.31 ppm) give a signal in the NOESY-spectrum.

Lithiation studies on **7** were performed, varying lithium base, temperature, reaction time and solvent, followed by quenching with methyl iodide. Crude product solutions were analyzed by GC-MS and ^1H -NMR spectroscopy, respectively. As summarized in Table 5, a second lithiation could not be achieved in one pot. Furthermore, attempts to deprotonate H_b selectively over H_a failed. The chemical shift of H_a and H_b have been determined above and can thus be used to determine the structure of **13b** (Figure 4).

Table 5 Findings for the lithiation of **7** and subsequent quench with methyl iodide. Conversion correlates to the area under the peak in the GC-MS chromatogram. No correction factor was taken into account. ^aLithiation was performed in-situ, thus a proper conversion cannot be given. ^bThe product was isolated, and the structure was determined by NMR.



entry	solvent	[min]	[°C]	lithium base	Conversion [%]
A	toluene/MTBE (2:1) ^a	60	-78 to r.t.	<i>t</i> -BuLi	-
C	toluene/MTBE (10/1)	60	-78 to r.t.	<i>n</i> -BuLi	6
D	toluene/MTBE/THF (10:1:5)	60	-78 to r.t.	<i>n</i> -BuLi	12
E	toluene	30	0	<i>n</i> -BuLi	25 ^b

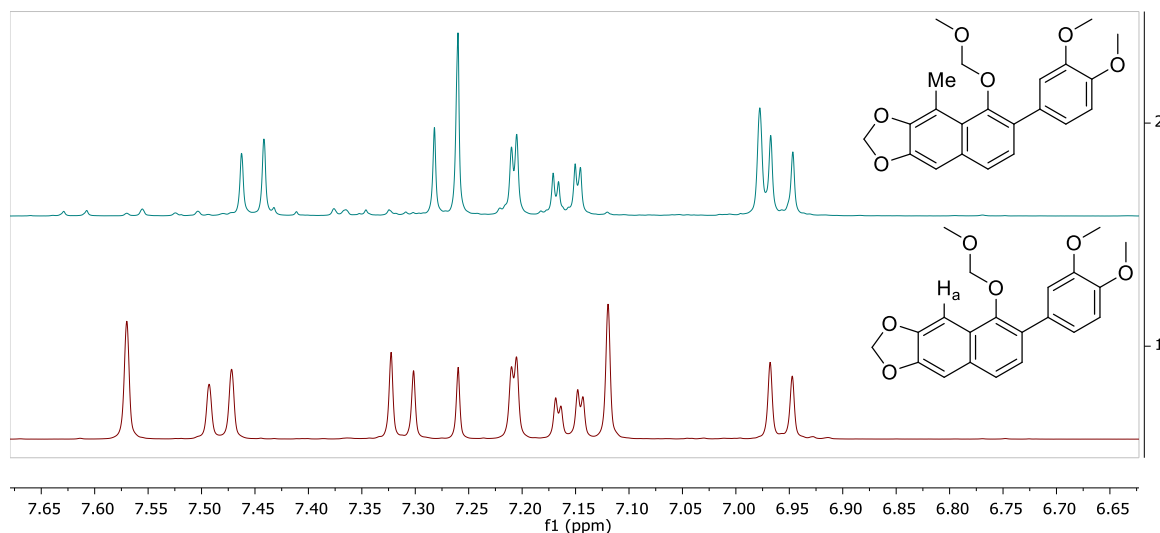
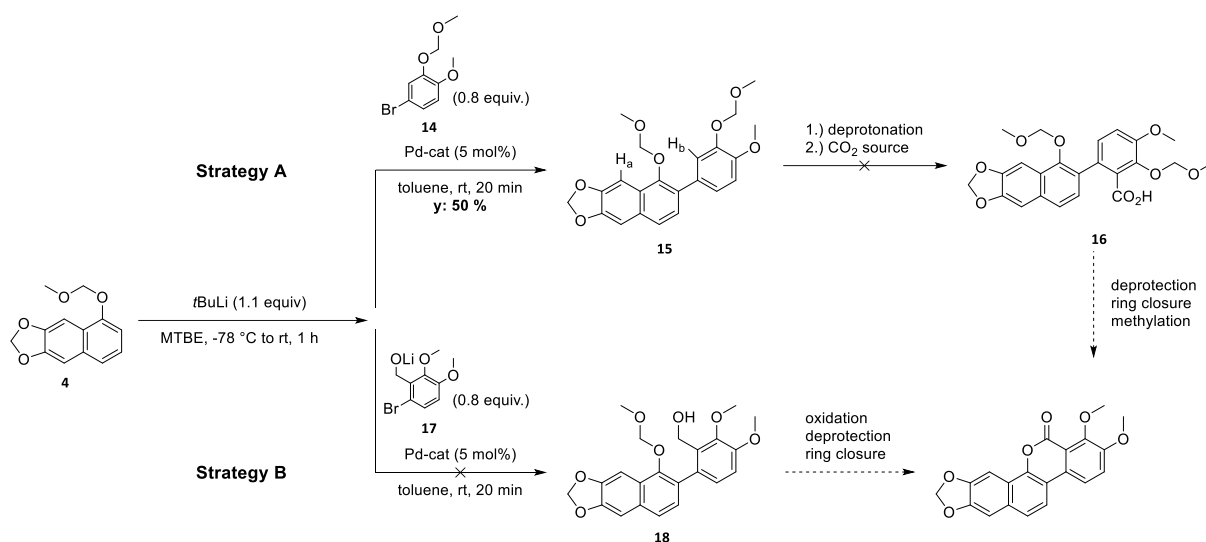


Figure 4 Stacked ¹H-NMR spectra of **13b** on top of **7**. Signal a (7.57 ppm) is missing from the top spectrum, indicating H_a has been substituted by a methyl group.

Alternative route development

Two workaround strategies have been developed to tackle this problem (Scheme 13). Strategy A introduces a MOM-ether in the aryl bromide. A cross-coupling reaction of **4** with **14** yields **15**. We hoped the phenolic MOM-ether would promote *ortho* lithiation, favoring the abstraction of H_b (thermodynamic) over H_a (kinetic). Lithiation studies were done on **15**, but no suitable conditions could be found to promote metalation at the desired position. Thermodynamic deprotonation is favored in apolar solvents at higher temperatures with *n*-BuLi over *t*-BuLi.^[108] However even when compound **15** was lithiated in pure toluene at r.t. with *n*-BuLi. D₂O-quench exclusively led to deuterium incorporation at the thermodynamic site, as indicated by the ²H NMR spectrum (Figure 5).



Scheme 13 Proposed workaround strategies for the synthesis of Arnottin I.

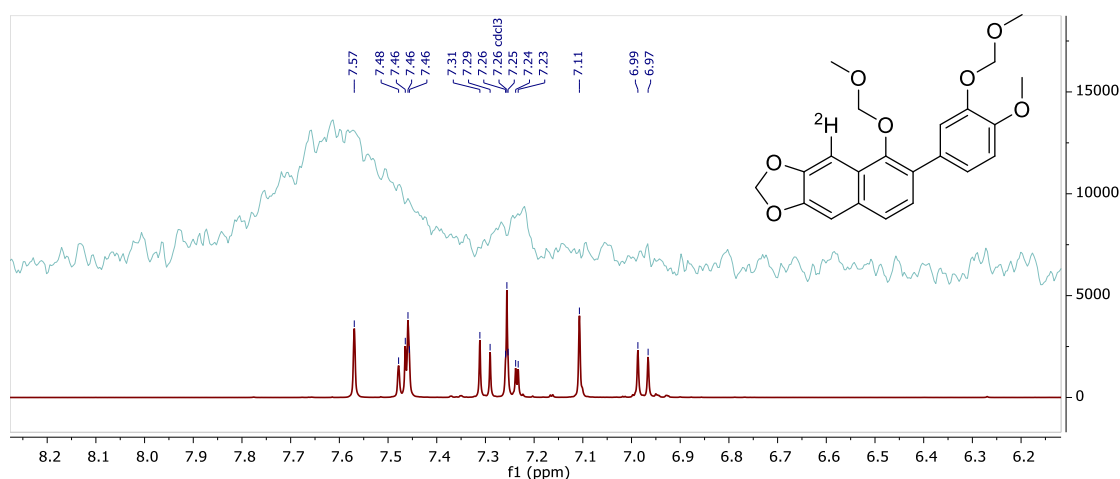
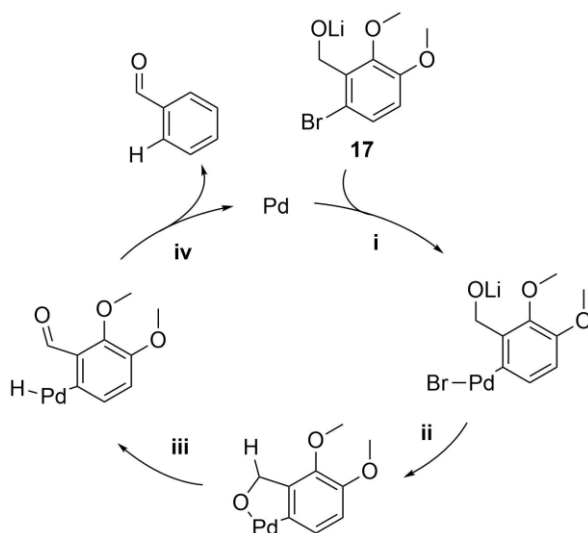


Figure 5. Deuterium NMR of **15** in CHCl₃ stacked on top of a proton NMR spectrum in CDCl₃.

Strategy B introduces a benzylic alcohol function in the aryl bromide **17**, followed by selective oxidation to the carboxylic acid.^[109,110] Deprotection of the MOM-ether and subsequent Fischer esterification to form the lactone in a cascade reaction would then yield Arnottin I. This route however failed in the cross-coupling step, due to the degradation of the aryl bromide. We propose a decomposition mechanism starting with an oxidative addition of the Ar-Br bond to the Pd-catalyst, followed by an intramolecular transmetalation from the lithium alkoxide. A β -hydride elimination converts the benzylic alcohol into a benzaldehyde, after which reductive elimination regenerates the catalyst.



Scheme 14 decomposition of **17** through (i) oxidative addition (ii) transmetalation (iii) beta-hydride elimination and (iv) reductive elimination to the corresponding benzaldehyde.

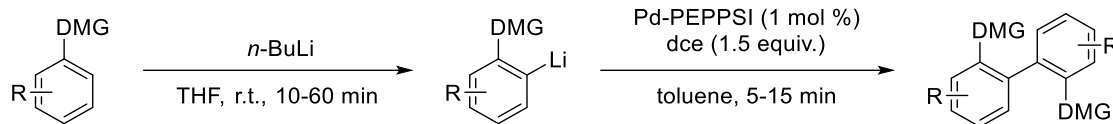
Although certainly Arnottin I could be obtained through means of aryllithium cross-coupling, we decided to abandon the project at this point. Additional protective groups would introduce at least two more steps, taking away much of the elegance of initial proposal and making this synthesis route unattractive compared to previously published ones.

Oxidative homo-coupling of aryllithium compounds

Method development

Oxidative homo-coupling of organolithium compounds have only been scarcely described in literature. Attempts at this have been made as early as 1998, using stoichiometric amounts of oxovanadium.^[97] Whilst we were developing our method for the what we thought was the first report of catalytic, oxidative homo-coupling of aryllithium compounds, Liu *et al* published on Mn catalyzed homo-coupling of *in-situ* generated organolithium reagents.^[111] Their method involves manganese oxide which is significantly less expensive than the Pd-PEPPSI catalysts. However, it is a two-step procedure and the reported substrate scope so far only contains three heterocycles.

We developed a method which allows for clean and fast coupling of aryllithium compounds at room temperature in up to quantitative yield without a tedious workup. A catalytic system was chosen consisting of Pd-PEPPSI IPent and Pd-PEPPSI SIPr (Table 6) catalyst, respectively, and dichloro-ethane (dce) as oxidant.

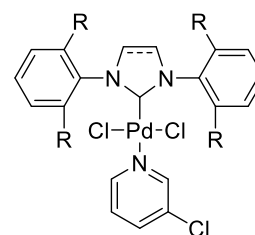


Scheme 15 General approach for the palladium-catalyzed homo-coupling of *in-situ* generated aryllithium compounds.

Aryllithium species are most commonly obtained either through lithium halogen exchange, or through direct deprotonation. The latter is done by exploiting directing metalation groups on the aromatic ring. These are usually lone pair donors, that will coordinate to the Li⁺ ion, thus directing the organolithium base towards deprotonating a proton near the directing group. MOM-protected α -naphthol (**19**) was chosen as a model substrate for the optimization of our method. We found, that **19** will fully convert to the aryllithium species within minutes at room temperature, when treated with *n*-BuLi in THF, crushing out as a colorless precipitate. The precipitate was dissolved by the addition of dry toluene, catalyst was added, followed by dichloro-ethane. Reactions carried out in pure THF were unsuccessful, as test experiments revealed. Table 6 summarizes our optimization process leading to optimal conditions: a reaction that can be done within minutes at room temperature. Upon addition of dichloro-ethane, the reaction mixture turned to pale yellow suspension within seconds, as LiCl precipitates from the solution, driving the reaction forward. When done on a bigger scale (5 mmol) the reaction proved to be highly exothermic. Gas formation could also be observed which is in agreement with the mentioned mechanism where ethylene gas is released. In control experiments with either no catalyst or no dichloro-ethane no conversion could be detected by GC-MS.

Table 6 Optimization table for the catalytic, oxidative coupling of methyl methoxy naphthol. All reactions are carried out on 1 mmol scale. Values for the conversion are calculated from the area under the peak in the GC-MS chromatogram. No correction factor was taken into account.

Entry	Pd-PEPPSI	cat-loading (mol%)	addition time (min)	T (°C)	conversion (%)
A	IPent	10	60	rt	93
B	IPent	5	30	40	96
C	IPent	2.5	45	40	88
D	IPent	1	30	40	80
E	IPent	1	5	40	92
F	IPent	1	direct	40	90
G	IPent	1	direct	rt	95
H	SIPr	10	60	rt	73
I	SIPr	5	30	40	84
J	SIPr	1	direct	r.t.	88



Pd-PEPPSI IPent: R = IPent, hashed is double bond

Pd-PEPPSI SIPr: R = IPr, hashed bond saturated

With the optimized conditions for both Pd-PEPPSI IPent (entry G), and Pd-PEPPSI SIPr (entry J) catalysts the applicability of this methodology was explored (Figure 6). When Pd-PEPPSI IPent was used, excellent yields were obtained for the homo-coupling of MOM-phenol (**20**) and MOM-naphthol (**21**). We found that Pd-PEPPSI SIPr consistently gave lower conversions than Pd-PEPPSI IPent, making us focus more on the latter.

The dimers **20** and **21** were obtained in similarly excellent yield. Although sterically less demanding, the dimerization of lithiated anisole was less successful. The lithiation of anisole is reported^[112] to be less trivial compared to the MOM-aryls, which explains the discrepancy. A larger excess of *n*-BuLi or addition of TMEDA would possibly help to quantitatively lithiate anisole.

We were particularly interested in the homo-coupling of thiophenes as oligothiophenes are widely used in material science.^[113–115] Using our methodology thiophenes dimers can be obtained (**23** and **25**). For the synthesis of **23** commercially available 2-thienyllithium solution was used. The degree of degradation of 2-thienyllithium was not determined, and instead the concentration given on the bottle was assumed to be correct. More interestingly, despite the insoluble nature of the lithiated dimers of **23** and **25**, it could still be converted into the its corresponding tetramer (**24** and **26**).

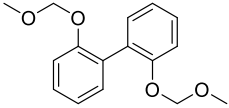
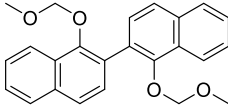
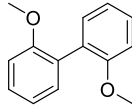
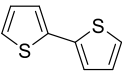
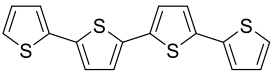
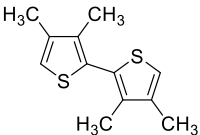
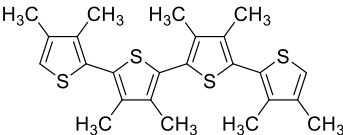
			
	20	21	22
Pd PEPPSI-IPent	92 %	97 %	60 %
Pd PEPPSI-SIPr	50 %	69 %	43 %
			
	23	24	25
Pd PEPPSI-IPent	^a 45 %	^b no yield determined	96 %
Pd PEPPSI-SIPr	-	-	32 %
			
			26
			76 %

Figure 6 Products obtained with optimized conditions for oxidative homo-coupling reactions with Pd-PEPPSI IPent. Yield in parentheses for when Pd-PEPPSI SIPr was used. ^a Commercially available thionyl lithium solution (1M in hexanes/THF) was used. ^b Due to time limitations and troublesome workup, a yield cannot be given (GC-MS conversion 96%).

Temperature Studies

We were interested in possibility of low temperature catalytic oxidative homo-coupling of aryllithium reagents. This would possibly broaden the functional group tolerance, hoping the coupling reaction

could outpace nucleophilic attack of the aryllithium to a carbon electrophile. To a solution **27** in THF *n*-BuLi was added at room temperature. Toluene and catalyst were added, and the reaction vessel was cooled down to -80 °C. Dichloro-ethane was added, and the mixture was stirred for 30 minutes before taking a sample. The sample was quickly quenched by the addition of methanol and checked for conversion by GC-MS. The cooling bath was warmed stepwise, and the process was repeated until room temperature was reached. In addition to the expected signal for the homo coupled product **20**, a peak was detected with an *m/z* value correlating with **28** in the GC-MS chromatogram (Figure 7).

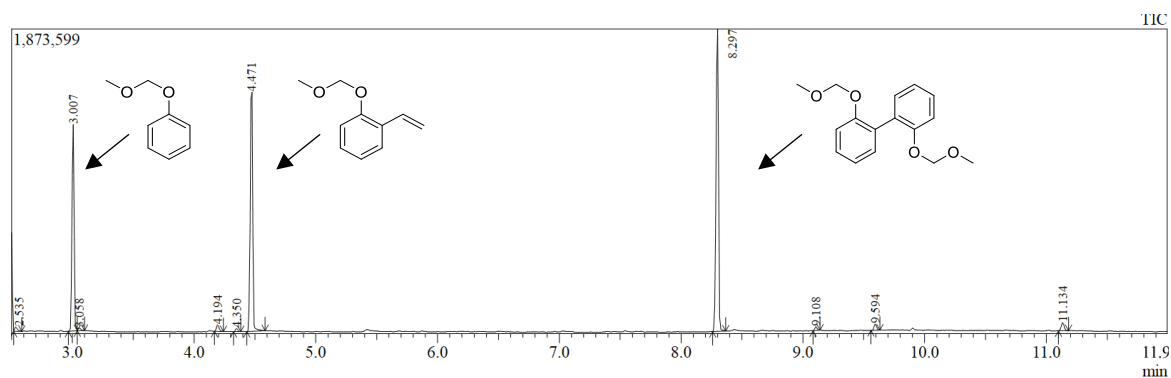


Figure 7 GC-MS of entry H in Table 7 showing the distribution of **27** : **28** : **20** with peaks indicated with the corresponding molecular structure.

Table 7 Distribution of MOM-phenol (**27**) to styrene **28** to MOM-phenol dimer **20** found at a given temperature in %. Values are calculated from the area under the peak in the GC-MS chromatogram. No correction factor was taken into account.

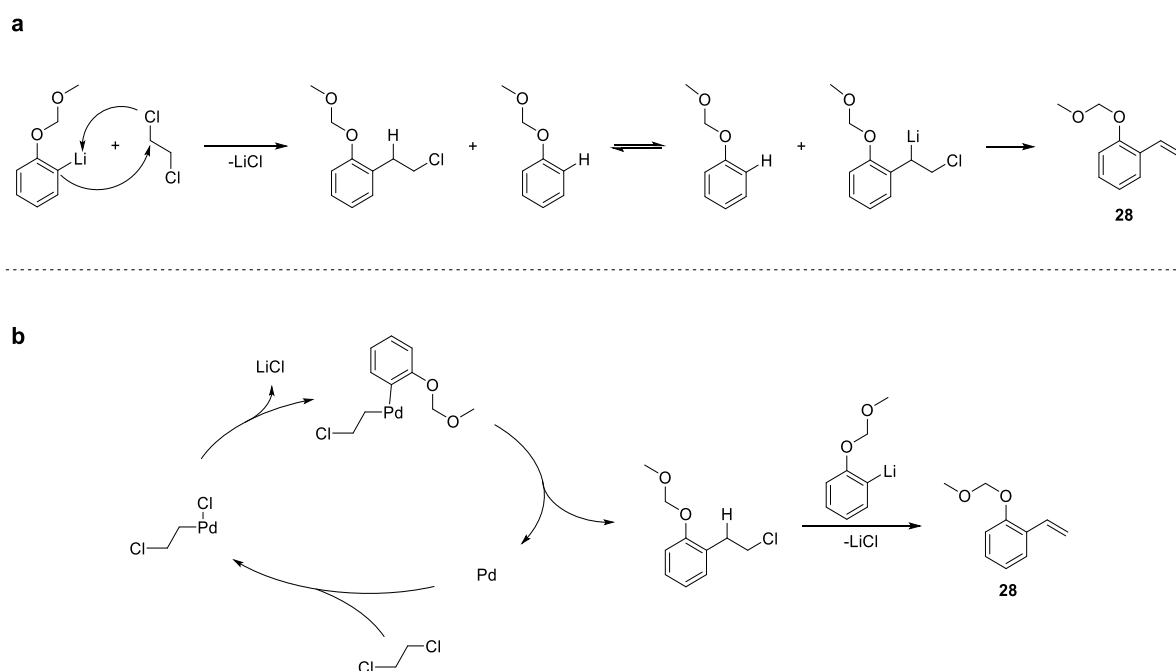
entry	bath temp. (°C)	IPent	SIPr
		27 : 28 : 20	27 : 28 : 20
A	-80	97 : <1 : 1	97 : <1 : <1
B	-70	95 : <1 : 2	97 : <1 : <1
C	-55	97 : <1 : 2	97 : <1 : <1
D	-40	98 : <1 : 1	97 : <1 : <1
F	-30	92 : 3 : 3	97 : <1 : <1
G	-20	76 : 13 : 8	91 : 3 : 1
H	0	10 : 16 : 73	23 : 32 : 39
I	r.t.	10 : 15 : 73	23 : 32 : 38

For the formation of this product we propose two mechanisms: a palladium independent, and a palladium dependent cross-coupling pathway (Scheme 16).

In the palladium independent mechanism dichloro-ethane is attacked by the lithiated MOM-naphthol in an S_N2 reaction (Scheme 16a). The newly generated benzylic proton is acidic, thus immediately deprotonated by another molecule of lithiated **27**. Olefin formation through elimination of LiCl irreversibly then generates the styrene derivative. This hypothesis could be tested by repeating the

experiment but without the addition of catalyst. Precautions must be made so to ensure there are no traces of palladium left (e.g. adsorbed on improperly washed glass equipment, or stirring bars).^[116]

Another possible alternative pathway would involve the cross-coupling of dichloro methane with an equivalent of lithiated MOM-phenol (Scheme 16b). Decomposition seems to start at the same temperature at which the homo-coupling reaction starts to proceed, suggesting the involvement of the palladium catalyst. The cross coupled product would again contain an acidic benzylic proton, which can undergo the same deprotonation-elimination process as described above. Possibly at lower temperatures lithiated MOM-phenol is present as aggregates or coordinated in another way that prevent it from undergoing a transmetalation. Upon raising the temperature, the dissociation energy is provided, thus the reaction takes place. Li-NMR experiments could be used to gain more information on the nature of lithiated MOM-phenol at low and ambient temperatures.

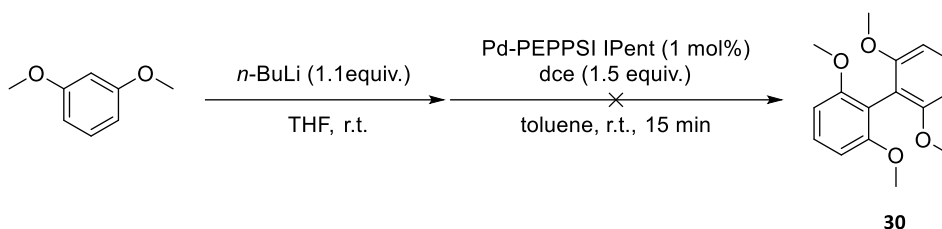


Scheme 16 Proposed mechanisms for the formation of **28** by a) a palladium-independent mechanism and b) a palladium-dependent mechanism.

Sterically hindered substrates

1,3-dimethoxybenzene posed as a model substrate for the development of reaction conditions suitable for the oxidative homo-coupling of sterically hindered substrates. When treated with *n*-BuLi in THF or diethyl ether 1,3-dimethoxybenzene is converted to the corresponding lithium-bis-*ortho*-dimethoxybenz-2-ide species (Scheme 17). However, the conditions developed above were not suitable to this

substrate in order to reach efficient product formation. We hypothesized a significant increase in conversion and reproducibility could be achieved by applying a reversed addition strategy. Yet, adding a suspension of aryllithium in toluene to a solution of catalyst and dichloroethane in toluene would give mediocre conversions at best at high catalyst loadings (Table 8). We were puzzled why the reaction will not go to completion, but experiments on oxidative hetero coupling revealed the catalyst might be deactivated.^b



Scheme 17 Desired dimerization of 1,3-dimethoxy benzene to form the sterically congested dimer **30**.

Furthermore, in the GC-MS chromatogram of crude product mixtures, we were able to assign a signal to the m/z of a coupling product between toluene and 1,3-dimethoxy benzene. We investigated the effect of toluene as a possible factor in the inhibition of coupling. Conversion was barely affected by varying the amount of toluene in a suspension of Pd-catalyst in hexane and dichloro-ethane, however. Exchanging toluene for a mixture of hexane and THF massively inhibited conversion. These control experiments let us to suggest, that the presence of THF will promote a pathway, that will render the catalyst inactive, thus lowering the conversion. Another explanation would be the presence of unreacted n -BuLi, decomposing the catalyst. Due to time limitations, the deactivation mechanism could not be further investigated, but solving this issue could be crucial for the development of a coupling procedure for sterically hindered substrates.

A way of quantifying the longevity of a catalyst is the turnover number (TON), which gives the mean number of converted product molecules per molecule of catalyst before the latter is deactivated or decomposes. With the above insights, we arrived at conditions with the highest TON. 1,3-dimethoxy benzene was lithiated in diethyl ether, followed by removal of the ethereal solvent in vacuo, before diluting it in dry toluene, and adding the aryllithium mixture over 5 minutes to a suspension of Pd-PEPPSI IPent (2.5 mol%) in hexane/dichloro-ethane at 60 °C. A conversion of 54 % was determined by

^b To a freshly prepared reaction mixture of lithium 1,3-dimethoxy benz-2-ide, Pd-PEPPSI IPent and dichloro ethane in toluene were added. Then phenyl lithium was added. In the product mixture no biphenyl was found, which otherwise would couple easily. This is an indication for deactivation of the catalyst.

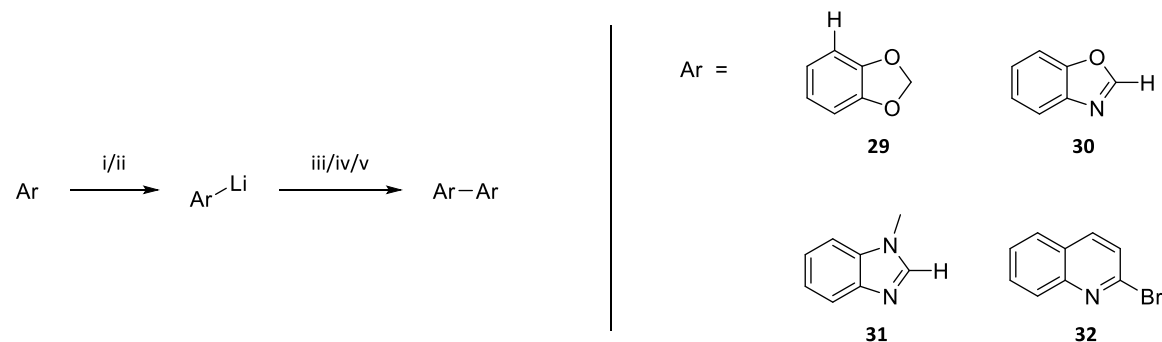
NMR, arriving at TON = 21.6. This rather poor TON shows the need for the determination of the mechanism by which the catalyst is deactivated in this reaction.

Table 8 Optimization table for the catalytic, oxidative homo-coupling of lithium 1,3-dimethoxy benz-2-ide employing reversed addition strategy. Values are calculated from the area under the peak in the GC-MS chromatogram. No correction factor was taken into account.

entry	cat-loading (mol%)	addition time (min)	temp. (°C)	conversion (%)
A	5	5	50	64
B	5	10	50	60
C	5	15	50	42
D	5	20	50	45
E	5	30	50	34
F	5	5	50	52
G	5	5	60	66
H	2.5	5	60	26
I	1	5	60	10
J	5	5	70	61

Preliminary Results

Expansion of the substrate scope to benzodioxole and *N*-heterocycles was upon the last things we attempted, and therefore only preliminary GC-MS data can be presented. The lithiation of these compounds is less straight forward than with the substrates presented so far. Benzodioxole will decompose to catechol and various butyl adducts when treated with *n*-BuLi or *t*-BuLi as found by GC-MS analysis.^[117] *N*-heterocyclic compounds on the other hand are easily deprotonated, and compounds **30**,^[118] **31**,^[119] and **32**^[120,121] have been lithiated and used in synthesis at low temperatures. However, as mentioned *vide supra* dimerization of **27** only occurred at ambient temperatures.



Scheme 18 Dimerization of substrates **29-32**. i) THF, Li-base, -78 °C, 30 min. ii) THF, Li-base, r.t., 20 min. iii) Pd-PEPPSI IPent (0.01 equiv.), dce (1.5 equiv.), toluene, -78 °C to r.t., 60 min. iv) Pd-PEPPSI IPent (0.01 equiv.), dce (1.5 equiv.), toluene, r.t., 15 min. v) Pd-PEPPSI IPent (0.01 equiv.), dce (1.5 equiv.), toluene, 40 °C, 15 min.

We attempted to lithiate substrates **29-32** at low temperature, then adding toluene, Pd-PEPPSI IPent catalyst and dichloro-ethane, before letting the mixture gradually warm up to r.t. (Table 9). This strategy was only partly successful for the dimerization of **30** and **32**. For the dimerization of **30** in particular entries C-F show that dimerization at lower temperatures results in lower conversion.

For a more generalized statement, more data must be gathered, and further experimentation will show if even these challenging compounds can be dimerized. From the data presented in this chapter, we can infer that lower temperatures will favor side-reactions with dichloro-ethane. Control experiments with other oxidants might reveal further insights in this manner. As was the case for 1,3-dimethoxy benzene, reversed addition might be a key strategy to increase conversion also in these compounds.

Table 9 Preliminary results for the coupling of substrates **29-32**. Conversion values are calculated from the area under the peak in the GC-MS chromatogram. No correction factor was taken into account. ^a Side products account for less than 5 % in the GC-MS chromatogram.

entry	Ar	Li-base (equiv.)	deprotonation conditions	dimerization conditions	conversion to dimer [%]
A	29	<i>n</i> -BuLi(1.1)	r.t., 20 min	r.t., 15 min	16
B	29	<i>t</i> -BuLi(1.1)	-78 °C, 30 min	-78 °C to r.t, 1 h	<1
C	30	<i>n</i> -BuLi(1.1)	-78 °C, 30 min	-78 °C to r.t, 1 h	8 ^a
D	30	<i>n</i> -BuLi(1.1)	r.t., 20 min	r.t., 15 min	66 ^a
E	30	<i>n</i> -BuLi(1.1)	r.t., 20 min	40 °C, 15 min	50 ^a
F	30	<i>n</i> -BuLi(1.1)	-78 °C, 30 min	r.t., 15 min	26 ^a
G	31	<i>n</i> -BuLi(1.1)	-78 °C, 30 min	-78 °C to r.t, 1 h	8
H	32	<i>t</i> -BuLi (2.2)	-78 °C, 30 min	-78 °C to r.t, 1 h	35

Conclusions and Prospect

We were able to successfully couple aryllithium compound **5** with bromo veratrole catalyzed by Pd-nanoparticles in toluene. The subsequent steps to obtain Arnottin however were unsuccessful, and we decided to abandon that project. The development of a method for the oxidative homo-coupling of *in-situ* generated aryllithium compounds was fruitful. We present a procedure to cleanly and quickly form C-C bonds from C-Li precursors in toluene with Pd-PEPPSI IPent, and Pd PEPPSI SIPr. This is done by employing oxidative homo-coupling with dichloro-ethane as an oxidant. Further development of the procedure to expand the substrate scope to heterocycles is highly anticipated, as is the development of oxidative hetero-coupling aryllithium compounds.

Experimental

All air-sensitive reactions were carried out under a nitrogen atmosphere using flame dried glassware employing standard Schlenk techniques. THF and toluene were dried and distilled over sodium. Thin layer chromatography: Merck silica gel 60, 0.25 mm. Compounds were visualized by UV, potassium permanganate, or Seebach staining solution. GC-MS (GC: HP6890; MS: HP5973) with an HP1 or HP5 column (Agilent Technologies: Palo Alto, Ca) was used for reaction and conversion control. Mass spectra were recorded on an AEI-MS-902 mass spectrometer (ES+), LTQ Orbitrap XL (ESI+ or ESI-). ^1H and ^{13}C -NMR were recorded on a Varian AMX400 (400 and 100.59 MHz, respectively). Chemical shift values are reported in ppm with the solvent resonant peak posing as the internal standard and are given in format: chemical shift (multiplicity, coupling constant in Hz, integration). Multiples are abbreviated as follows: s = singlet, d = doublet, t = triplet, q = quartet, br = broad, m = multiplet. All starting materials were purchased from common chemical suppliers and used without further purification.

General procedure for oxidative coupling of unhindered compounds (**20** - **26**):

In a flame dried, nitrogen flushed Schlenk tube was added *n*-BuLi (1.1 mmol, 1.6 M in hexanes) to a stirred solution of substrate (1 mmol) in THF (500 μL) at room temperature (**20-22**), or 0 $^\circ\text{C}$ (**23-26**), respectively. The mixture was stirred until lithiation was complete, dry toluene (5 mL) was added, followed by Pd-PEPPSI IPent (7.9 mg, 0.01 mmol) and then dichloro-ethane (120 μL , 1.5 mmol) in one portion. The reaction mixture was stirred for 15 minutes, during which a colorless precipitate formed. The product mixture was quenched by the addition of few drops of MeOH, filtered through a plug of silica, and the solvent was evaporated under reduced pressure.

5,6-dibromobenzo[d][1,3]dioxole (**1**)

Benzo-1,3-dioxole (2.00 g, 16.4 mmol) were dissolved in acetonitrile (150 mL), and NBS (6.12 g, 34.4 mmol) was added, followed by TMSCl (100 μL , 8.2 mmol), upon which the solution turned yellow. After 16 h, the solution was quenched by the addition aqueous sodium metabisulfite solution (3 mL). The mixture was reduced to a volume of about 50 mL, and the formed precipitate was redissolved by the addition of methylene chloride. The solution was washed with water, extracted with methylene chloride (3 x 20 mL), and the combined organic phases were washed with brine, and dried over MgSO_4 . Removal

of the solvent under reduced pressure gave 4.575 g (99 %) of **1** as colorless solid. The crude product was recrystallized from ethanol.

5,8-dihydro-5,8-epoxynaphtho[2,3-d][1,3]dioxole (**2**)

A flame dried Schlenk flask was charged with **1** (2.98 g, 10.6 mmol), evacuated and flushed with nitrogen three times. Furan (15 mL) and tetrahydrofuran (15 mL) were added, the solution was cooled to -78 °C and *n*-BuLi (1.6 M in hexane, 7.5 mL) was added dropwise over 10 minutes. The yellow solution was stirred at -78 °C for 10 min, the cooling bath was removed, and the reaction vessel was allowed to warm to room temperature. After 2 h, the solution was quenched by the addition of water (20 mL) and extracted with methylene chloride (3 x 20 mL). The combined organic phases were washed with brine, dried over MgSO₄, and the solvent was evaporated under reduced pressure. The crude product was recrystallized from ethanol and subsequently washed with pentane (3 x 10 mL) to give **2** in 57 % yield.

¹H NMR (400 MHz, cdcl₃) δ = 7.04 (t, *J*=1.0, 2H), 6.83 (s, 2H), 5.94 (d, *J*=1.4, 1H), 5.89 (d, *J*=1.4, 1H), 5.64 (s, 2H).

naphtho[2,3-d][1,3]dioxol-5-ol (**3**)

To a stirred solution of **2** (850 mg, 1.59 mmol) in methylene chloride (40 mL) was added *p*-toluene sulfonic acid monohydrate (61 mg, 0.32 mmol). The solution was stirred at rt for 2 h and then quenched by the addition of water (10 mL). The phases were separated, the aqueous phase was extracted with methylene chloride (3 x 10 mL). The combined organic phases were poured onto aqueous NaOH (1 M, 5 mL), the phases were separated, and the aqueous phase was acidified by the addition of aqueous 1 M HCl. Methylene Chloride was added to dissolve the precipitate, the phases were separated, and the aqueous phase was extracted with methylene chloride (3 x 10 mL). The combined organic phases were dried over MgSO₄ and the solvent was evaporated under reduced pressure to give 617 mg (73 %) as a colorless solid. The crude product was used without further purification.

¹H NMR (400 MHz, cdcl₃) δ = 7.48 (s, 1H), 7.26 (d, *J*=3.3, 1H), 7.15 (dd, *J*=8.2, 7.5, 1H), 7.09 (s, 1H), 6.69 (dd, *J*=7.5, 1.0, 1H), 6.04 (s, 2H), 5.01 (s, 1H).

5-(methoxymethoxy)naphtho[2,3-d][1,3]dioxole (**4**)

To a suspension of NaH (842 mg, 60 weight% in mineral oil, 21.1 mmol) in dry THF was added **3** (1.80 g, 9.57 mmol), and after 10 minutes of stirring MOMCl (815 μL, 10.53 mmol) was added. After stirring for 16 h, the reaction mixture was quenched with aqueous NaOH (1M, 5 mL), the phases were separated,

and the aqueous phase was extracted with diethyl ether (3 x 5 mL). The combined organic phases were washed with brine, dried over MgSO₄ and the solvent was evaporated under reduced pressure. Final purification by SiO₂ flash chromatography gave 1.52 g (68 %) of **4** as a colorless solid.

mp 64.9 °C

¹H NMR (400 MHz, cdcl₃) δ = 7.56 (s, 1H), 7.32 (dt, *J*=8.2, 1.0, 1H), 7.22 (t, *J*=7.9, 1H), 7.09 (s, 1H), 6.99 (dd, *J*=7.7, 1.1, 1H), 6.04 (s, 2H), 5.35 (s, 2H), 3.54 (s, 3H). ¹³C NMR (101 MHz, cdcl₃) δ = 152.6, 148.0, 147.5, 131.9, 124.6, 122.6, 120.9, 107.4, 103.9, 101.1, 98.9, 95.0, 77.5, 77.2, 76.8, 56.4.

HRMS: *m/z* calc. for C₁₃H₁₂O₄H [M+1]: 233.08084; found: 233.08061.

6-(3,4-dimethoxyphenyl)-5-(methoxymethoxy)naphtho[2,3-d][1,3]dioxole (**7**)

A flame dried, N₂ flushed Schlenk flask was charged with **4** (30 mg, 0.129 mmol), MTBE (1.0 mL) was added, and the solution was cooled to -78 °C. *t*-BuLi (1.7 M in pentane, 85 μL, 0.14 mmol) were added dropwise, the cooling bath was removed, and the reaction mixture was stirred at room temperature for 30 min. The reddish slurry was diluted in toluene to a volume of 5 mL and was added to a solution of **1** (30 mg, 0.15 mmol) and Pd-nanoparticles (5 mol%) in toluene (1 mL) via syringe pump over 30 minutes. After complete addition the solution was quenched by the addition of water (10 mL), the phases were separated, and the aqueous phase was washed with ethyl acetate (3 x 10 mL). The combined organic phases were washed with brine, dried over MgSO₄, and the solvent was evaporated under reduced pressure. Purification by SiO₂ flash chromatography (pentane/ethyl acetate 95:5 to 85:20) gave 22 mg (47 %) of **7** as a colorless solid.

¹H NMR (400 MHz, cdcl₃) δ = 7.57 (s, 1H), 7.48 (d, *J*=8.4, 1H), 7.31 (d, *J*=8.4, 1H), 7.21 (d, *J*=2.0, 1H), 7.16 (dd, *J*=8.2, 2.0, 1H), 7.12 (s, 1H), 6.96 (d, *J*=8.3, 1H), 6.06 (s, 2H), 4.77 (s, 2H), 3.94 (s, 3H), 3.93 (s, 3H), 3.31 (d, *J*=0.6, 3H). ¹³C NMR (101 MHz, cdcl₃) δ = 149.7, 148.8, 148.4, 148.3, 148.0, 132.0, 131.4, 129.0, 127.2, 126.0, 123.4, 122.0, 113.1, 111.3, 103.9, 101.3, 99.6, 99.4, 77.5, 77.2, 76.8, 57.9, 56.1, 56.1.

6-(3,4-dimethoxyphenyl)-5-(methoxymethoxy)-4-methylnaphtho[2,3-d][1,3]dioxole (**13b**)

¹H NMR (400 MHz, cdcl₃) δ = 7.45 (d, *J*=8.4, 1H), 7.28 (s, 1H), 7.21 (d, *J*=1.9, 1H), 7.16 (dd, *J*=8.2, 2.0, 1H), 7.00 – 6.92 (m, 2H), 6.04 (s, 2H), 4.64 (s, 2H), 3.94 (s, 6H), 3.08 (s, 3H), 2.78 (s, 3H).

4-bromo-1-methoxy-2-(methoxymethoxy)benzene (**14**)

To a solution of 4-bromo-2-methoxy phenol (1.94 g, 9.65 mmol) and diisopropyl ethyl amine (3.32 mL, 33.8 mmol) in dry methylene chloride (20 mL), chloromethoxy methane (0.953 mL, 12.9 mmol) was

added at 0° C under N₂ atmosphere. After complete addition, the cooling bath was removed, and the solution was stirred at rt for 16 h. The reaction was quenched by the addition of water (20 mL), the phases were separated, and the aqueous phase was extracted with methylene chloride (3 x 15 mL). The combined organic phases were washed with brine, dried over MgSO₄, and the solvent was evaporated under reduced pressure. Purification by SiO₂ flash chromatography (pentane/ethyl acetate 95:5) gave 2.16 g (90 %) of 14 as a colorless oil.

¹H NMR (400 MHz, cdCl₃) δ = 7.29 (d, *J*=2.4, 1H), 7.10 (dd, *J*=8.6, 2.3, 1H), 6.76 (d, *J*=8.6, 1H), 5.21 (s, 2H), 3.85 (s, 3H), 3.51 (s, 3H).

6-(4-methoxy-3-(methoxymethoxy)phenyl)-5-(methoxymethoxy)naphtho[2,3-d][1,3]dioxole (15)

A flame dried, N₂ flushed Schlenk flask was charged with 4 (115 mg, 0.495 mmol), MTBE (1.5 mL) was added, and the solution was cooled to -78 °C. *t*-BuLi (1.7 M in pentane, 320 μL, 0.544 mmol) were added dropwise, the cooling bath was removed, and the reaction mixture was stirred at room temperature for 30 min. The reddish slurry was diluted in toluene to a volume of 15 mL and was added to a solution of 14 (94 mg, 0.381 mmol) and Pd-nanoparticles (5 mol%) in toluene (1 mL) via syringe pump over 30 minutes. After complete addition the solution was quenched by the addition of water (10 mL), the phases were separated, and the aqueous phase was washed with ethyl acetate (3 x 10 mL). The combined organic phases were washed with brine, dried over MgSO₄, and the solvent was evaporated under reduced pressure. Purification by SiO₂ flash chromatography (pentane/ethyl acetate 95:5 to 85:20) gave 90 mg (48 %) of 15 as a colorless solid.

¹H NMR (400 MHz, cdCl₃) δ = 7.57 (s, 1H), 7.50 – 7.43 (m, 2H), 7.30 (d, *J*=8.4, 1H), 7.25 (dd, *J*=8.3, 2.1, 1H), 7.11 (s, 1H), 6.98 (d, *J*=8.4, 1H), 6.05 (s, 2H), 5.27 (s, 2H), 4.77 (s, 2H), 3.93 (s, 3H), 3.54 (s, 3H), 3.32 (s, 3H). ¹³C NMR (101 MHz, cdCl₃) δ = 149.8, 149.2, 148.3, 148.0, 146.3, 132.1, 131.4, 128.7, 127.2, 126.0, 123.8, 123.4, 118.4, 111.8, 103.9, 101.3, 99.6, 99.5, 95.8, 77.5, 77.2, 76.8, 57.8, 56.4, 56.1, 56.1.

6-bromo-2,3-dimethoxyphenyl)methanol (17H)

In a flask was dissolved 2,3-dimethoxy benzyl alcohol (500 mg, 2.97 mmol) in acetonitrile (5 mL), and NBS (555 mg, 3.12 mmol) was added. The solution was stirred to completion (TLC) at room temperature. The solvent was removed on the rotavap, the residue taken up in diethyl ether, the insoluble succinimide filtered off, and the filtrate was washed with 1M NaOH (2 x 5 mL). The organic layer was dried over MgSO₄, the solvent evaporated under reduced pressure. The crude product was recrystallized from EtOAc/pentane to give 321 mg (43 %) 17H as colorless solid.

^1H NMR (400 MHz, cdCl_3) δ = 7.27 (d, $J=8.8$, 1H), 6.77 (d, $J=8.8$, 1H), 4.83 (s, 2H), 3.90 (s, 3H), 3.86 (s, 3H), 2.33 (s, 1H).

Methoxy methoxy benzene

In a flame dried, nitrogen flushed Schlenk flask phenol (5.00 g, 53.1 mmol) was dissolved in dry THF (150 mL), and the solution was placed into an ice bath. NaH (60% dispersion in mineral oil, 3.53 g, 58.4 mmol) was added portion wise, and the mixture was stirred for 20 minutes. MOMOCl (4.44 mL, 58.4 mmol) was added through syringe over 5 minutes. The reaction mixture was stirred at r.t. for 2 h, before quenching it by the addition of water (20 mL). Diethyl ether (50 mL) was added, the phases separated, and the organic phase was washed with aqueous NaOH (1M, 2 x 20 mL), water (10 mL) and brine (20 mL). The organic phase was dried over MgSO_4 , and the solvent was evaporated under reduced pressure. Purification by SiO_2 chromatography gave 4.15 g (56 %) of pure methoxy methoxy benzene as colorless oil.

^1H NMR (400 MHz, cdCl_3) δ = 7.38 – 7.18 (m, 3H), 7.07 (t, $J=7.3$, 1H), 5.06 (s, 2H), 3.34 (s, 3H).

1-(Methoxymethoxy)naphthalene (**19**)

In a flame dried, nitrogen flushed Schlenk flask alpha-naphthol (5.78 g, 40 mmol) was dissolved in dry dmf (40 mL), and the solution was placed into an ice bath. NaH (60% dispersion in mineral oil, 1.92 g, 48 mmol) was added portion wise, and the mixture was stirred for 1 h. MOMOCl (3.54 mL, 44 mmol) was added through syringe over 10 minutes. The reaction mixture was stirred at r.t. for 3 h, before quenching it by the addition of water (20 mL). Diethyl ether (50 mL) was added, the phases separated, and the organic phase was washed with aqueous NaOH (1M, 2 x 20 mL), water (10 mL) and brine (20 mL). The organic phase was dried over MgSO_4 , and the solvent was evaporated under reduced pressure. Purification by SiO_2 chromatography gave 4.27 g (56 %) of pure **19** as colorless oil.

^1H NMR (400 MHz, cdCl_3) δ = 8.31 – 8.25 (m, 1H), 7.85 – 7.78 (m, 1H), 7.49 (d, $J=8.8$, 3H), 7.38 (t, $J=7.9$, 1H), 7.10 (d, $J=7.6$, 1H), 5.41 (s, 2H), 3.56 (s, 3H).

2,2'-bis(methoxymethoxy)-1,1'-biphenyl (**20**)

^1H NMR (400 MHz, cdCl_3) δ = 7.38 – 7.18 (m, 3H), 7.07 (t, $J=7.3$, 1H), 5.06 (s, 2H), 3.34 (s, 3H).

1,1'-bis(methoxymethoxy)-2,2'-binaphthalene (**21**)

^1H NMR (400 MHz, cdCl_3) δ = 8.32 (dd, $J=8.0, 1.7$, 1H), 7.91 (dd, $J=7.4, 1.8$, 1H), 7.75 (d, $J=8.5$, 1H), 7.66 (d, $J=8.5$, 1H), 7.57 (pd, $J=6.8, 1.5$, 2H), 4.94 (s, 2H), 3.08 (s, 3H). ^{13}C NMR (101 MHz, cdCl_3) δ = 150.9, 134.5, 129.6, 128.8, 128.1, 128.0, 126.5, 126.3, 124.0, 122.8, 99.7, 77.5, 77.2, 76.8, 57.2.

2,2'-dimethoxy-1,1'-biphenyl (22)

^1H NMR (400 MHz, cdCl_3) δ = 7.37 – 7.29 (m, 2H), 7.05 – 6.95 (m, 4H), 3.78 (s, 6H).

2,2'-bithiophene (23)

^1H NMR (400 MHz, cdCl_3) δ = 7.24 – 7.16 (m, 4H), 7.02 (dd, $J=5.0, 3.7$, 2H).

3,3',4,4'-tetramethyl-2,2'-bithiophene (25)

^1H NMR (400 MHz, cdCl_3) δ = 6.93 (s, 2H), 2.18 (d, $J=1.2$, 7H), 2.02 (s, 7H).

3,3',3'',3''',4,4',4'',4'''-octamethyl-2,2':5',2'':5'',2'''-quaterthiophene (26)

^1H NMR (400 MHz, cdCl_3) δ = 6.95 (s, 2H), 2.20 (s, 6H), 2.12 (s, 6H), 2.09 (s, 6H), 2.08 (s, 6H). ^{13}C NMR (101 MHz, cdCl_3) δ = 138.1, 136.7, 136.6, 136.4, 130.3, 129.8, 129.7, 120.9, 77.5, 77.2, 76.8, 15.6, 14.4, 14.3, 13.7.

References

-
- [1] "The Nobel Prize in Chemistry 2010," <https://www.nobelprize.org/prizes/chemistry/2010/press-release/>.
 - [2] P. Garcia, M. Malacria, C. Aubert, V. Gandon, L. Fensterbank, *ChemCatChem* **2010**, *2*, 493–497.
 - [3] M. O. Akram, P. S. Shinde, C. C. Chintawar, N. T. Patil, *Org. Biomol. Chem.* **2018**, *16*, 2865–2869.
 - [4] T. Morita, M. Akita, T. Satoh, F. Kakiuchi, M. Miura, *Org. Lett.* **2016**, *18*, 4598–4601.
 - [5] Y. Na, S. Park, S. B. Han, H. Han, S. Ko, S. Chang, *J. Am. Chem. Soc.* **2004**, *126*, 250–258.
 - [6] G. W. Kabalka, G. Dong, B. Venkataiah, *Org. Lett.* **2003**, *5*, 893–895.
 - [7] Y.-T. Tsoi, Z. Zhou, W.-Y. Yu, *Org. Lett.* **2011**, *13*, 5370–5373.
 - [8] J. Zhang, T.-P. Loh, *Chem. Commun.* **2012**, *48*, 11232–11234.
 - [9] S. Thapa, B. Shrestha, S. K. Gurung, R. Giri, *Org. Biomol. Chem.* **2015**, *13*, 4816–4827.
 - [10] A. Piontek, E. Bisz, M. Szostak, *Angew. Chem. Int. Edit.* **2018**, *57*, 11116–11128.
 - [11] A. Fürstner, A. Leitner, M. Méndez, H. Krause, *J. Am. Chem. Soc.* **2002**, *124*, 13856–13863.
 - [12] L. Guo, W. Srimontree, C. Zhu, B. Maity, X. Liu, L. Cavallo, M. Rueping, *Nat. Commun.* **2019**, *10*, 1–6.
 - [13] B. M. Rosen, K. W. Quasdorf, D. A. Wilson, N. Zhang, A.-M. Resmerita, N. K. Garg, V. Percec, *Chem. Rev.* **2011**, *111*, 1346–1416.
 - [14] C. Glaser, *Ber. Dtsch. Chem. Ges.* **1869**, *2*, 422–424.
 - [15] C. C. C. Johansson Seechurn, M. O. Kitching, T. J. Colacot, V. Snieckus, *Angew. Chem. Int. Edit.* **2012**, *51*, 5062–5085.
 - [16] R. F. Heck, *Synlett* **2006**, *2006*, 2855–2860.
 - [17] R. F. Heck, *J. Am. Chem. Soc.* **1968**, *90*, 5546–5548.
 - [18] R. F. Heck, *J. Am. Chem. Soc.* **1968**, *90*, 5518–5526.

- [19] R. F. Heck, *J. Am. Chem. Soc.* **1968**, *90*, 5531–5534.
- [20] R. F. Heck, *J. Am. Chem. Soc.* **1968**, *90*, 5538–5542.
- [21] R. F. Heck, *J. Am. Chem. Soc.* **1968**, *90*, 5542–5546.
- [22] R. F. Heck, *J. Am. Chem. Soc.* **1968**, *90*, 5526–5531.
- [23] R. F. Heck, *J. Am. Chem. Soc.* **1968**, *90*, 5535–5538.
- [24] R. J. P. Corriu, J. P. Masse, *J. Chem. Soc., Chem. Commun.* **1972**, *0*, 144a–144a.
- [25] K. Tamao, Y. Kiso, K. Sumitani, M. Kumada, *J. Am. Chem. Soc.* **1972**, *94*, 9268–9269.
- [26] K. Tamao, K. Sumitani, M. Kumada, *J. Am. Chem. Soc.* **1972**, *94*, 4374–4376.
- [27] M. Yamamura, I. Moritani, S.-I. Murahashi, *Journal of Organometallic Chemistry* **1975**, *91*, C39–C42.
- [28] S. Murahashi, M. Yamamura, K. Yanagisawa, N. Mita, K. Kondo, *J. Org. Chem.* **1979**, *44*, 2408–2417.
- [29] A. O. King, N. Okukado, E. Negishi, *J. Chem. Soc., Chem. Commun.* **1977**, 683–684.
- [30] E. Negishi, A. O. King, N. Okukado, *J. Org. Chem.* **1977**, *42*, 1821–1823.
- [31] D. Azarian, S. S. Dua, C. Eaborn, D. R. M. Walton, *J. Organomet. Chem.* **1976**, *117*, C55–C57.
- [32] M. Kosugi, Y. Shimizu, T. Migita, *J. Organomet. Chem.* **1977**, *129*, C36–C38.
- [33] S. Baba, E. Negishi, *J. Am. Chem. Soc.* **1976**, *98*, 6729–6731.
- [34] H. A. Dieck, R. F. Heck, *J. Org. Chem.* **1975**, *40*, 1083–1090.
- [35] N. Miyaoura, A. Suzuki, *J. Chem. Soc., Chem. Commun.* **1979**, 866–867.
- [36] T. Hayashi, M. Konishi, Y. Kobori, M. Kumada, T. Higuchi, K. Hirotsu, *J. Am. Chem. Soc.* **1984**, *106*, 158–163.
- [37] A. F. Littke, G. C. Fu, *Angew. Chem. Int. Edit.* **1998**, *37*, 3387–3388.
- [38] A. F. Littke, G. C. Fu, *J. Org. Chem.* **1999**, *64*, 10–11.
- [39] A. F. Littke, C. Dai, G. C. Fu, *J. Am. Chem. Soc.* **2000**, *122*, 4020–4028.
- [40] C. Dai, G. C. Fu, *J. Am. Chem. Soc.* **2001**, *123*, 2719–2724.
- [41] F. Paul, J. Patt, J. F. Hartwig, *Organometallics* **1995**, *14*, 3030–3039.
- [42] V. P. W. Böhm, C. W. K. Gstöttmayr, T. Weskamp, W. A. Herrmann, *J. Organomet. Chem.* **2000**, *595*, 186–190.
- [43] N. Marion, S. P. Nolan, *Acc. Chem. Res.* **2008**, *41*, 1440–1449.
- [44] S. Caddick, F. G. N. Cloke, G. K. B. Clentsmith, P. B. Hitchcock, D. McKerrecher, L. R. Titcomb, M. R. V. Williams, *J. Organomet. Chem.* **2001**, *617–618*, 635–639.
- [45] K. Arentsen, S. Caddick, F. G. N. Cloke, A. P. Herring, P. B. Hitchcock, *Tetrahedron Lett.* **2004**, *45*, 3511–3515.
- [46] R. F. Heck, J. P. Nolley, *J. Org. Chem.* **1972**, *37*, 2320–2322.
- [47] A. Biffis, P. Centomo, A. Del Zotto, M. Zecca, *Chem. Rev.* **2018**, *118*, 2249–2295.
- [48] K. Kaneda, M. Higuchi, T. Imanaka, *J. Mol. Catal.* **1990**, *63*, L33–L36.
- [49] S. Mukhopadhyay, G. Rothenberg, A. Joshi, M. Baidossi, Y. Sasson, *Adv. Synth. Catal.* **2002**, *344*, 348–354.
- [50] Y. M. A. Yamada, S. M. Sarkar, Y. Uozumi, *J. Am. Chem. Soc.* **2012**, *134*, 3190–3198.
- [51] D. Heijnen, F. Tosi, C. Vila, M. C. A. Stuart, P. H. Elsinga, W. Szymanski, B. L. Feringa, *Angew. Chem. Int. Edit.* **2017**, *56*, 3354–3359.
- [52] S. H. L. Thoonen, B.-J. Deelman, G. van Koten, *J. Organomet. Chem.* **2004**, *689*, 2145–2157.
- [53] A. Hafner, M. Meisenbach, J. Sedelmeier, *Org. Lett.* **2016**, *18*, 3630–3633.
- [54] T. Leermann, F. R. Leroux, F. Colobert, *Org. Lett.* **2011**, *13*, 4479–4481.
- [55] J. Takagi, K. Takahashi, T. Ishiyama, N. Miyaoura, *J. Am. Chem. Soc.* **2002**, *124*, 8001–8006.
- [56] E. J. Corey, T. M. Eckrich, *Tetrahedron Lett.* **1984**, *25*, 2415–2418.
- [57] R. H. Wollenberg, K. F. Albizati, R. Peries, *J. Am. Chem. Soc.* **1977**, *99*, 7365–7367.
- [58] M. E. Jung, L. A. Light, *Tetrahedron Lett.* **1982**, *23*, 3851–3854.
- [59] N. PraveenGanesh, S. d’Hond, P. Y. Chavant, *J. Org. Chem.* **2007**, *72*, 4510–4514.
- [60] A. J. Leusink, H. A. Budding, J. W. Marsman, *J. Organomet. Chem.* **1967**, *9*, 285–294.
- [61] Henry. Gilman, Wright. Langham, A. L. Jacoby, *J. Am. Chem. Soc.* **1939**, *61*, 106–109.
- [62] G. Wittig, G. Pieper, G. Fuhrmann, *Ber. Dtsch. Chem. Ges. (A and B Series)* **1940**, *73*, 1193–1197.
- [63] H. J. Reich, *Chem. Rev.* **2013**, *113*, 7130–7178.

- [64] H. L. Lewis, T. L. Brown, *J. Am. Chem. Soc.* **1970**, *92*, 4664–4670.
- [65] J. F. McGarrity, C. A. Ogle, *J. Am. Chem. Soc.* **1985**, *107*, 1805–1810.
- [66] G. Fraenkel, M. Henrichs, M. Hewitt, B. M. Su, *J. Am. Chem. Soc.* **1984**, *106*, 255–256.
- [67] S. Bywater, D. J. Worsfold, *J. Organomet. Chem.* **1967**, *10*, 1–6.
- [68] Walter. Bauer, W. R. Winchester, P. von R. Schleyer, *Organometallics* **1987**, *6*, 2371–2379.
- [69] M. Weiner, G. Vogel, R. West, *Inorg. Chem.* **1962**, *1*, 654–658.
- [70] R. D. Thomas, M. T. Clarke, R. M. Jensen, T. Corby. Young, *Organometallics* **1986**, *5*, 1851–1857.
- [71] Walter. Bauer, W. R. Winchester, P. von R. Schleyer, *Organometallics* **1987**, *6*, 2371–2379.
- [72] V. Snieckus, *Chem. Rev.* **1990**, *90*, 879–933.
- [73] P. Beak, R. A. Brown, *J. Org. Chem.* **1982**, *47*, 34–46.
- [74] D. W. Slocum, C. A. Jennings, *J. Org. Chem.* **1976**, *41*, 3653–3664.
- [75] P. Beak, A. Tse, J. Haawkins, C.-W. Chen, S. Mills, *Tetrahedron* **1983**, *39*, 1983–1989.
- [76] P. Krawczuk, *n.d.*, *10*.
- [77] I. Funes-Ardoiz, F. Maseras, *ACS Catal.* **2018**, *8*, 1161–1172.
- [78] C. Liu, H. Zhang, W. Shi, A. Lei, *Chem. Rev.* **2011**, *111*, 1780–1824.
- [79] L. Jin, Y. Zhao, L. Zhu, H. Zhang, A. Lei, *Adv. Synth. Catal.* **2009**, *351*, 630–634.
- [80] Y. Zhao, H. Wang, X. Hou, Y. Hu, A. Lei, H. Zhang, L. Zhu, *J. Am. Chem. Soc.* **2006**, *128*, 15048–15049.
- [81] I. Funes-Ardoiz, F. Maseras, *ACS Catal.* **2018**, *8*, 1161–1172.
- [82] M. S. Maji, T. Pfeifer, A. Studer, *Angew. Chem. Int. Edit.* **2008**, *47*, 9547–9550.
- [83] C. Amatore, C. Cammoun, A. Jutand, *Eur. J. Org. Chem.* **2008**, *2008*, 4567–4570.
- [84] W. Liu, A. Lei, *Tetrahedron Letters* **2008**, *49*, 610–613.
- [85] G. Kiefer, L. Jeanbourquin, K. Severin, *Angew. Chem. Int. Edit.* **2013**, *52*, 6302–6305.
- [86] G. Kiefer, L. Jeanbourquin, K. Severin, *Angew. Chem. Int. Edit.* **2013**, *52*, 6302–6305.
- [87] R. A. Stockland, R. F. Jordan, *J. Am. Chem. Soc.* **2000**, *122*, 6315–6316.
- [88] R. A. Stockland, S. R. Foley, R. F. Jordan, *J. Am. Chem. Soc.* **2003**, *125*, 796–809.
- [89] S. G. Gaynor, *Macromolecules* **2003**, *36*, 4692–4698.
- [90] A. E. Carpenter, A. J. McNeece, B. R. Barnett, A. L. Estrada, C. C. Mokhtarzadeh, C. E. Moore, A. L. Rheingold, C. L. Perrin, J. S. Figueroa, *J. Am. Chem. Soc.* **2014**, *136*, 15481–15484.
- [91] T. Nagano, T. Hayashi, *Org. Lett.* **2005**, *7*, 491–493.
- [92] Z. Zhou, W. Xue, *J. Organomet. Chem.* **2009**, *694*, 599–603.
- [93] M. Yamamura, I. Moritani, S.-I. Murahashi, *J. Organomet. Chem.* **1975**, *91*, C39–C42.
- [94] J. Buter, D. Heijnen, C. Vila, V. Hornillos, E. Otten, M. Giannerini, A. J. Minnaard, B. L. Feringa, *Angew. Chem. Int. Edit.* **2016**, *55*, 3620–3624.
- [95] V. Hornillos, M. Giannerini, C. Vila, M. Fañanás-Mastral, B. L. Feringa, *Org. Lett.* **2013**, *15*, 5114–5117.
- [96] M. Giannerini, V. Hornillos, C. Vila, M. Fañanás-Mastral, B. L. Feringa, *Angew. Chem. Int. Edit.* **2013**, *52*, 13329–13333.
- [97] T. Ishikawa, A. Ogawa, T. Hirao, *Organometallics* **1998**, *17*, 5713–5716.
- [98] Y. Liu, J. Bergès, Y. Zaid, F. O. Chahdi, A. Van Der Lee, D. Harakat, E. Clot, F. Jaroschik, M. Taillefer, *J. Org. Chem.* **2019**, *84*, 4413–4420.
- [99] H. Ishii, T. Ishikawa, M. Murota, Y. Aoki, T. Harayama, *J. Chem. Soc., Perkin Trans. 1* **1993**, *0*, 1019–1022.
- [100] T. Hosoya, E. Takashiro, T. Matsumoto, K. Suzuki, *J. Am. Chem. Soc.* **1994**, *116*, 1004–1015.
- [101] J. V. Suárez-Meneses, E. Bonilla-Reyes, E. A. Blé-González, M. C. Ortega-Alfaro, R. A. Toscano, A. Cordero-Vargas, J. G. López-Cortés, *Tetrahedron* **2014**, *70*, 1422–1430.
- [102] S. Madan, C.-H. Cheng, *J. Org. Chem.* **2006**, *71*, 8312–8315.
- [103] M. J. Moschitto, D. R. Anthony, C. A. Lewis, *J. Org. Chem.* **2015**, *80*, 3339–3342.
- [104] T. Maibunkaew, C. Thongsornkleeb, J. Tummatorn, A. Bunrit, S. Ruchirawat, *Synlett* **2014**, *25*, 1769–1775.
- [105] R. G. F. Giles, A. B. Hughes, M. V. Sargent, *J. Chem. Soc., Perkin Trans. 1* **1991**, 1581.
- [106] K. Antien, G. Viault, L. Pouységu, P. A. Peixoto, S. Quideau, *Tetrahedron* **2017**, *73*, 3684–3690.
- [107] R. Shimizu, H. Egami, Y. Hamashima, M. Sodeoka, *Angew. Chem. Int. Edit.* **2012**, *51*, 4577–4580.

- [108] M. R. Winkle, R. C. Ronald, *J. Org. Chem.* **1982**, *47*, 2101–2108.
- [109] M. Mirza-Aghayan, M. Molaee Tavana, R. Boukherroub, *Tetrahedron Lett.* **2014**, *55*, 342–345.
- [110] G. An, H. Ahn, K. A. D. Castro, H. Rhee, *Synthesis* **2010**, *2010*, 477–485.
- [111] Y. Liu, J. Bergès, Y. Zaid, F. Ouazzani Chahdi, A. Van der Lee, D. Harakat, E. Clot, F. Jaroschik, M. Taillefer, *J. Org. Chem.* **2019**, *84*, 4413–4420.
- [112] D. W. Slocum, T. K. Reinscheld, C. B. White, M. D. Timmons, P. A. Shelton, M. G. Slocum, R. D. Sandlin, E. G. Holland, D. Kusmic, J. A. Jennings, et al., *Organometallics* **2013**, *32*, 1674–1686.
- [113] L. Zhang, N. S. Colella, B. P. Cherniawski, S. C. B. Mannsfeld, A. L. Briseno, *ACS Appl. Mater. Interfaces* **2014**, *6*, 5327–5343.
- [114] I. F. Perepichka, D. F. Perepichka, *Handbook of Thiophene-Based Materials: Applications in Organic Electronics and Photonics, 2 Volume Set*, John Wiley & Sons, **2009**.
- [115] Ph. Leclère, M. Surin, P. Viville, R. Lazzaroni, A. F. M. Kilbinger, O. Henze, W. J. Feast, M. Cavallini, F. Biscarini, A. P. H. J. Schenning, et al., *Chem. Mater.* **2004**, *16*, 4452–4466.
- [116] E. O. Pentsak, D. B. Eremin, E. G. Gordeev, V. P. Ananikov, *ACS Catal.* **2019**, *9*, 3070–3081.
- [117] S. Cabiddu, A. Maccioni, P. P. Piras, M. Secci, *J. Organomet. Chem.* **1977**, *136*, 139–146.
- [118] S. S. Moore, G. M. Whitesides, *J. Org. Chem.* **1982**, *47*, 1489–1493.
- [119] K. Kawasaki, M. Masubuchi, K. Morikami, S. Sogabe, T. Aoyama, H. Ebiike, S. Niizuma, M. Hayase, T. Fujii, K. Sakata, et al., *Bioorg. Med. Chem. Lett.* **2003**, *13*, 87–91.
- [120] H. Gilman, T. Soddy, *J. Org. Chem.* **1957**, *22*, 565–566.
- [121] M. Ishikura, I. Oda, M. Kamada, M. Terashima, *Synthetic Commun.* **1987**, *17*, 959–967.

Appendix

NMR-Spectra

LS1-023recryst_20181009171922 — — 20181009164625 —

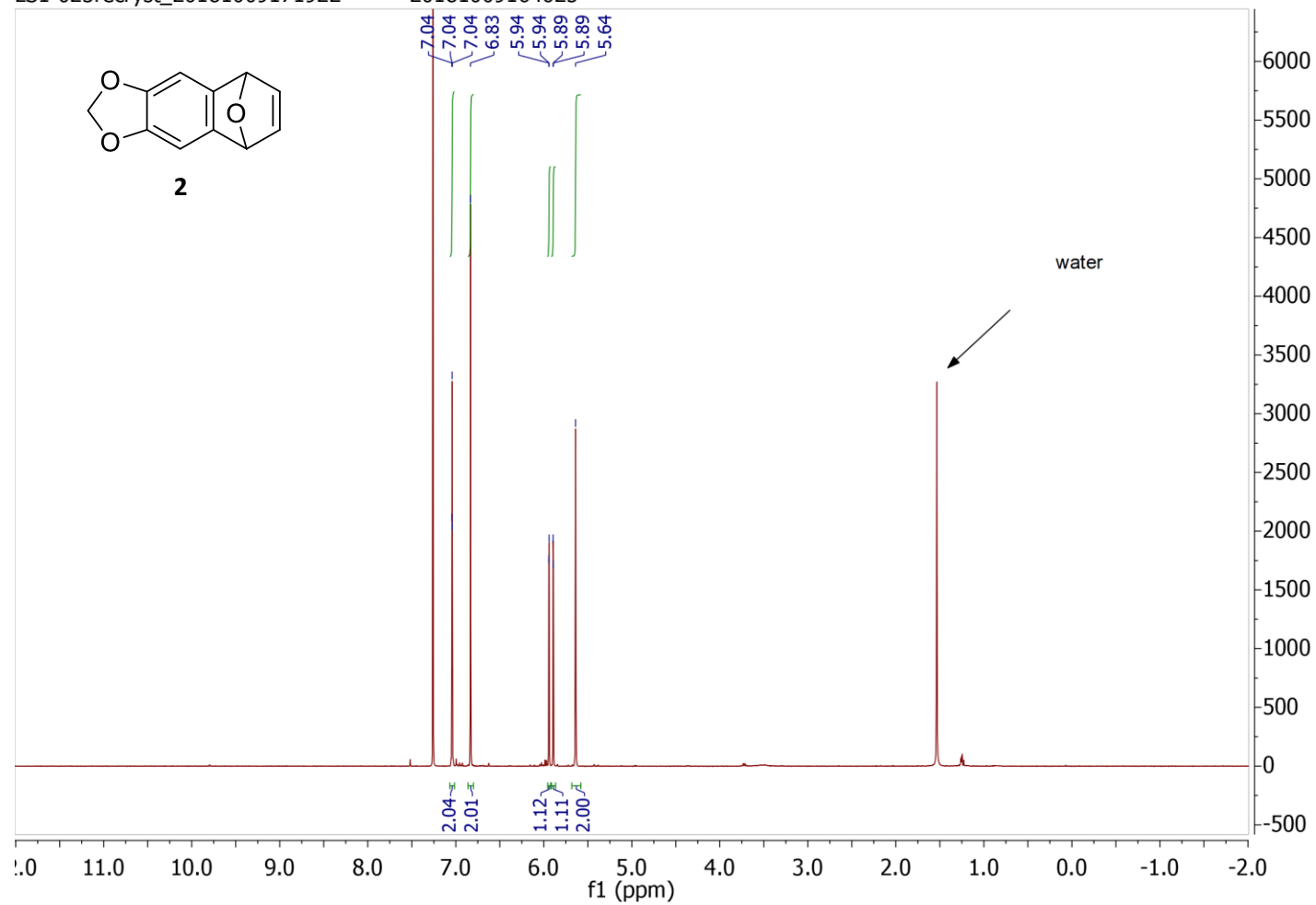


Figure 8 ¹H-NMR spectrum of **2**

LS1-027-dried_20181012145904 — — 20181012142023 —

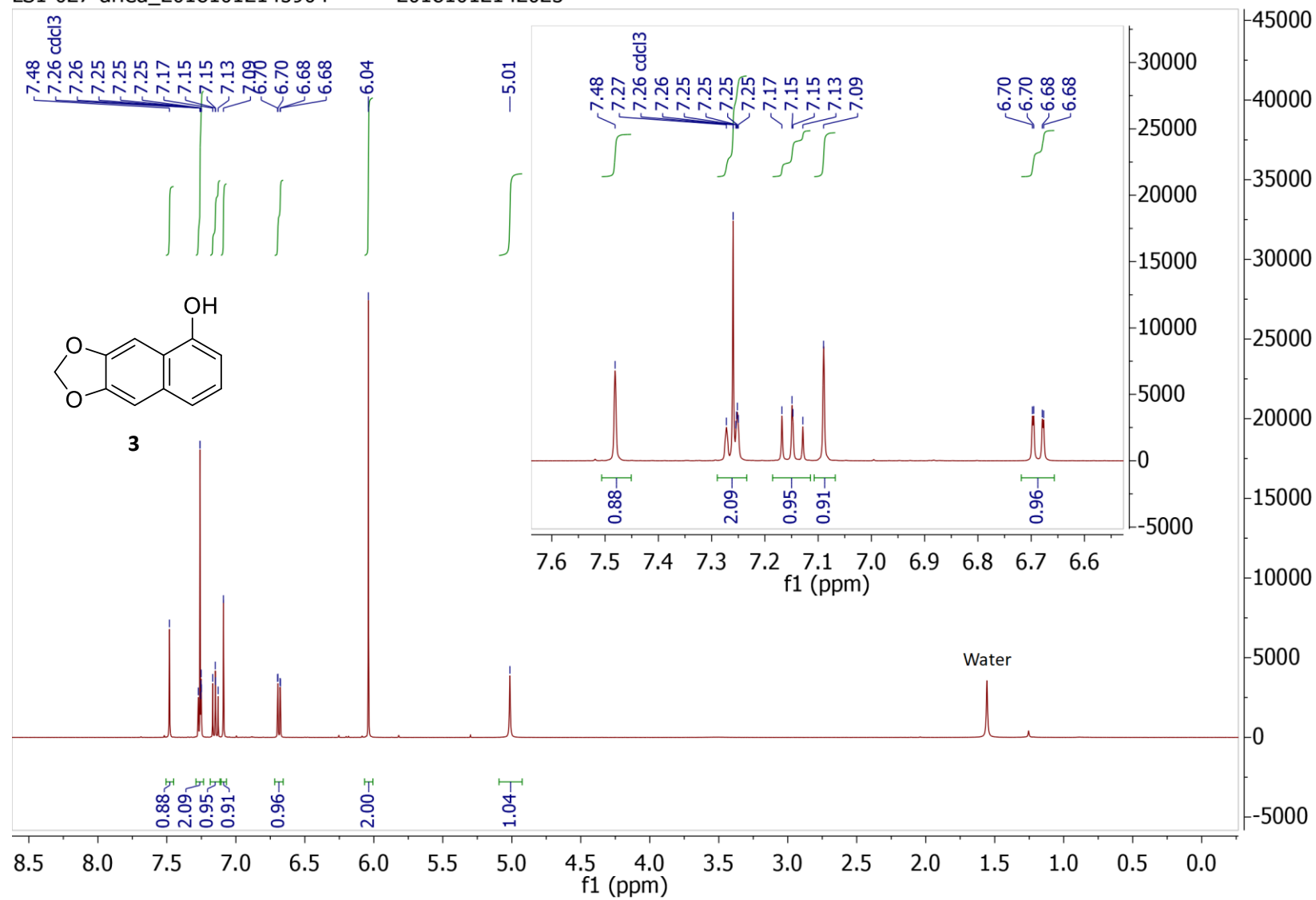


Figure 9 ¹H-NMR spectrum of **3**

LS1-031-1H_20181017075458 — — 20181016154621 —

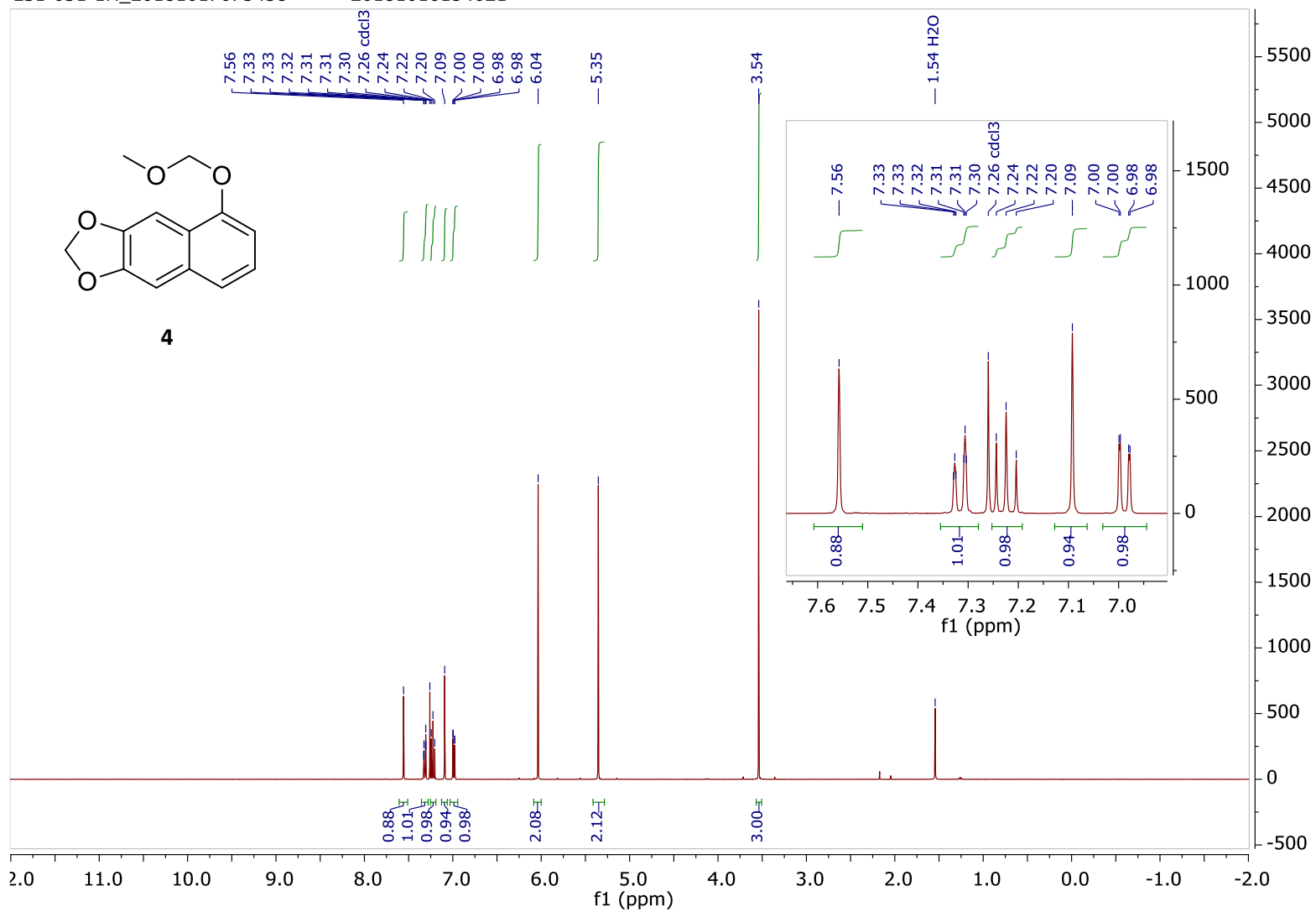


Figure 10 ¹H-NMR spectrum of 4

LS1-031-13C_20181017083814 — — 20181016154641 —

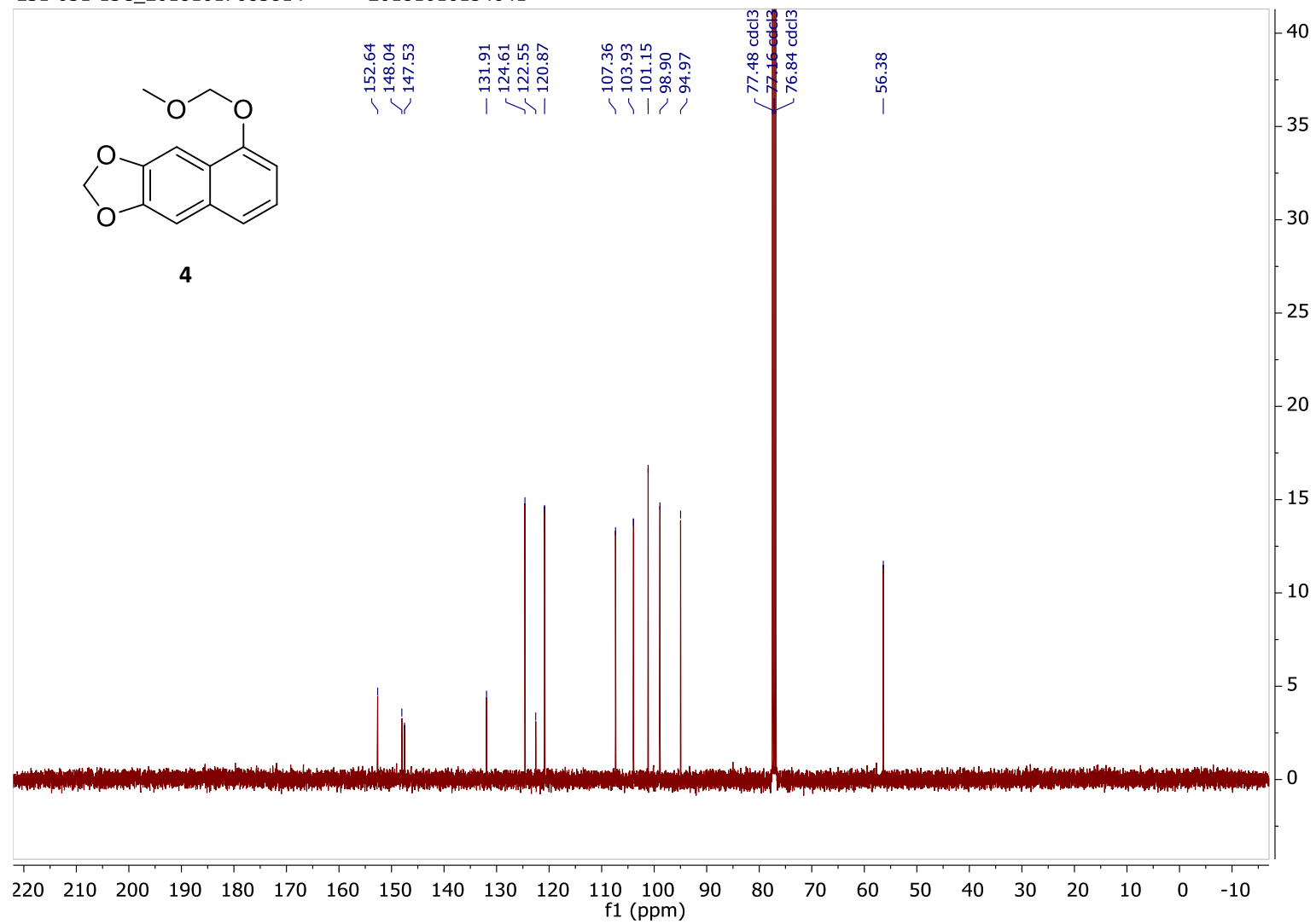


Figure 11 ¹³C-NMR spectrum of 4

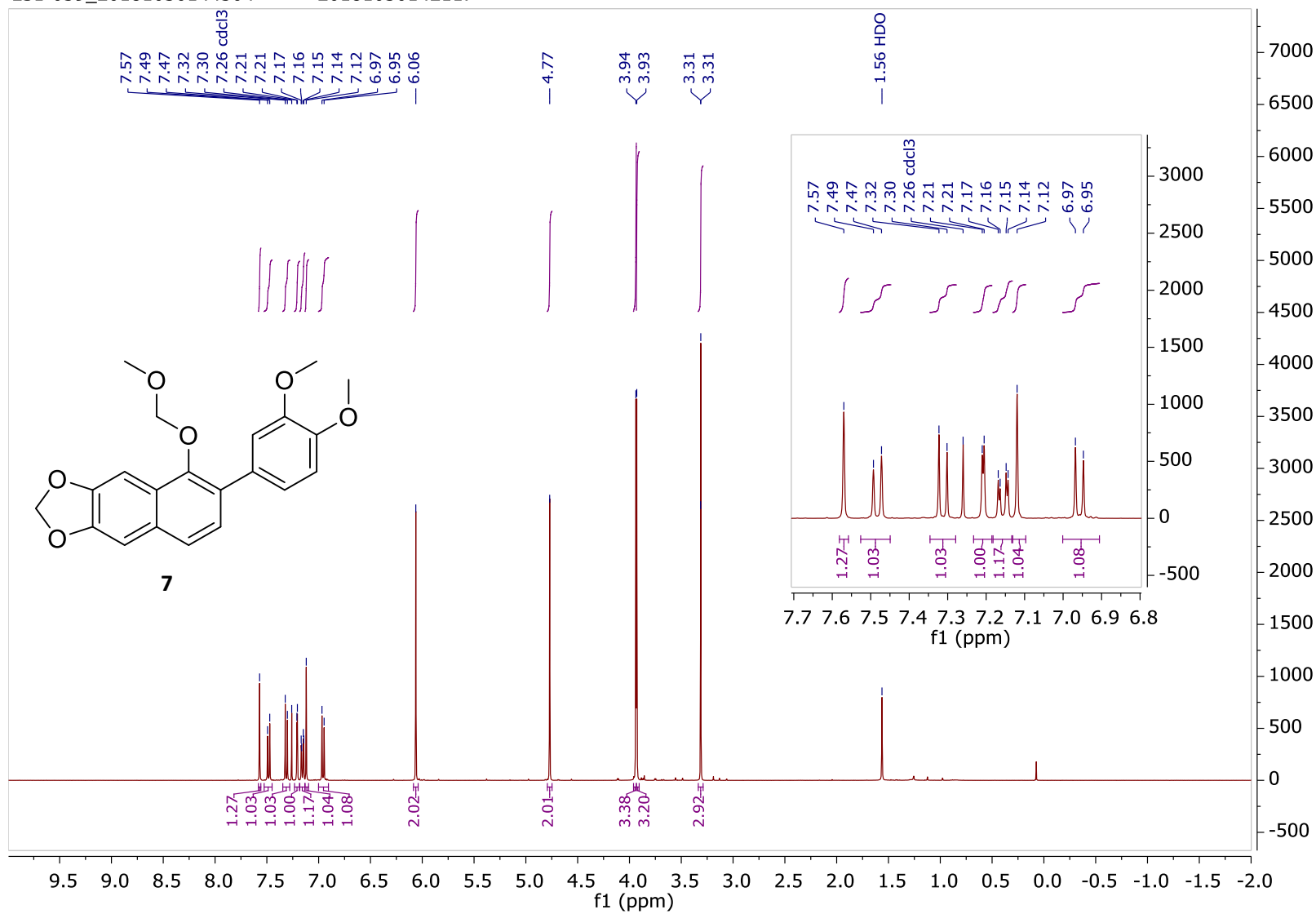


Figure 12 ¹H-NMR spectrum of 7

LS1-059_20181030145359 — — 20181030142209 —

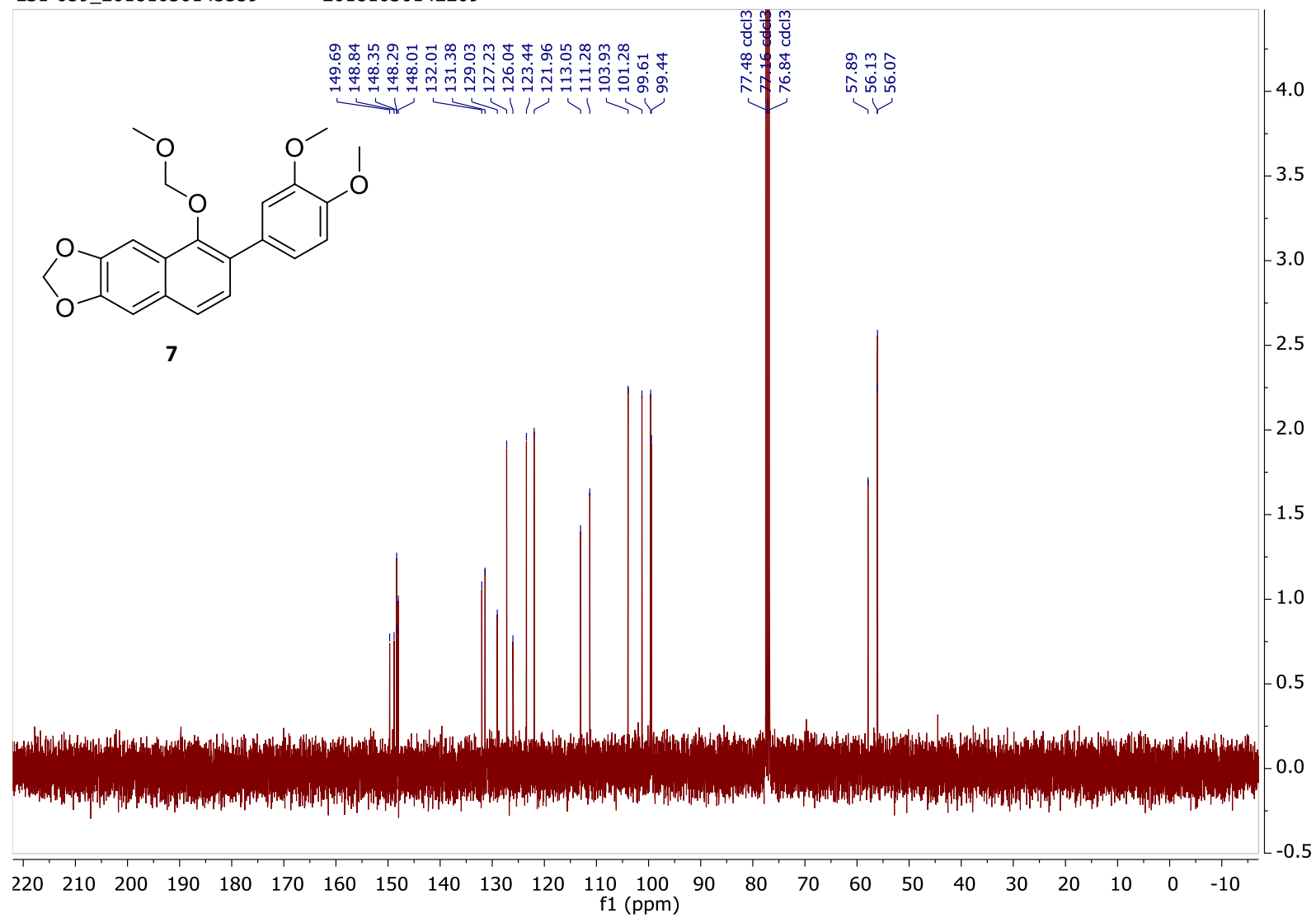


Figure 13 $^{13}\text{C-NMR}$ spectrum of **7**

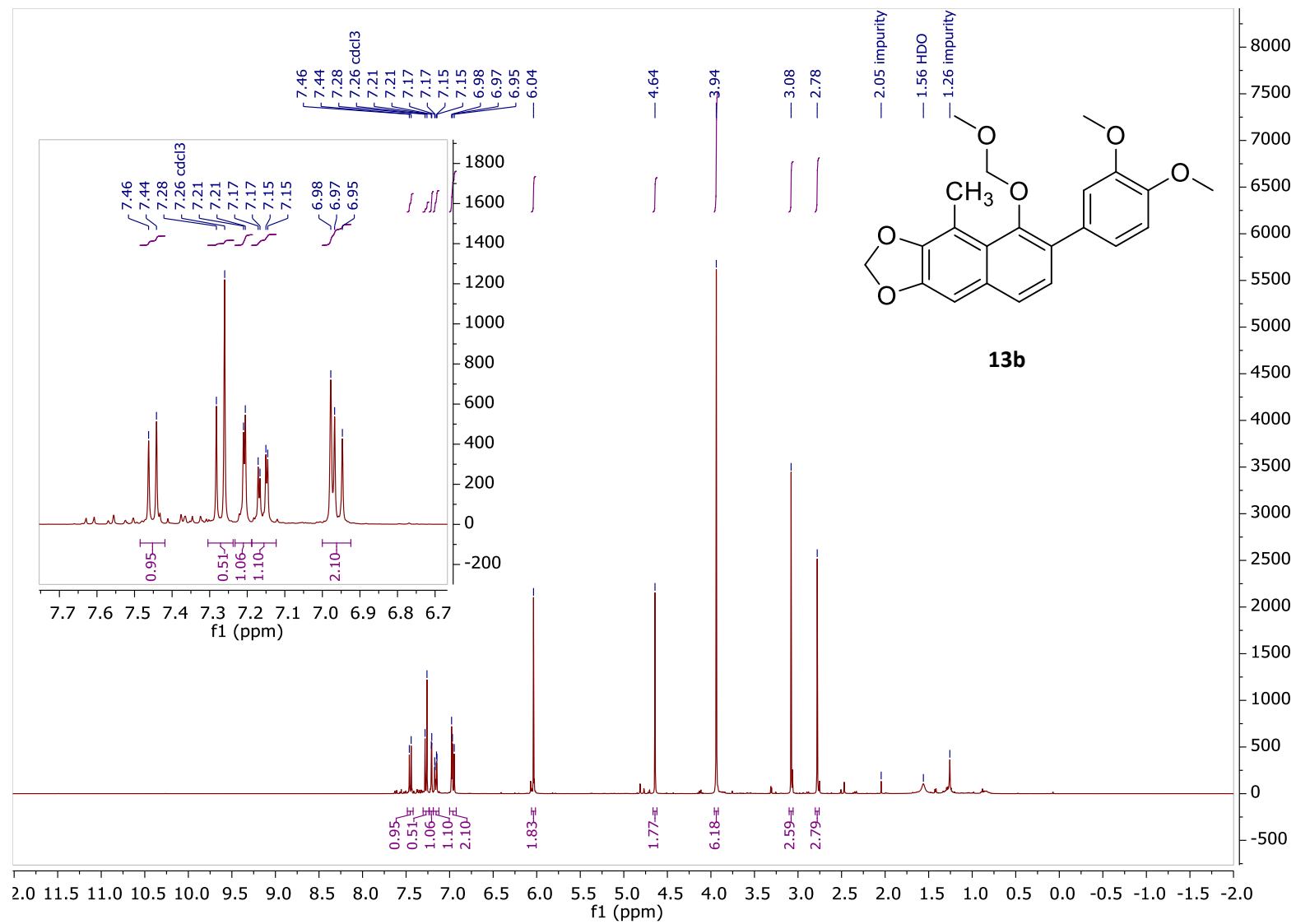


Figure 14 ¹H-NMR spectrum of **13b**

LS1-087_20181120131626 — — 20181120130918 —

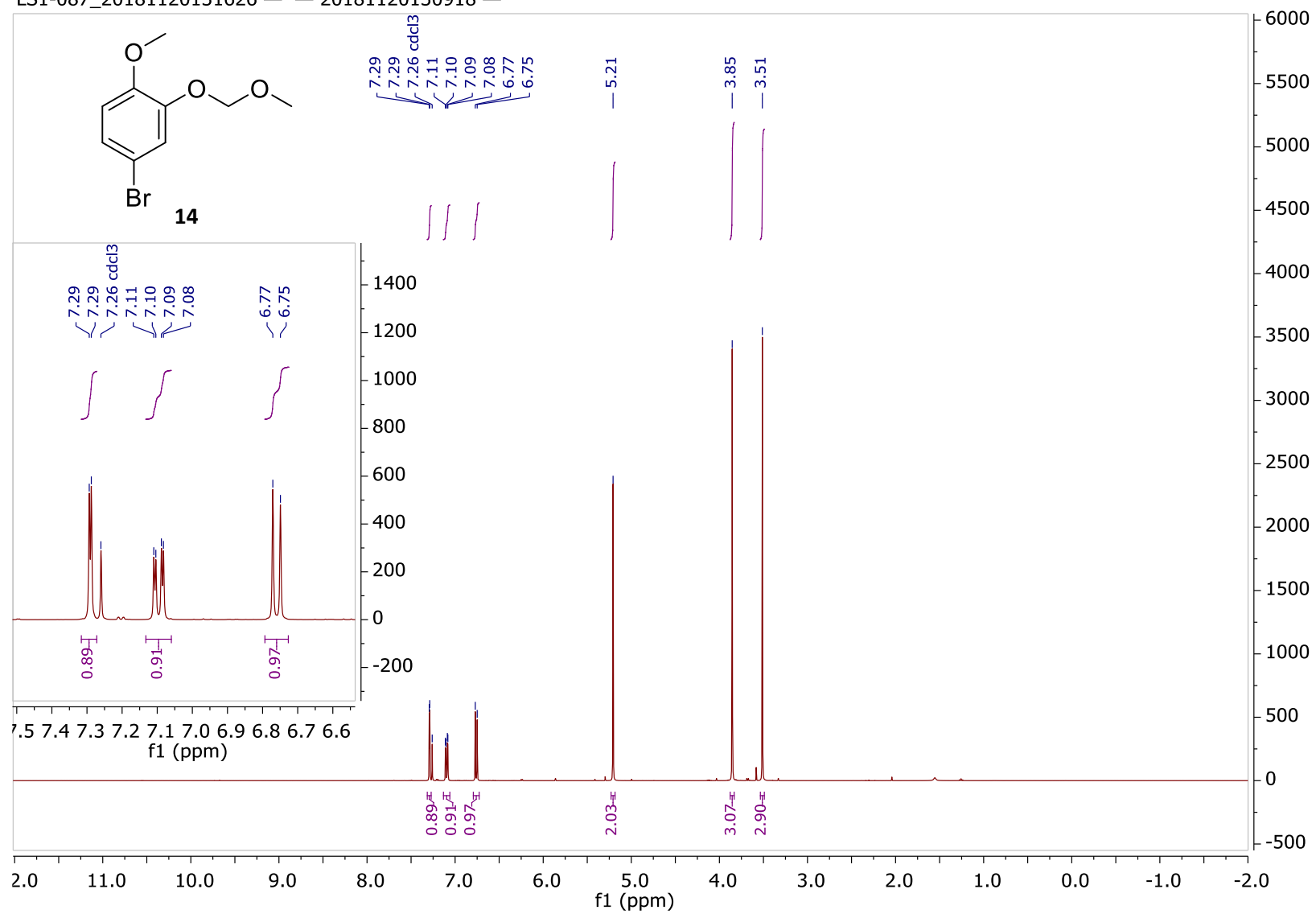


Figure 15 ¹H-NMR spectrum of **14**

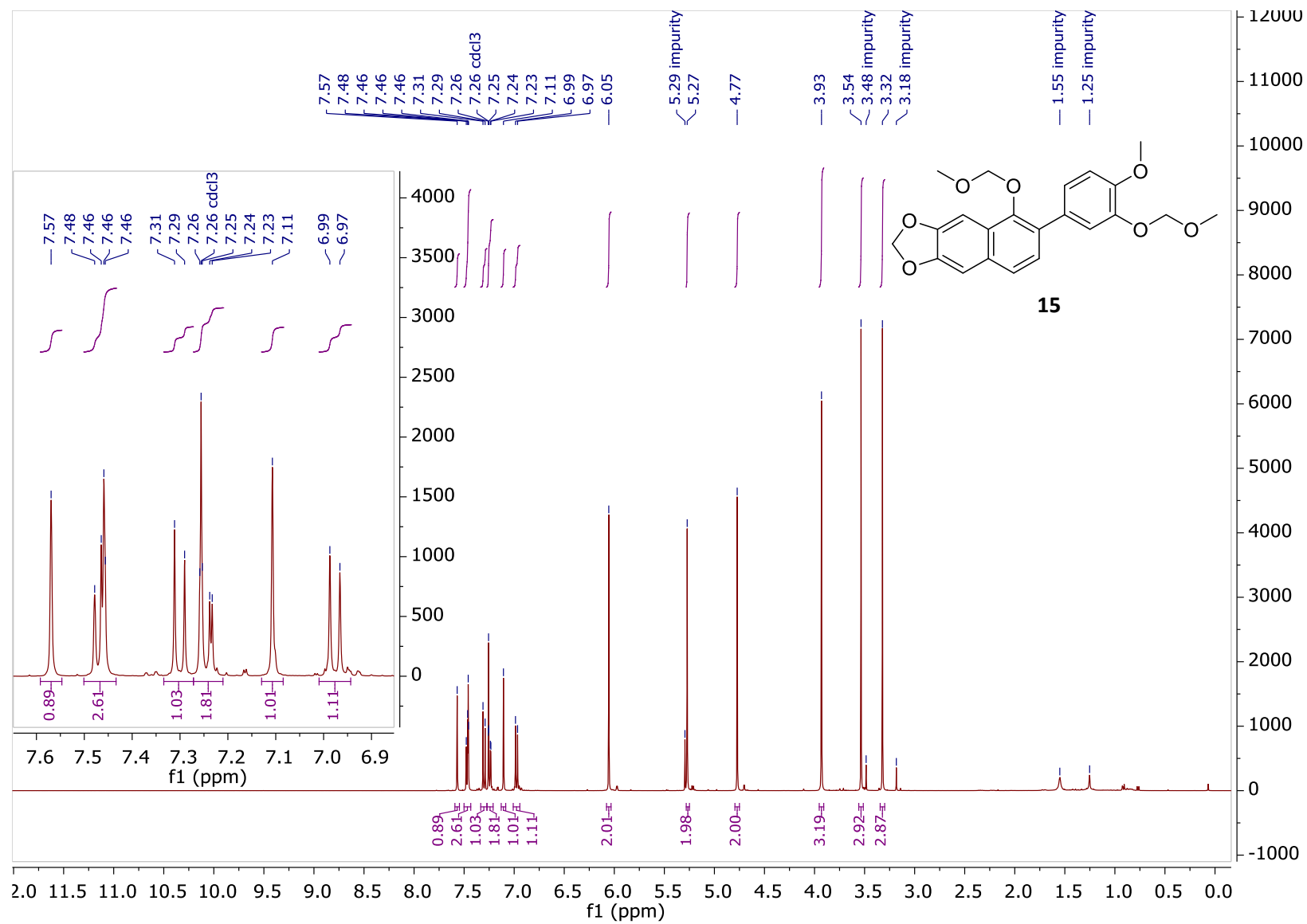


Figure 16 ¹H-NMR spectrum of **15**

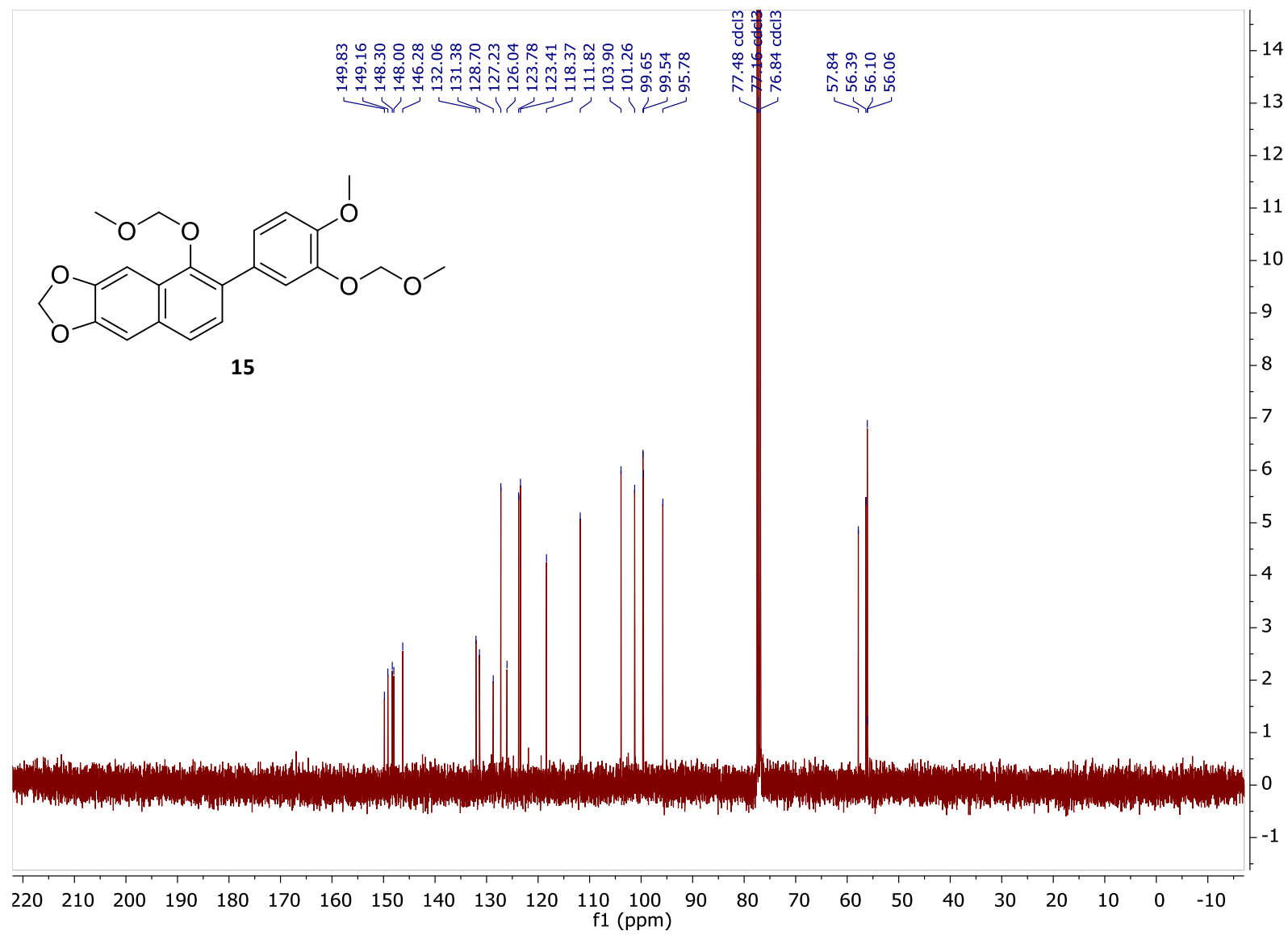


Figure 17 ^{13}C -NMR spectrum of **15**

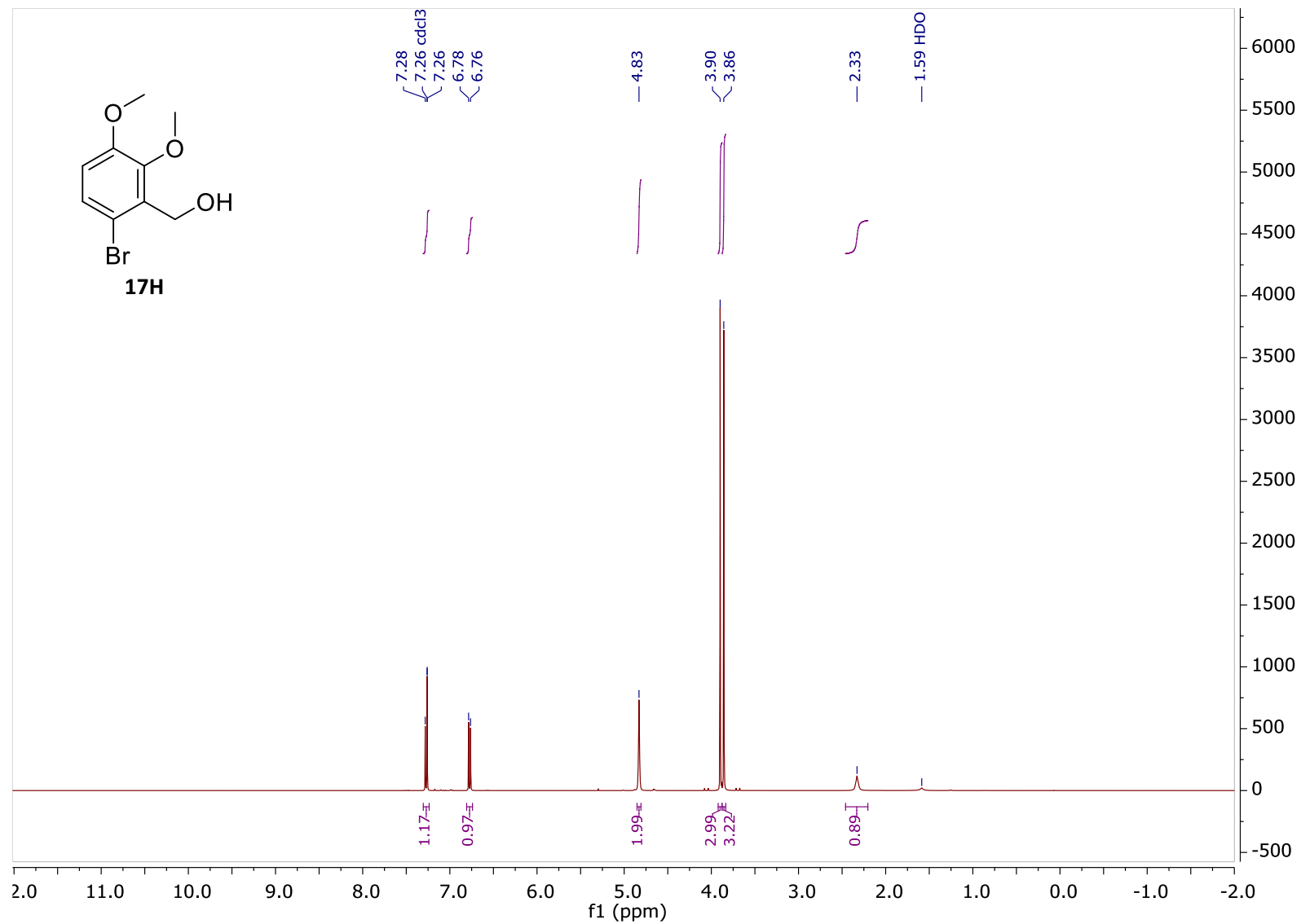


Figure 18 ¹H-NMR spectrum of **17H**

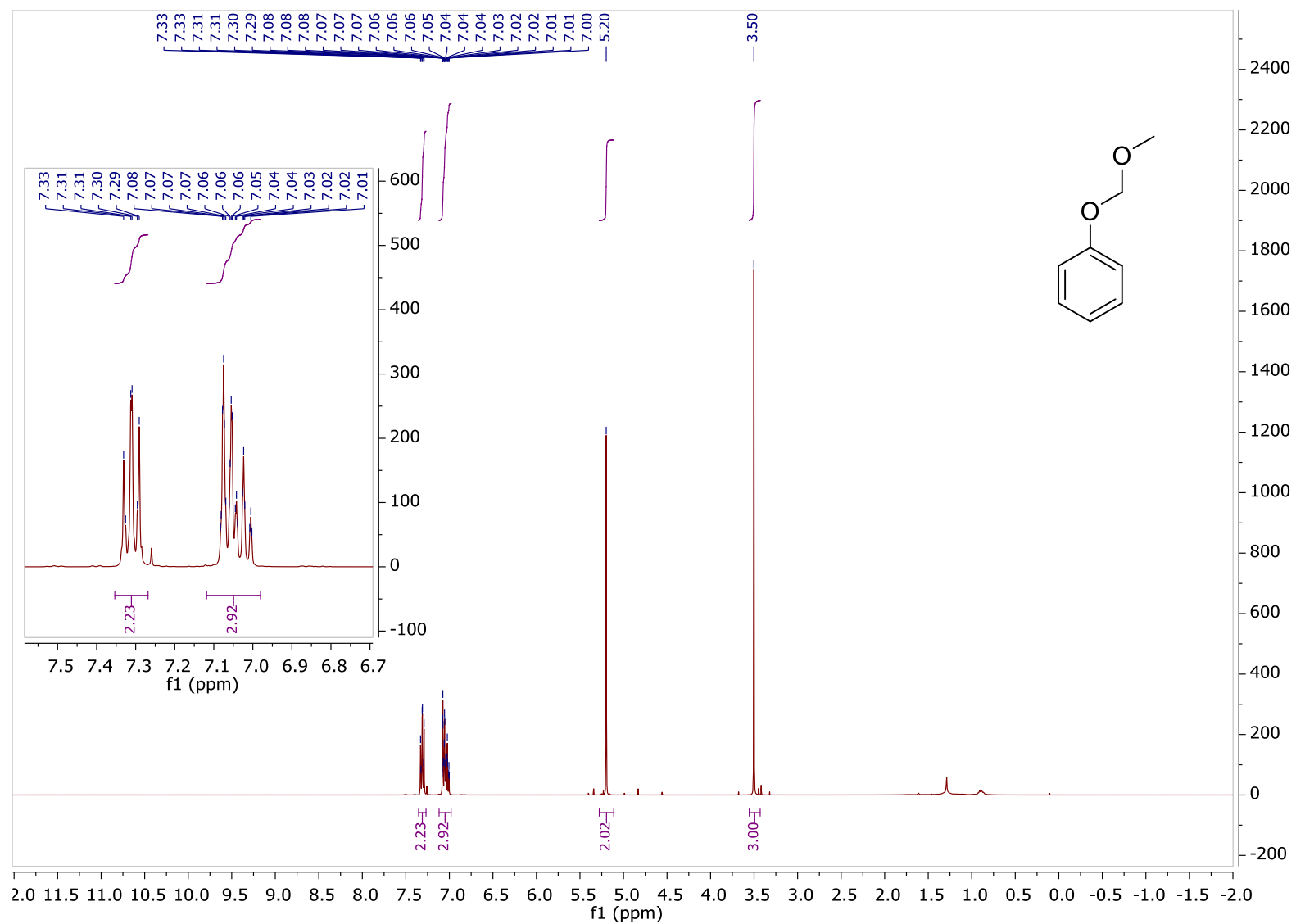


Figure 19 ¹H-NMR spectrum of methyl methoxy phenol

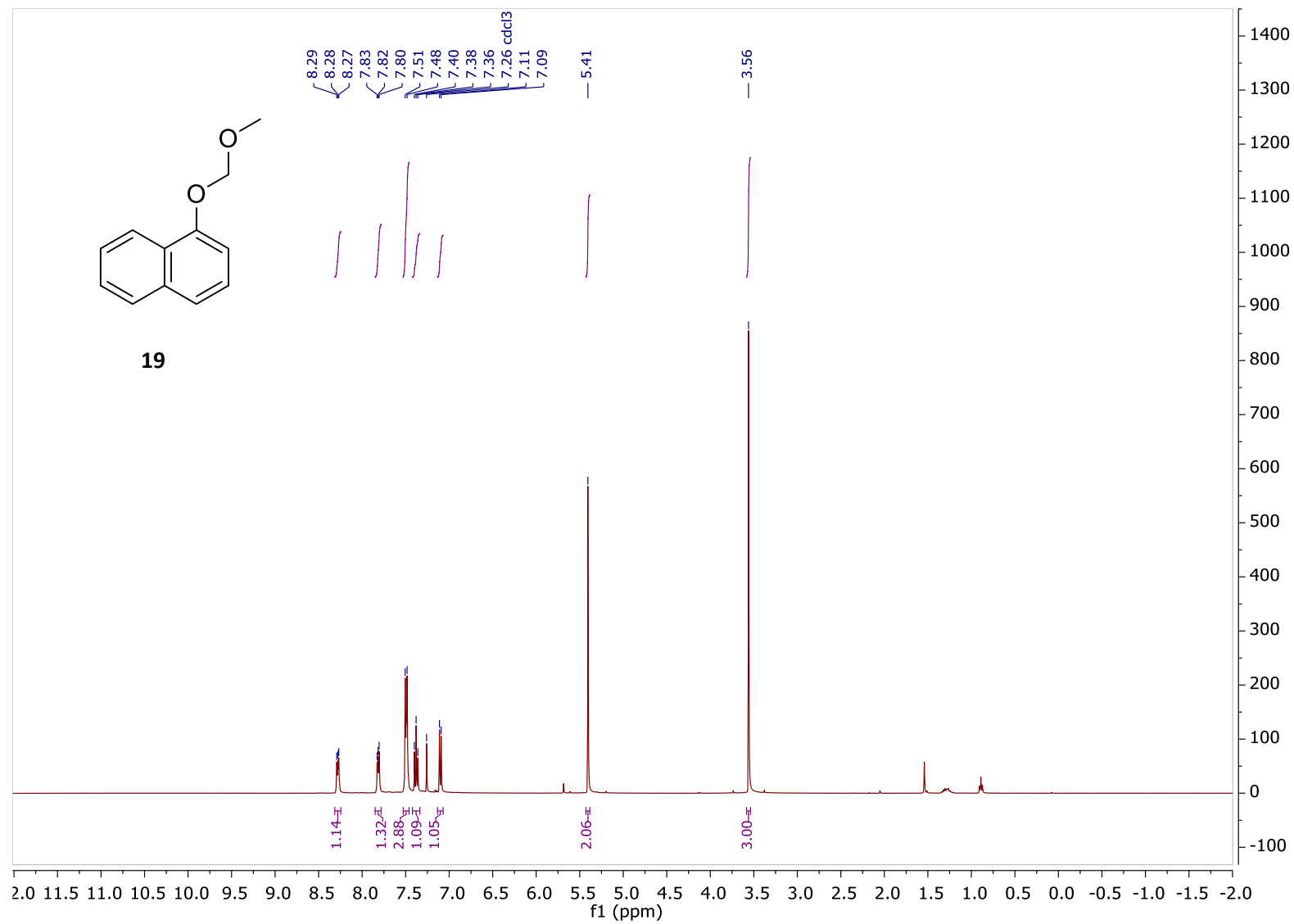


Figure 20 ¹H-NMR spectrum of methyl methoxy naphthol

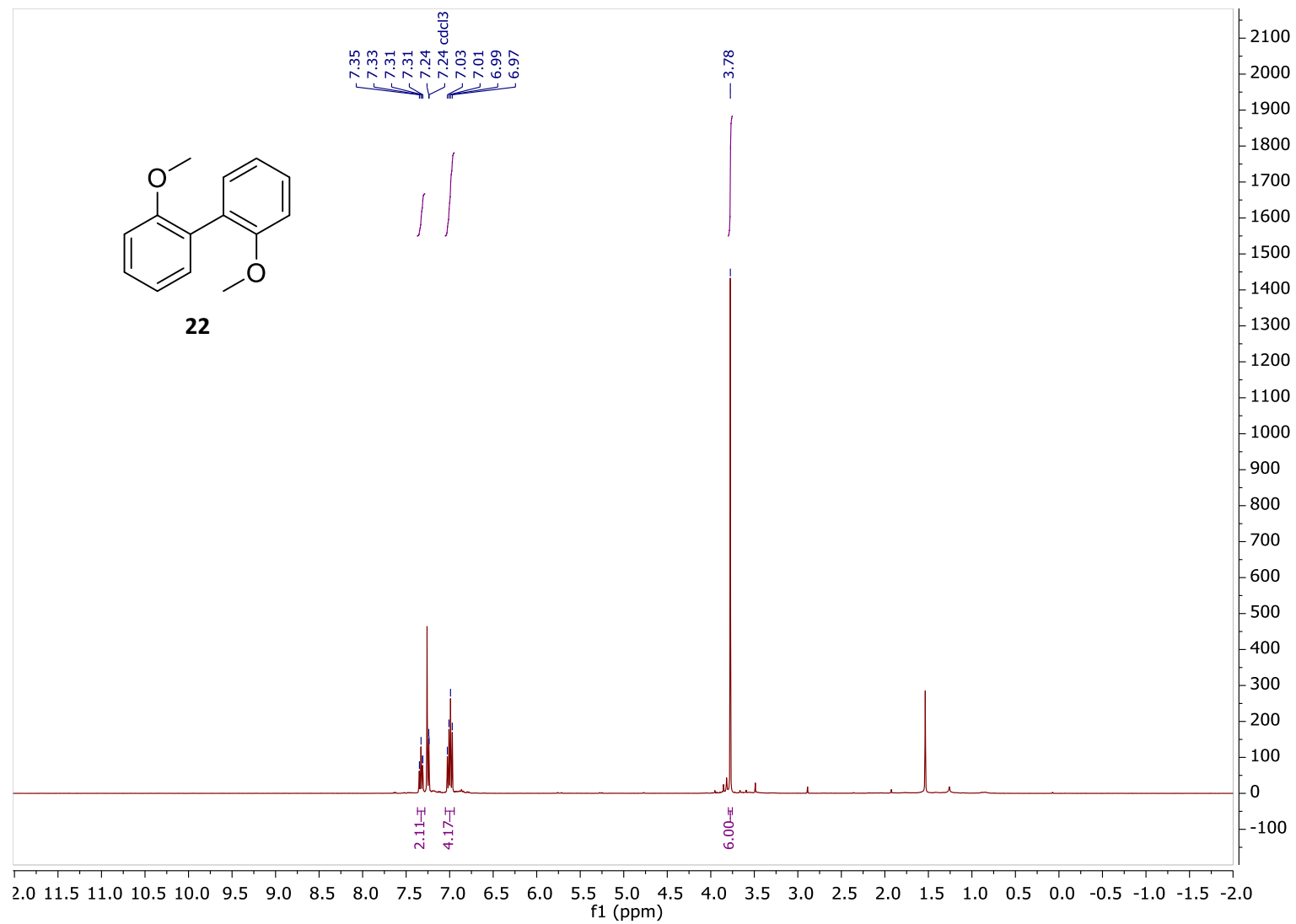


Figure 21 ¹H-NMR spectrum of **22**

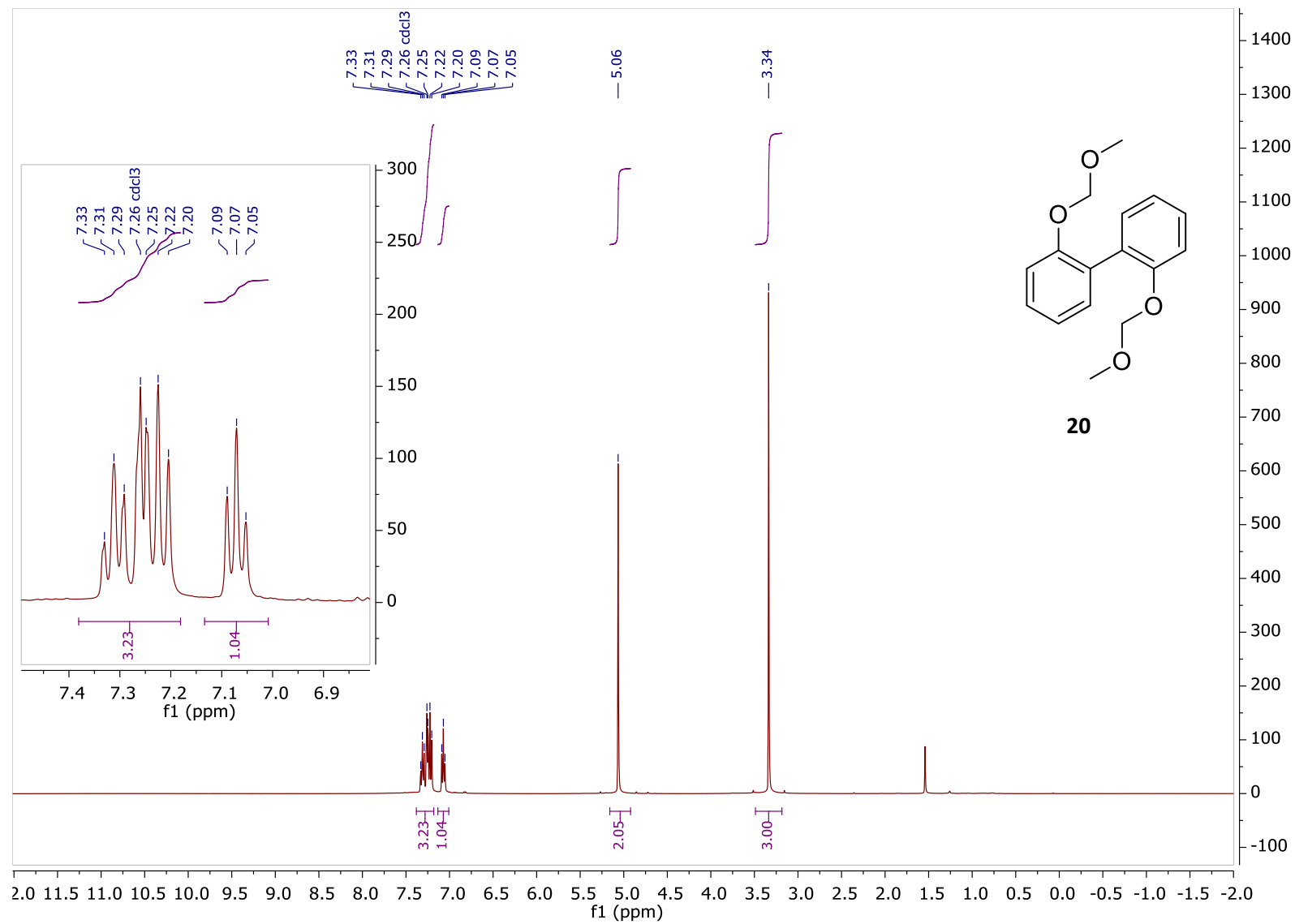


Figure 22 ¹H-NMR spectrum of **20**

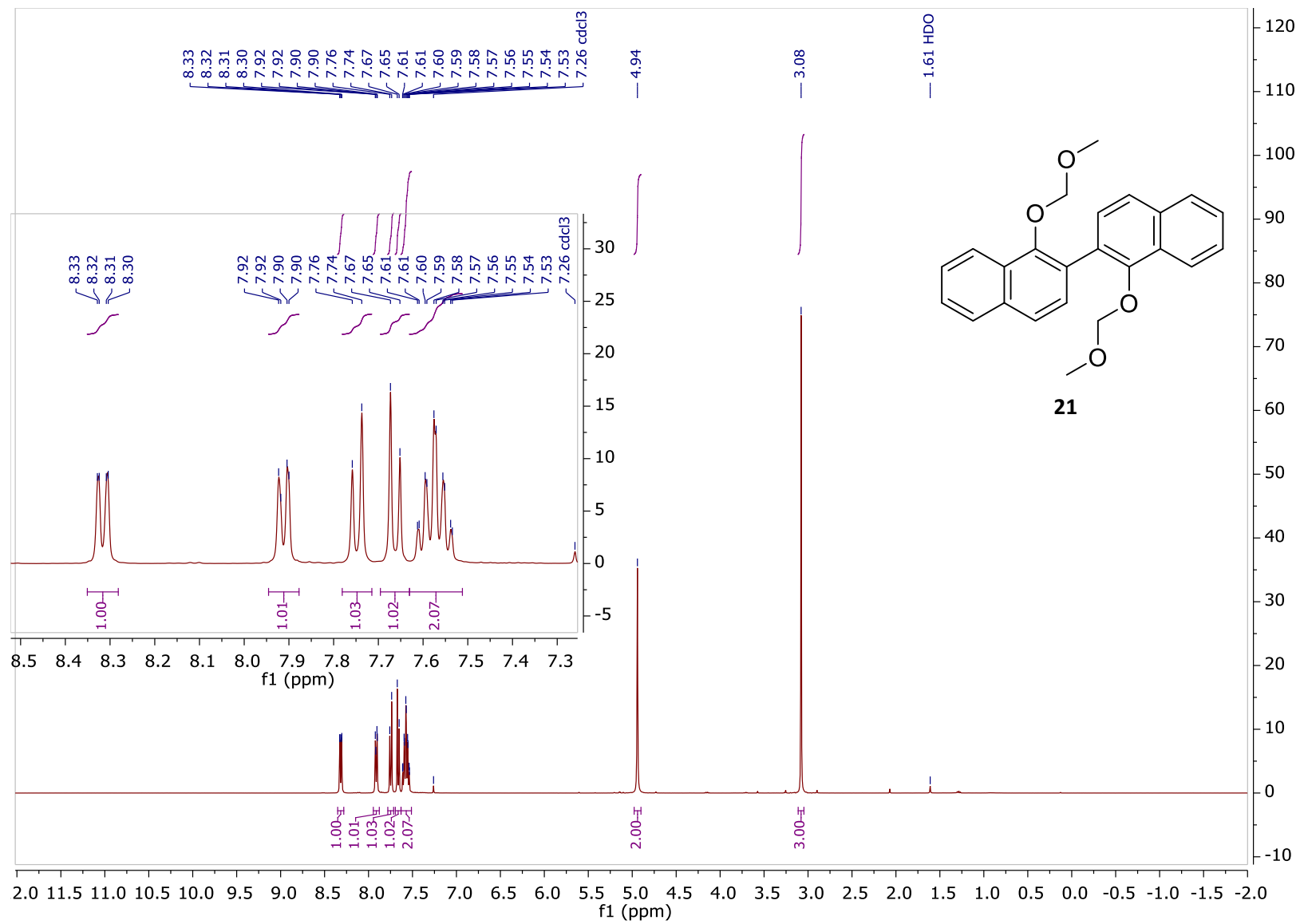


Figure 23 ¹H-NMR spectrum of **21**

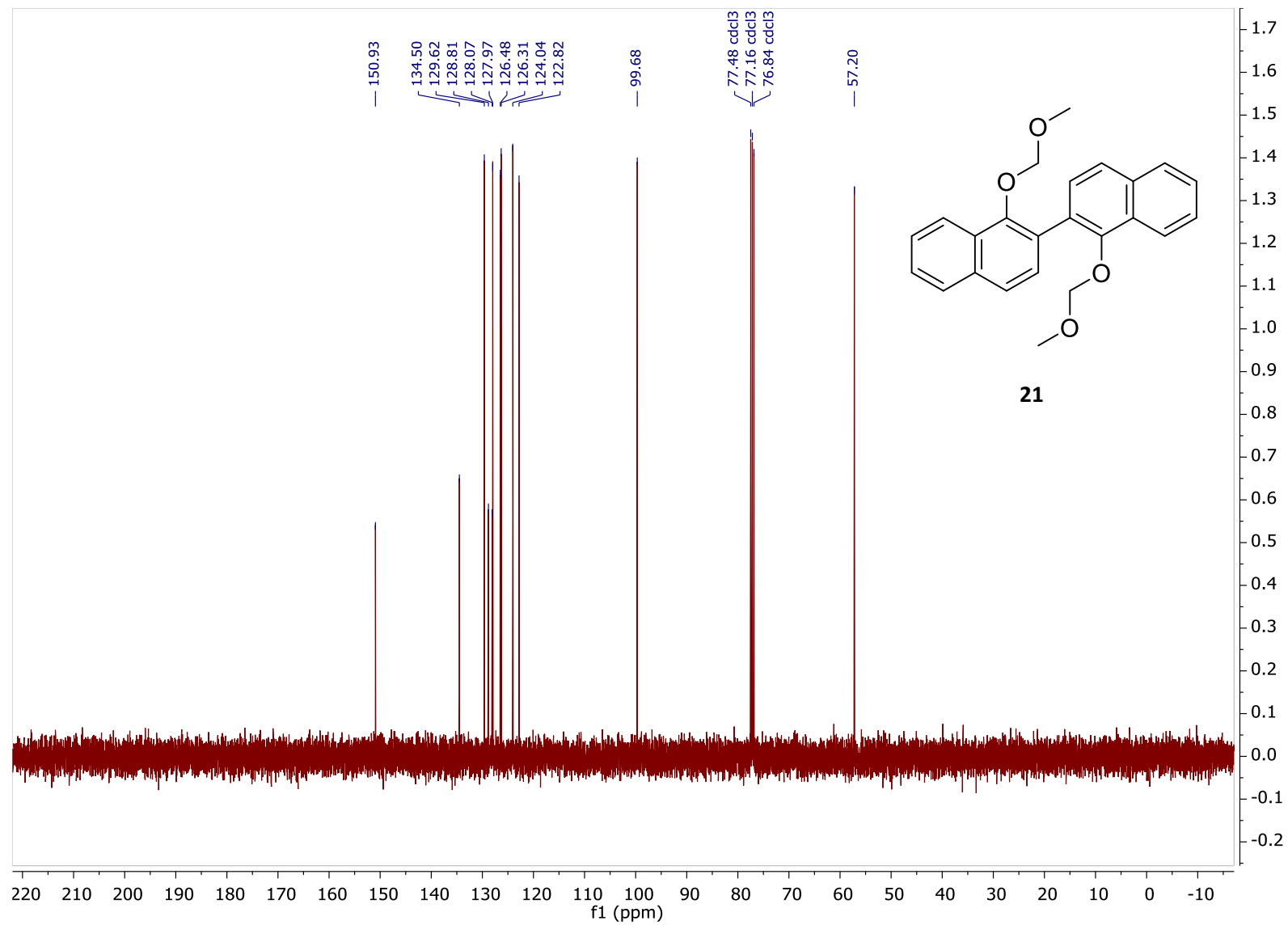


Figure 24 ^{13}C -NMR spectrum of **21**

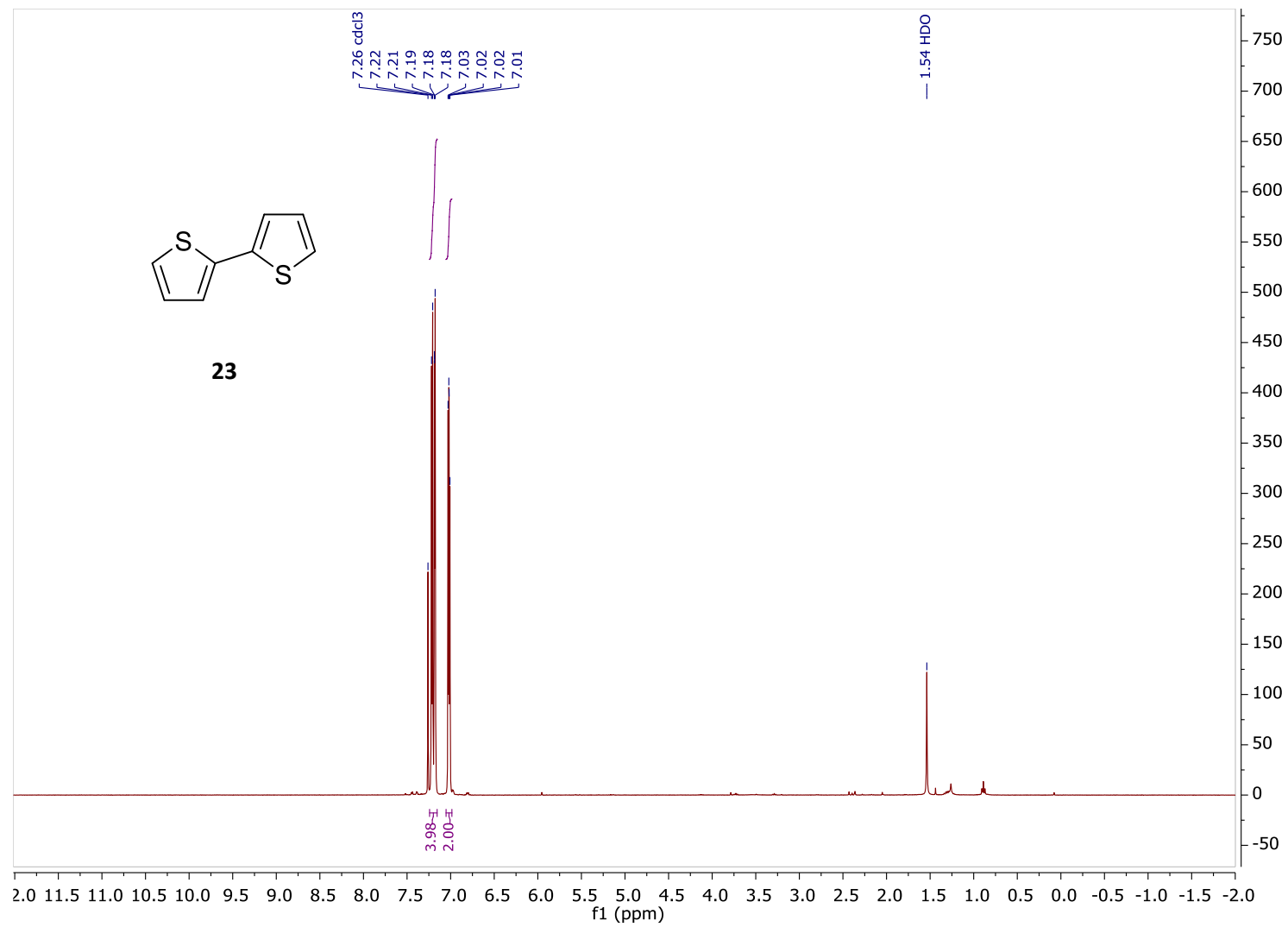


Figure 25 $^1\text{H-NMR}$ spectrum of **23**

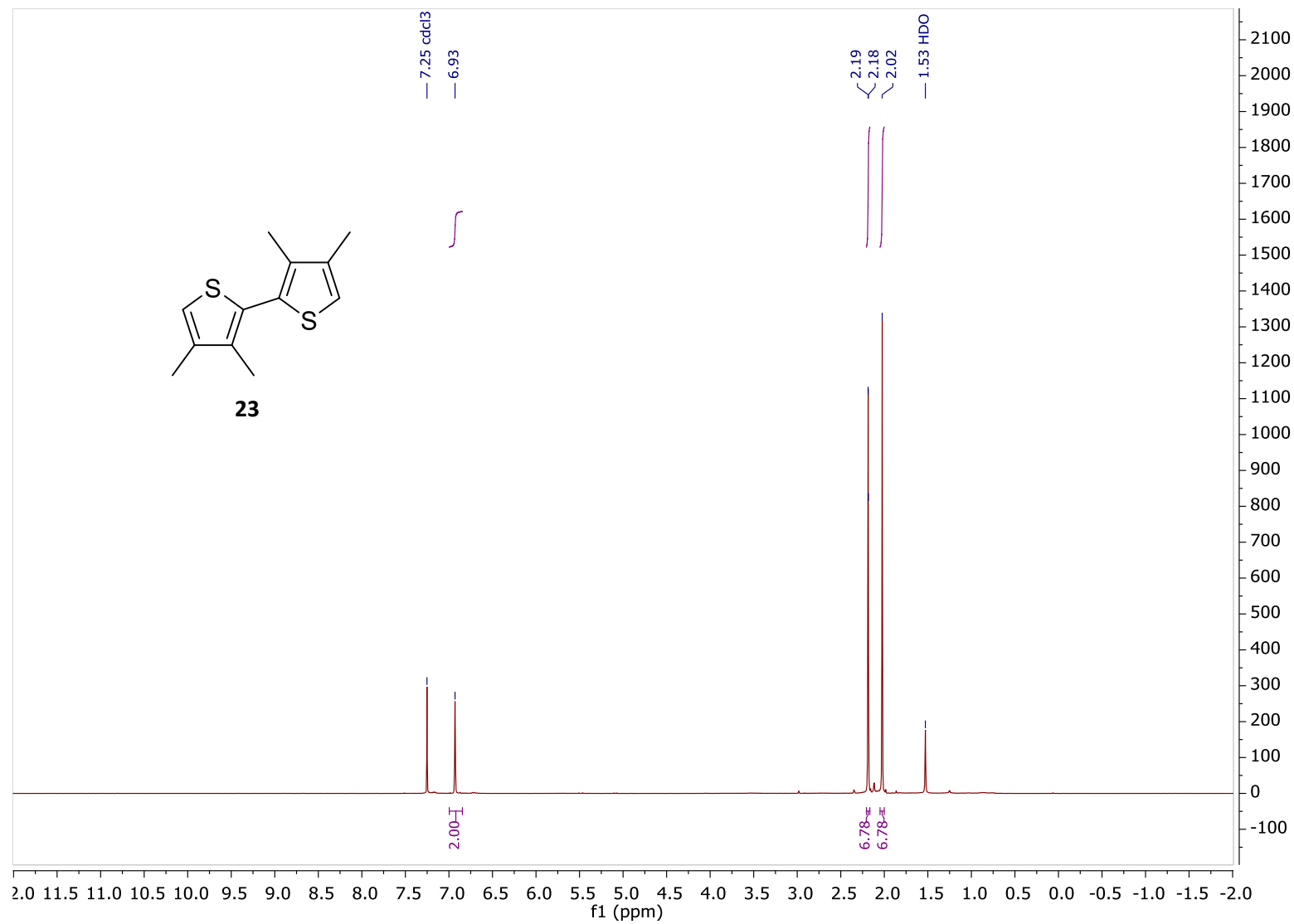


Figure 26 ¹H-NMR spectrum of **23**

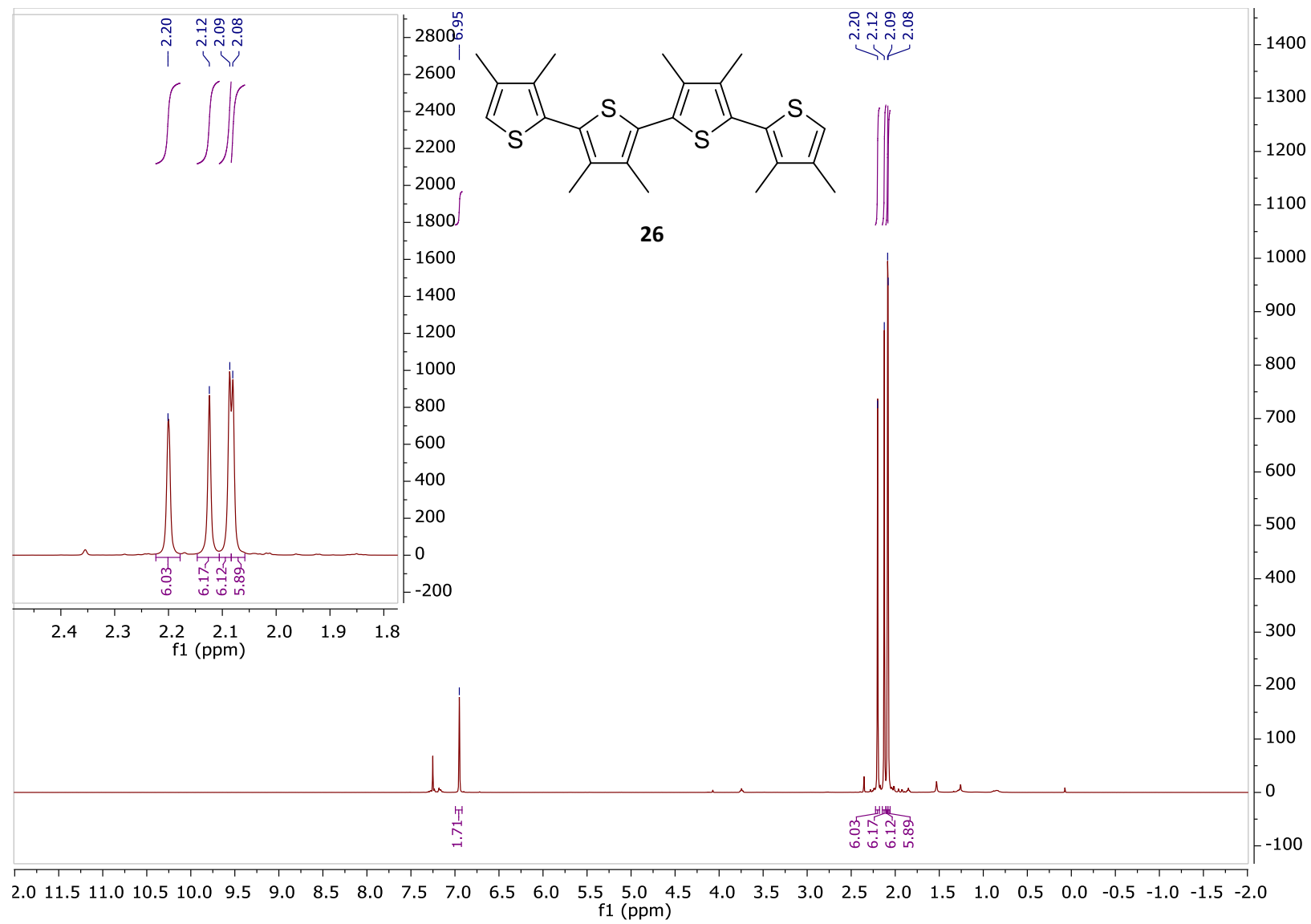


Figure 27 ¹H-NMR spectrum of **26**

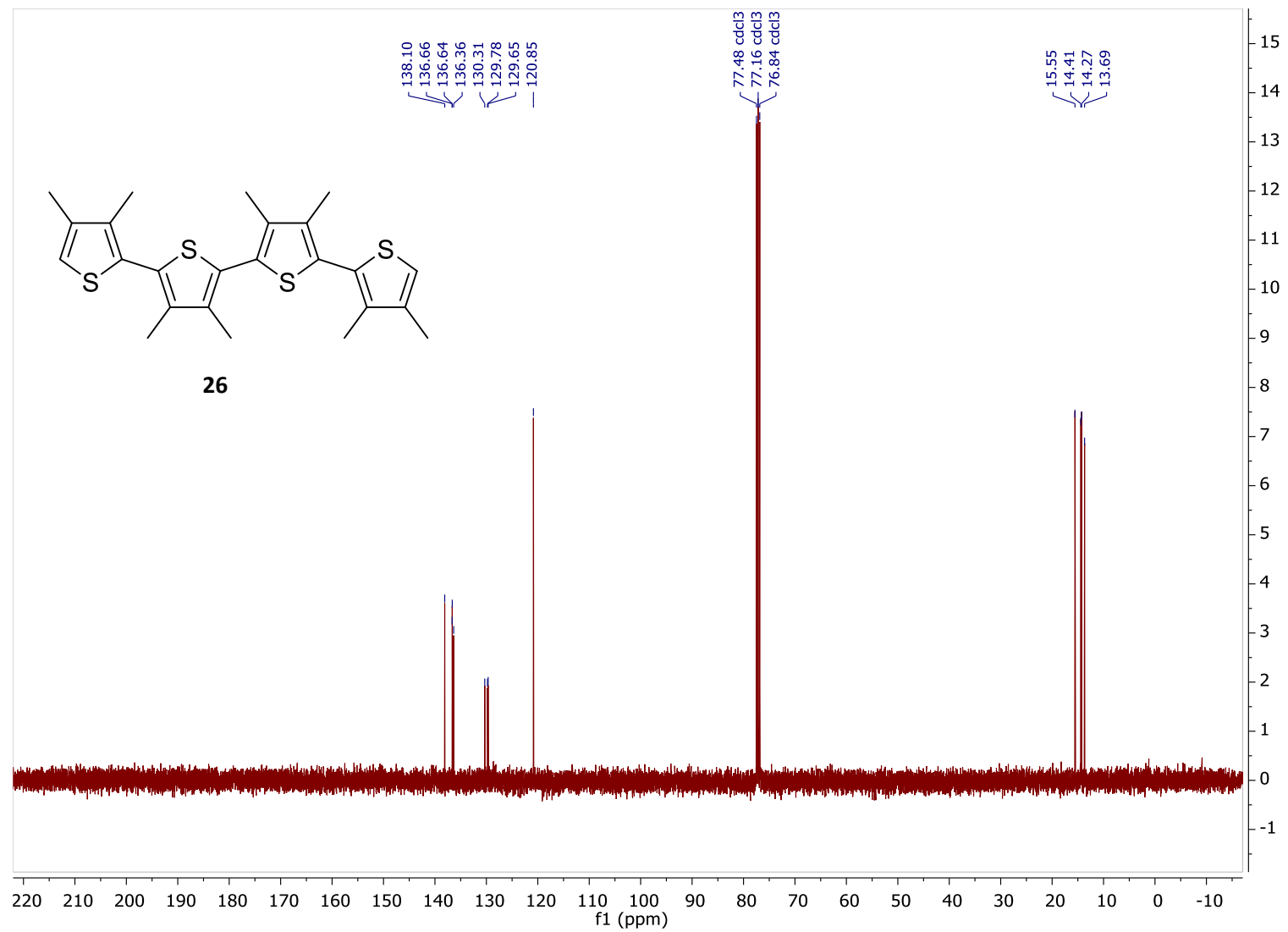
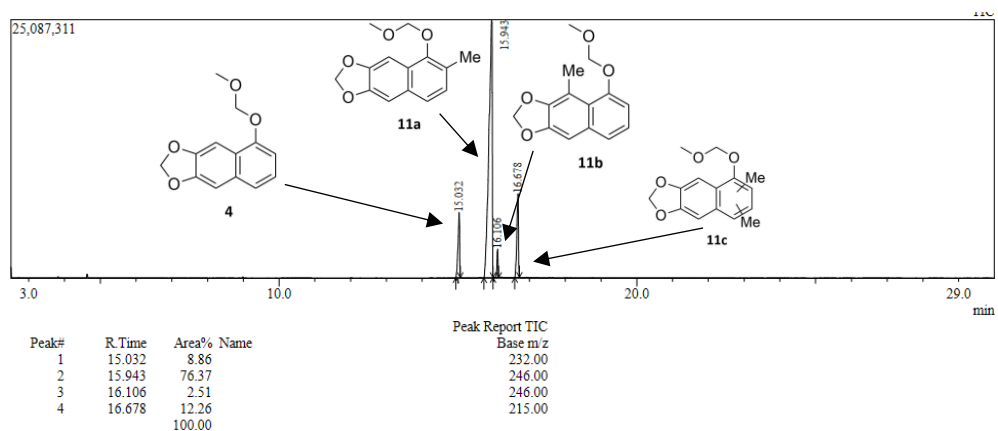


Figure 28 ^{13}C -NMR spectrum of **26**

GC-MS Chromatograms

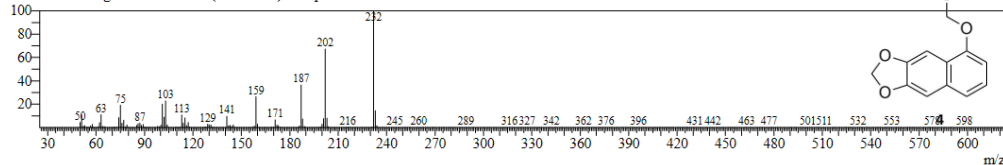


Peak# 1 R.Time:15.032(Scan#:1505)

MassPeaks:407

RawMode:Averaged 15.025-15.042(1504-1506)

BG Mode:Averaged 15.067-15.083(1509-1511) Group 1 - Event 1 Scan

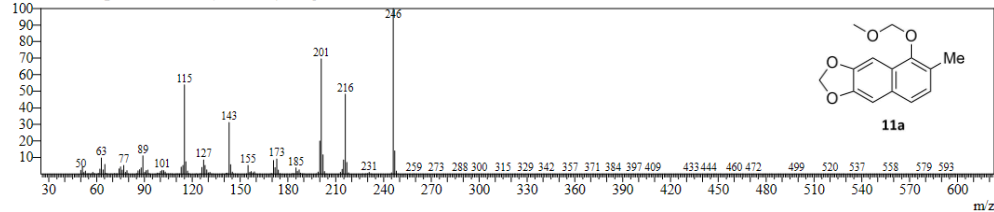


Peak# 2 R.Time:15.943(Scan#:1614)

MassPeaks:450

RawMode:Averaged 15.933-15.950(1613-1615)

BG Mode:Averaged 15.983-16.000(1619-1621) Group 1 - Event 1 Scan

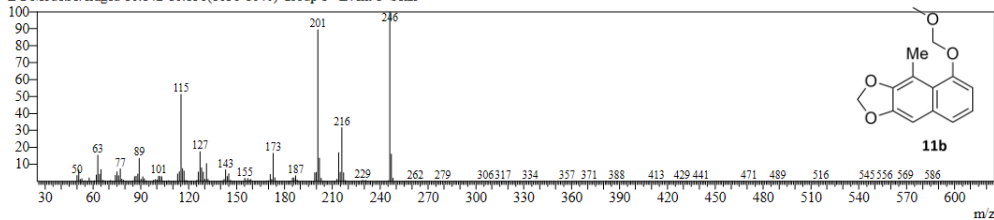


Peak# 3 R.Time:16.106(Scan#:1634)

MassPeaks:395

RawMode:Averaged 16.100-16.117(1633-1635)

BG Mode:Averaged 16.142-16.158(1638-1640) Group 1 - Event 1 Scan



Peak# 4 R.Time:16.678(Scan#:1702)

MassPeaks:413

RawMode:Averaged 16.667-16.683(1701-1703)

BG Mode:Averaged 16.717-16.733(1707-1709) Group 1 - Event 1 Scan

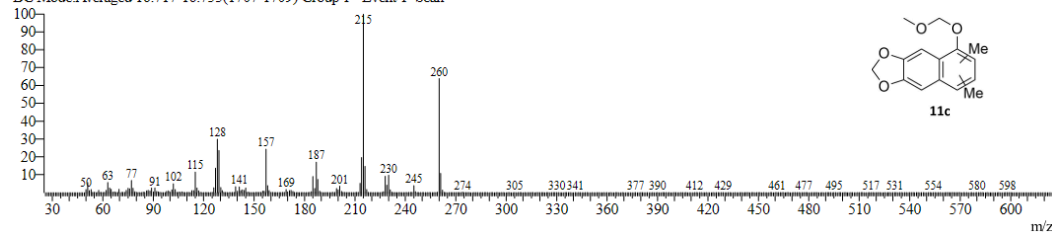
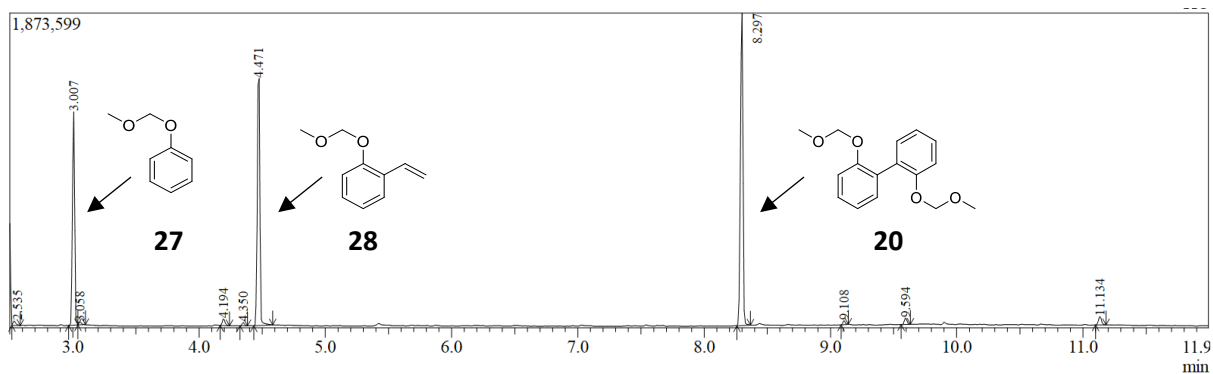


Figure 29 GC-MS chromatogram of a mixture of **4**, **11a**, **11b**, and **11c** from lithiation of **4** in MTBE with subsequent MeI-quench.



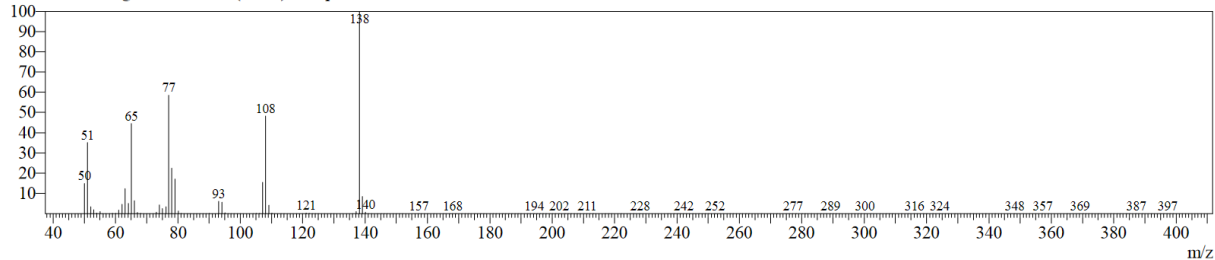
Peak#	R. Time	Area%	Name	Base m/z
1	2.535	0.60		94.10
2	3.007	23.53		138.15
3	3.058	0.39		91.10
4	4.194	0.94		166.10
5	4.350	0.36		138.15
6	4.471	32.30		91.10
7	8.297	39.34		198.05
8	9.108	0.46		198.05
9	9.594	0.85		226.10
10	11.134	1.23		216.15
		100.00		

Peak#:2 R. Time:3.007(Scan#:62)

MassPeaks:223

RawMode:Averaged 3.000-3.017(61-63)

BG Mode:Averaged 3.042-3.058(66-68) Group 1 - Event 1 Scan

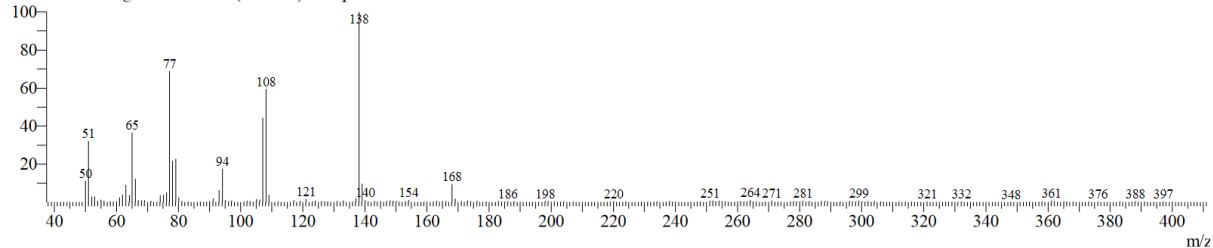


Peak#:5 R. Time:4.350(Scan#:223)

MassPeaks:189

RawMode:Averaged 4.342-4.358(222-224)

BG Mode:Averaged 4.383-4.400(227-229) Group 1 - Event 1 Scan



Peak#:6 R. Time:4.471(Scan#:238)

MassPeaks:234

RawMode:Averaged 4.467-4.483(237-239)

BG Mode:Averaged 4.583-4.600(251-253) Group 1 - Event 1 Scan

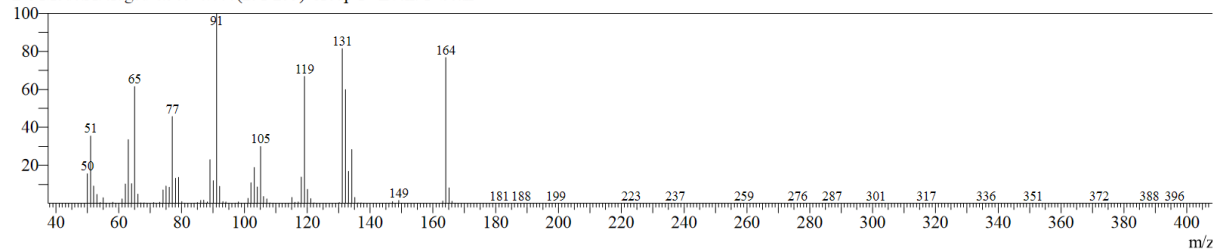
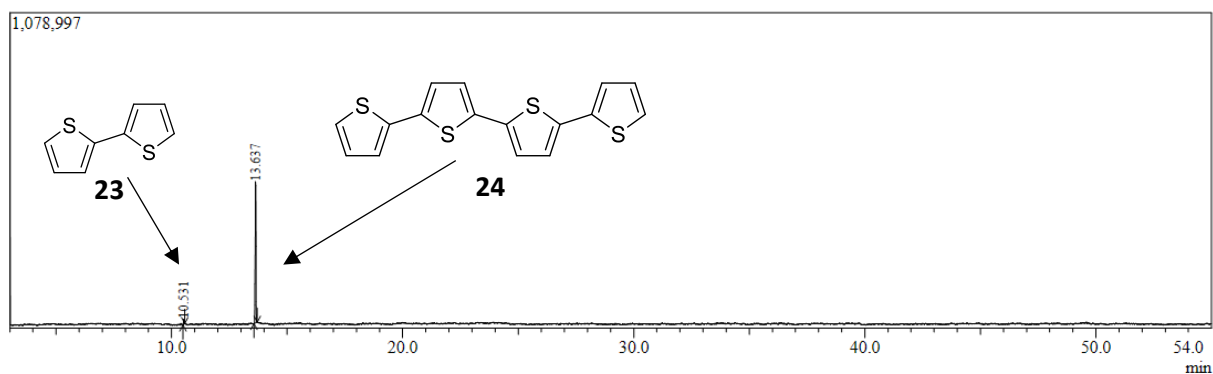


Figure 30 GC-MS chromatogram of the temperature study of the dimerization of **27** taken at 0 °C with Pd-PEPPSI SIPr as catalyst.



Peak#	R.Time	Area%	Name	Base m/z
1	10.531	3.16		261.00
2	13.637	96.84		330.00

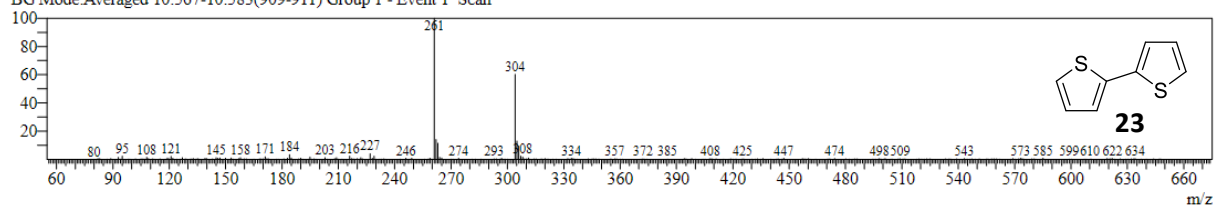
Peak Report TIC

Peak#:1 R.Time:10.531(Scan#:905)

MassPeaks:333

RawMode:Averaged 10.525-10.542(904-906)

BG Mode:Averaged 10.567-10.583(909-911) Group 1 - Event 1 Scan



Peak#:2 R.Time:13.637(Scan#:1277)

MassPeaks:408

RawMode:Averaged 13.625-13.642(1276-1278)

BG Mode:Averaged 13.708-13.725(1286-1288) Group 1 - Event 1 Scan

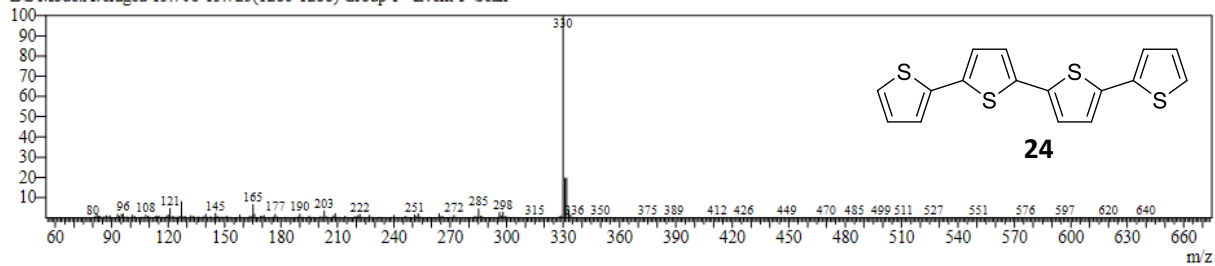
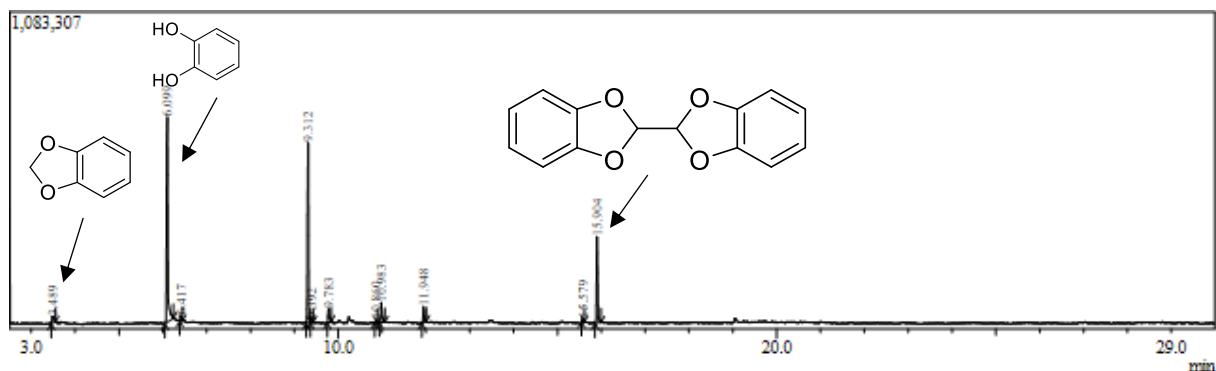
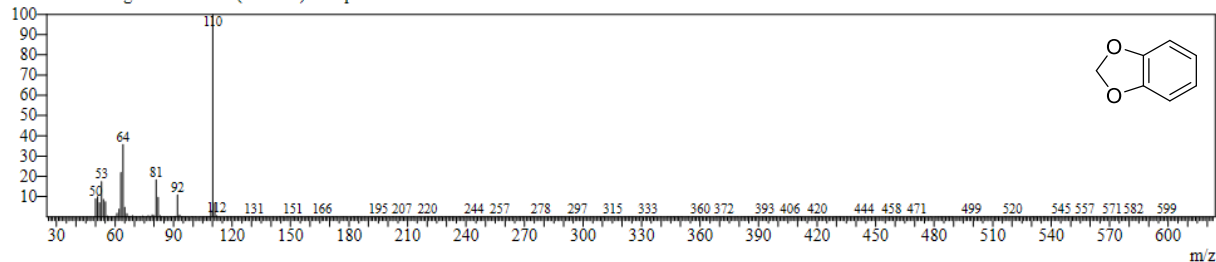


Figure 31 GC-MS chromatogram of the product solution of the dimerization of **23** to **24**

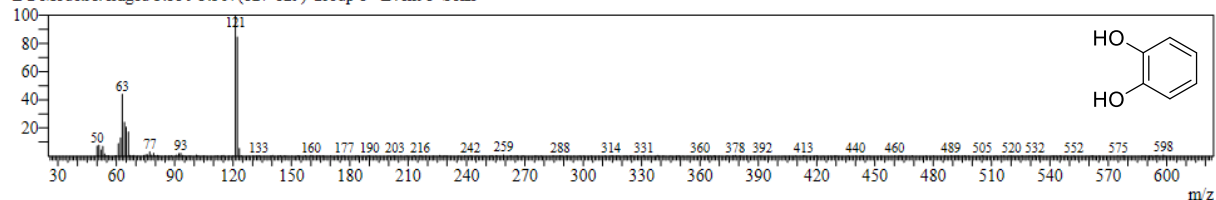


Peak#	R.Time	Area%	Name	Base m/z
1	3.489	1.95		121.15
2	6.099	39.24		110.10
3	6.417	0.80		148.15
4	9.312	30.97		110.10
5	9.392	0.71		110.10
6	9.783	2.91		121.15
7	10.860	0.48		135.15
8	10.983	3.69		103.10
9	11.948	2.99		131.15
10	15.579	0.57		135.15
11	15.904	15.69		242.10
		100.00		

Peak#2 R.Time:6.099(Scan#:433)
 MassPeaks:390
 RawMode:Averaged 6.092-6.108(432-434)
 BG Mode:Averaged 6.242-6.258(450-452) Group 1 - Event 1 Scan



Peak#1 R.Time:3.489(Scan#:120)
 MassPeaks:254
 RawMode:Averaged 3.483-3.500(119-121)
 BG Mode:Averaged 3.550-3.567(127-129) Group 1 - Event 1 Scan



Peak#11 R.Time:15.904(Scan#:1609)
 MassPeaks:330
 RawMode:Averaged 15.892-15.908(1608-1610)
 BG Mode:Averaged 15.992-16.008(1620-1622) Group 1 - Event 1 Scan

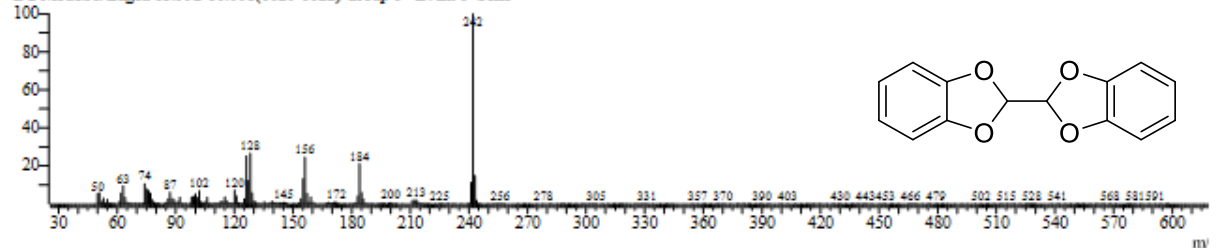
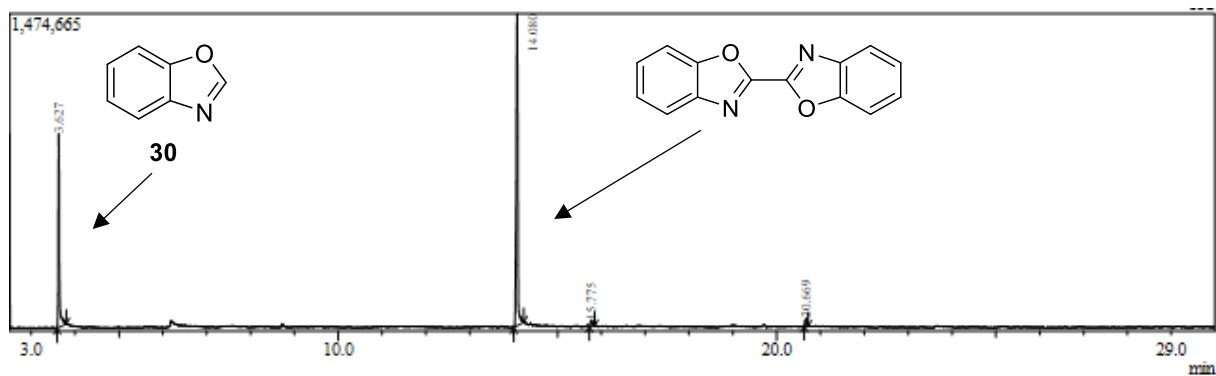
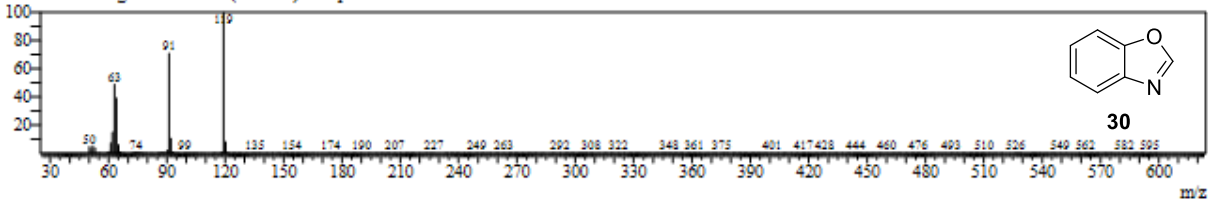


Figure 32 GC-MS Chromatogram of the product solution of the dimerization of 29



Peak#	R.Time	Area%	Name	Base m/z
1	3.627	31.31		119.10
2	14.080	65.67		178.15
3	15.775	1.48		178.15
4	20.669	1.55		245.25
		100.00		

Peak#1 R.Time:3.627(Scan#:136)
 MassPeaks:287
 RawMode:Averaged 3.617-3.633(135-137)
 BG Mode:Averaged 3.800-3.817(157-159) Group 1 - Event 1 Scan



Peak#2 R.Time:14.080(Scan#:1391)
 MassPeaks:360
 RawMode:Averaged 14.075-14.092(1390-1392)
 BG Mode:Averaged 14.233-14.250(1409-1411) Group 1 - Event 1 Scan

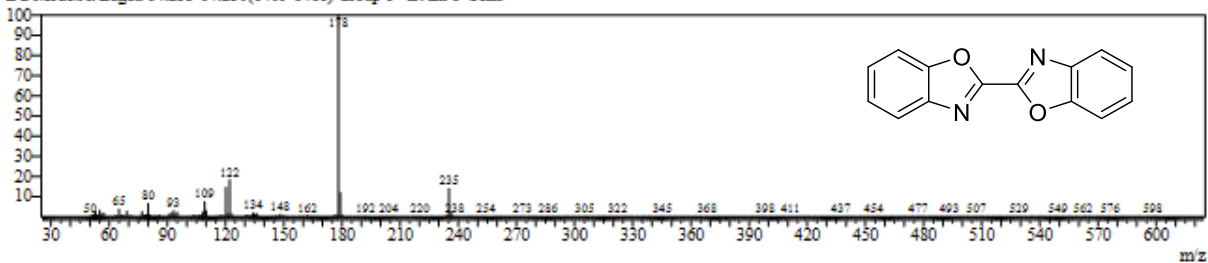
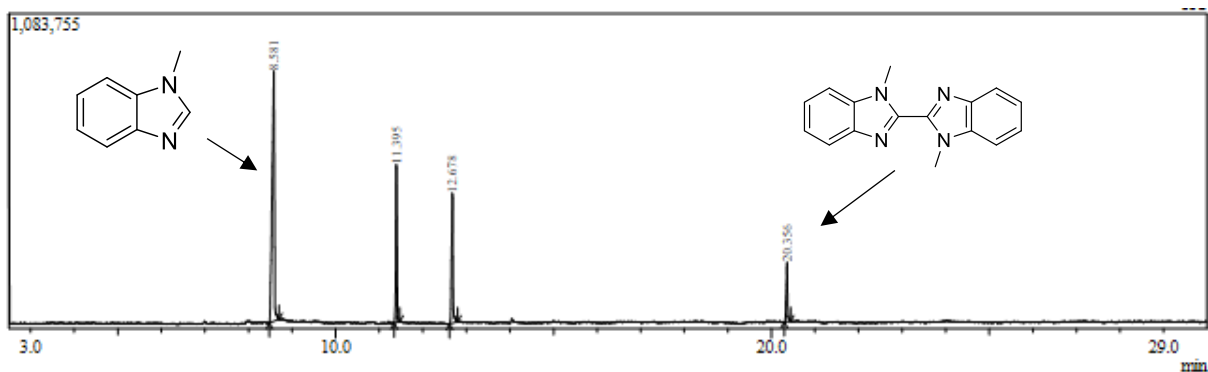


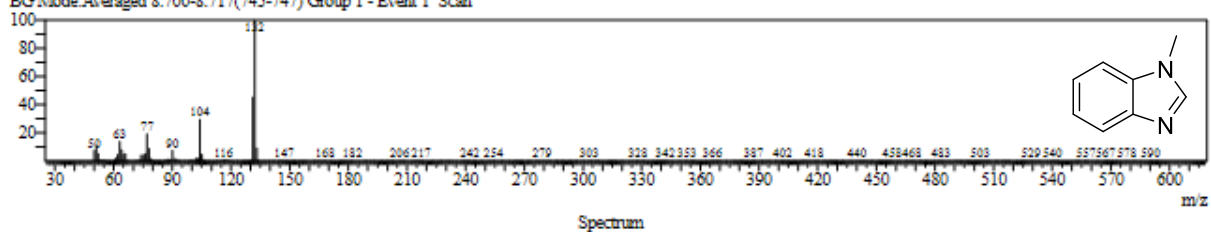
Figure 33 GC-MS Chromatogram of the product solution of the dimerization of **30**



Peak#	R.Time	Area%	Name	Base m/z
1	8.581	55.61		132.15
2	11.395	18.14		147.20
3	12.678	18.43		146.20
4	20.356	7.83		261.15
		100.00		

Peak Report TIC

Peak#1 R.Time:8.581(Scan#:731)
 MassPeaks:323
 RawMode:Averaged 8.575-8.592(730-732)
 BG Mode:Averaged 8.700-8.717(745-747) Group 1 - Event 1 Scan



Peak#4 R.Time:20.356(Scan#:2144)
 MassPeaks:360
 RawMode:Averaged 20.350-20.367(2143-2145)
 BG Mode:Averaged 20.442-20.458(2154-2156) Group 1 - Event 1 Scan

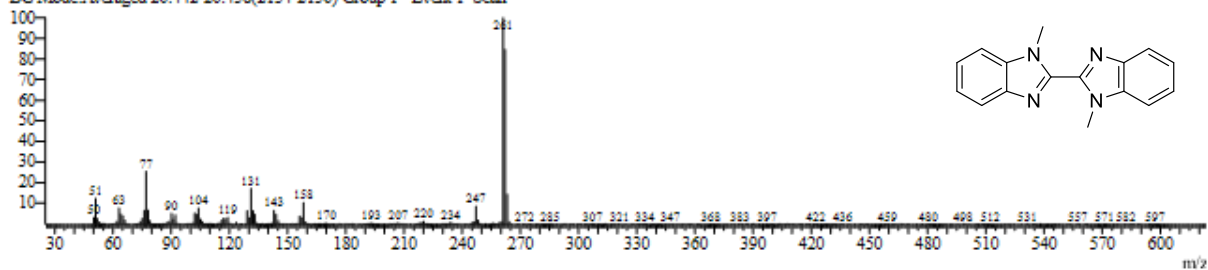
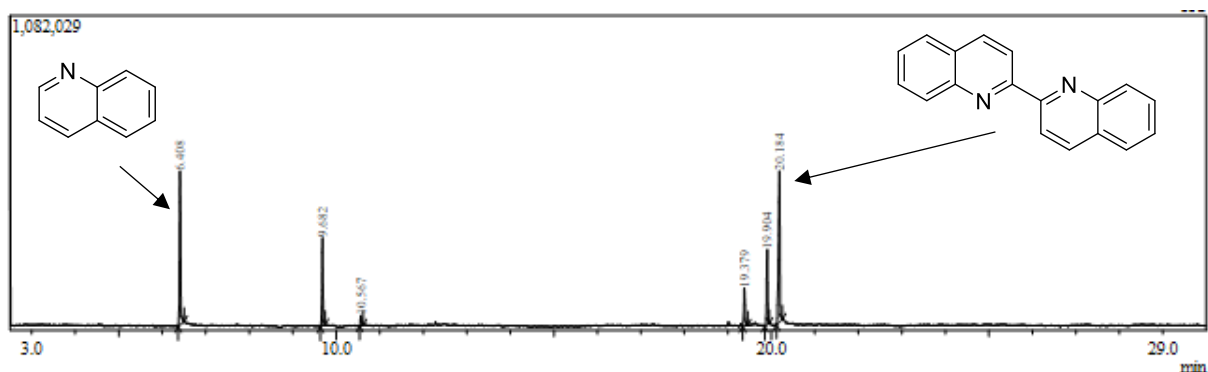


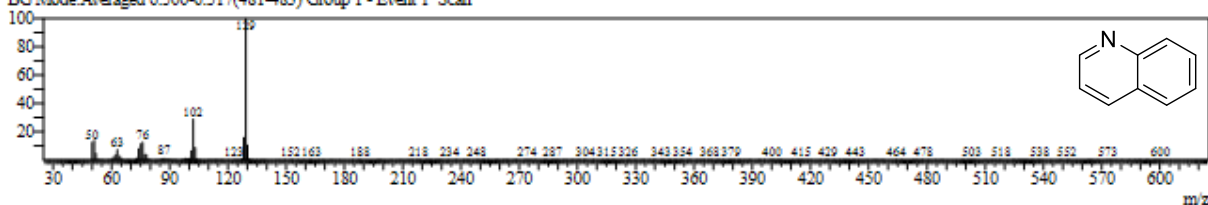
Figure 34 GC-MS chromatogram of the product solution of the dimerization of **31**



Peak Report TIC

Peak#	R. Time	Area%	Name	Base m/z
1	6.408	27.56		129.15
2	9.682	14.36		170.15
3	10.567	1.86		130.15
4	19.379	7.35		144.20
5	19.904	13.86		158.15
6	20.184	35.02		256.15
		100.00		

Peak# 1 R. Time: 6.408 (Scan# 470)
 MassPeaks: 285
 RawMode: Averaged 6.400-6.417 (469-471)
 BG Mode: Averaged 6.500-6.517 (481-483) Group 1 - Event 1 Scan



Peak# 6 R. Time: 20.184 (Scan# 2123)
 MassPeaks: 346
 RawMode: Averaged 20.175-20.192 (2122-2124)
 BG Mode: Averaged 20.258-20.275 (2132-2134) Group 1 - Event 1 Scan

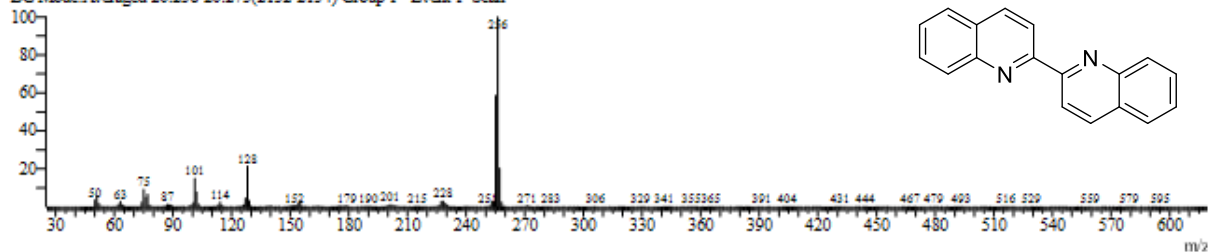


Figure 35 GC-MS Chromatogram of the product solution of the dimerization of **32**